ECOHYDROLOGY OF A GREAT LAKES COASTAL RIDGE-SWALE WETLAND SYSTEM

by

Martha L. Carlson

A dissertation submitted in partial fulfillment
of the requirements for the degree of
Doctor of Philosophy
(Natural Resources and Environment)
in The University of Michigan
2009

Doctoral Committee:

Professor Michael J. Wiley, Chair
Professor Deborah E. Goldberg
Professor Donald R. Zak
Professor Douglas A. Wilcox, The College at Brockport, State University of New York

DEDICATION

To my husband, Bob;
my sisters, Lee Ann and Sandy;
my mother and father, Sheila and Tom,
without whose love, encouragement,
and support this would not have been possible.

ACKNOWLEDGMENTS

I owe the utmost gratitude to the following:

My advisor and committee chair, Dr. Michael J. Wiley of the University of Michigan School of Natural Resources and Environment, for his insightful analysis and thoughtful critique.

My long-time mentor, Dr. Douglas A. Wilcox of the College at Brockport, State University of New York, for his constant encouragement and support.

My committee members, Dr. Deborah Goldberg and Dr. Don Zak.

Dr. Steve Baedke of James Madison University for the inspiration to study evapotranspiration in ridge-swale wetlands, for his thoughtful advice and scientific assistance, and for providing me with water-chemistry data.

Dr. Todd Thompson of the Indiana Geological Survey for his thoughtful advice and assistance and for providing GPR and sediment-core data.

Dr. Jim Meeker of Northland College and Valena Hoffman for providing plant identification expertise.

My field assistants, Robert Mazur, Morgan Crutcher, Miriam Allersma, Erin Murphy, Amelia Letvin, and Kelly Iknayan for slugging through the mud with me.

Dr. Todd Rasmussen of the University of Georgia, who provided me with code for performing regression deconvolution and insightful interpretation of unaccountable fluctuations in my data set.

Lee Ann C. LeBlanc, Taryn Dentinger, and Robert Mazur for their reviews of various versions of my dissertation and for helping me along the way.

The USGS Global Change Research Program, the University of Michigan School of Natural Resources and Environment, and Rackham Graduate School who provided funding for this research.

CONTENTS

LIST OF TABLES

LIST OF FIGURES

LIST OF SYMBOLS AND ABBREVIATIONS

Symbol	Definition of Variable	Units	Source
B	barometric pressure	kPa	
BE	barometric efficiency		Ferris et al. (1962), Gonthier (2007)
D_s	depth from substrate to predepositional surface	l (length)	
D_w	depth of water	l	
ET_{ASCE}	actual evapotranspiration predicted from PET_{ASCE}	$l\ t^{-1}$ (length per unit time)	Allen et al. (2005)
ET_G	actual evapotranspiration calculated from diurnal water-table fluctuations	$l\ t^{-1}$	Loheide (2008)
ET_C	composite of ET_G and scaled PET	$l\ t^{-1}$	
G_{net}	net groundwater flow	$l\ t^{-1}$	
G_{rec}	groundwater recovery	$l\ t^{-1}$	Loheide (2008)
G_{perc}	net percolation gain or loss	$l\ t^{-1}$	
H_s	soil heat flux	$MJ\ m^{-2}\ h^{-1}$	Allen et al. (1998)
H_t	total head		
K	hydraulic conductivity	$l\ t^{-1}$	Bouwer (1989)
LAI_c	leaf area index of the canopy	m^2 leaf m^{-2} ground	LI-COR (1992)
LAI_g	leaf area index of the ground-cover vegetation	m^2 leaf m^{-2} ground	Measured

PET_{ASCE}	ASCE-PM standardized reference evapotranspiration	$l\ t^{-1}$	Allen et al. (2006)
PET_{PM}	potential evapotranspiration, Penman-Monteith	$l\ t^{-1}$	Monteith (1965), Shuttleworth (1993), Souch et al. (1996, 1998)
PET_{QUAD}	potential evapotranspiration, quadratic solution to Penman-Monteith	$l\ t^{-1}$	Paw and Gao (1988)
R_a	extraterrestrial radiation	$MJ\ m^{-2}\ h^{-1}$	Allen et al. (1998)
R_n	net radiation	$MJ\ m^{-2}\ h^{-1}$	Allen et al. (1998)
R_{nl}	outgoing net longwave radiation	$MJ\ m^{-2}\ h^{-1}$	Allen et al. (1998)
R_{ns}	incoming net shortwave radiation	$MJ\ m^{-2}\ h^{-1}$	
R_s	measured incoming shortwave radiation	$MJ\ m^{-2}\ h^{-1}$	
R_{so}	clear-sky solar radiation	$MJ\ m^{-2}\ h^{-1}$	Allen et al. (1998)
S_y	specific yield	dim.	Bouwer (1989), Gerla (1992)
S_{ya}	specific yield of air (standing water)	dim.	Hill and Neary (2007)
S_{ys}	specific yield of soil and sediments	dim.	Hill and Neary (2007)
S_{yc}	composite specific yield of above- and below-ground components	dim.	
T or T_a	air temperature	°C	Measured
W	water-surface elevation head	l	
c_p	specific heat of air at constant pressure	$MJ\ kg^{-1}\ °C^{-1}$	Shuttleworth (1993)
dh/dt	change in water-table elevation over time	$l\ t^{-1}$	

e_s	saturation vapor pressure	kPa	Shuttleworth (1993)
e_a	actual vapor pressure	kPa	Allen et al. (1998)
h	water-table elevation		
l	length		
m	slope of the line tangent to the predawn portion of the water-level curve	$l\ t^{-1}$	White (1932)
r_a	aerodynamic resistance	$s\ m^{-1}$	Souch et al. (1998)
r_s	surface/canopy resistance	$s\ m^{-1}$	Souch et al. (1998)
t	time		
u	wind speed at 2 m height	$m\ s^{-1}$	Measured
Δ	slope of the saturation vapor pressure curve at air temperature	$kPa\ °C^{-1}$	Shuttleworth (1993)
ΔS	change in storage	l	
α	daily mean short-wave solar radiation coefficient, albedo	dim.	Shuttleworth (1993), Allen et al. (1998)
γ	psychometric constant	$kPa\ °C^{-1}$	Shuttleworth (1993)
λ	latent heat of vaporization	$MJ\ kg^{-1}$	Shuttleworth (1993)
ρ_a	density of air	$kg\ m^{-3}$	Shuttleworth (1993)
ρ_w	density of liquid water	$kg\ m^{-3}$	Allen et al. (2006)

Abbreviation	**Definition**
d	day
h	hour
s	second
mm	millimeter

m	meter
kg	kilogram
kPa	kilopascal
°C	degree Celsius
MJ	Megajoule
dim.	dimensionless

ABSTRACT

ECOHYDROLOGY OF A GREAT LAKES COASTAL RIDGE-SWALE WETLAND SYSTEM

by

Martha L. Carlson

Chair: Michael J. Wiley

Interactions between wetland plants and the water table influence trajectories of vegetation change and resulting community responses to climate change. The specific dynamics, however, are not well defined, in part because of complexities associated with climate, physiography, and underlying geology. In this study, the dynamic interactions of vegetation with the water table were examined in a coastal ridge-swale wetland system on Lake Huron. I modified a riparian-zone method for estimating evapotranspiration (ET) and shallow groundwater flow and applied it to this structurally and vegetatively complex site. I then explored how observed variability in wetland water balance arises through interactions between plants, physiography, and hydrogeology and examined inter-annual climatic effects. Finally, I used path analytic techniques to examine the dynamic nature of feedbacks between plant water use, indexed by ET, and water availability, indexed by soil moisture.

Average daily evapotranspiration rates for the 15 wetlands in the study ranged from 5.5 mm d^{-1} (SD 1.6) to 8.1 mm d^{-1} (SD 2.5). Over the growing season, the mean ET rate was 894 mm (SD 98) in 2006 (wet year) and 924 mm (SD 89) in 2007 (dry year). Shallow groundwater flux rates associated with ET averaged 681 mm (SD 79) in 2006 and 705 mm (SD 81) in 2007.

Annual climatic variability (precipitation in particular) strongly affected the causal interactions between soil water availability and plant water use. A strong positive feedback was observed in a wet year, whereas a weaker interaction was observed in a dry year, along with some indication of water limitation.

Underlying geology substantially affected plant-hydrology interactions in two important ways. Sandy substrates permitted considerable water loss, systematically lowering the water table and reducing soil moisture. In swales that recharged the water table, water availability had a stronger causal effect on plant water use.

Effects of vegetation may be equally important, especially when considering ecosystem response to climate change. Although soil moisture had a strong negative effect on ET, vegetation (tree species in particular) reduced soil moisture in a way that facilitated ET, especially under wet climatic conditions.

CHAPTER 1

Introduction

1.1 Overview

Vegetation and the water table interact strongly in wetland systems. Vegetation often appears to be organized into distinct communities related to site hydrology, particularly hydroperiod and water level (Harris and Marshall 1963, Wilcox and Simonin 1987, Kantrud et al. 1989, Noest 1994, Poiani et al. 1996, Mitsch and Gosselink 2000, Henszey et al. 2004, Leyer 2005, van Geest et al. 2005, Dwire et al. 2006). Plant transpiration also influence local groundwater hydrology; daily water-table fluctuations driven by evapotranspiration (ET) move water from ground to atmosphere, creating a head differential that draws shallow groundwater toward the source of loss (e.g., Meyboom 1966, Laczniak et al. 1991, Gerla 1992, Doss 1993, Reiner 2002, Loheide et al. 2005). Although effects of vegetation on water levels and the reverse are routinely observed, we do not have a comprehensive theory about the nature of the broader bidirectional system of interactions and the implied feedback that drives wetland development and maintenance in the landscape. Compounding this complexity, the underlying geology, physiography, and climate (precipitation in particular) of a specific wetland affect the system of interactions as well. Because these interactions influence trajectories of vegetation change, observed plant-community response to impending climate change likely will depend on the nature of feedbacks between plant water use and water availability. A better understanding of these ecohydrological interactions will be important for understanding potential effects of climate change on wetlands, as well as their long-term management and conservation.

This study investigated dynamics controlling plant water use and availability in a ridge-swale wetland system on Michigan's Lake Huron shoreline. At this site, coastal processes in an embayment with high sediment supply have led to the preservation of a

strand plain comprised of approximately 90 former beach ridges and their intervening swales, many of which support wetlands (Thompson, personal communication, May 30, 2005). My objectives were: 1) develop a methodology for estimating ET and shallow groundwater flow in rain-prone, dynamic wetlands, 2) explore how variation in swale hydrology arises through interactions between plants and site hydrogeology, and 3) examine how the complex hydrology of the system is related to the structure and function of its vegetative community.

1.2 Background

Ecohydrological interactions have been of interest to wetland ecologists for some time (e.g., White 1932, Troxell 1936, Meyboom, 1966). Emerging critical issues concerning climate change and water-resource management have led to a resurgence in the pursuit to understand how plants and hydrology interact to determine site water balance and community structure. Ecohydrology, as defined by Rodriguez-Iturbe (2000), is "the science which seeks to describe the hydrologic mechanisms that underlie ecological patterns and processes." Often used interchangeably, hydroecology, then, is the study of interactions between bodies of water and their ecological components (Hancock et al. 2009). This dissertation seeks to strike a balance between these subtle differences in definition to describe the mutual interactions between vegetation and hydrology in a vegetationally and structurally complex wetland system in the Great Lakes.

Research in coastal wetland areas of the eastern United States identified linkages between subsurface flow, plant transpiration, and water levels in salt marshes (Dacey and Howes 1984, Ursino et al. 2004, Marani et al. 2006). Due, in part, to the scarcity of water in semiarid regions of the world, increasing interest is arising to examine the coupled relationship between soil water, groundwater, and plant community composition (Breshears and Barnes 1999, Huxman et al. 2005, Seyfried et al. 2005, Caylor et al. 2006). Less emphasis has been placed on these interactions in humid regions (Rodriguez-Iturbe et al. 2007), and the mechanisms and spatiotemporal aspects behind these dynamics are still poorly understood in any ecosystem. Blöschl (2001), for example, stated that we need to better our understanding of spatiotemporal variation in hydrologic

systems. Rodriguez-Iturbe (2000) named ecohydrologic dynamics as an exciting research frontier. Kirchner (2006) also specified a need to recognize spatiotemporal variation of hydrologic processes explicitly in data collection and field experiments.

Because wetlands are often surface expressions of the water table, they are locations where surface water and groundwater interact and thus tend toward hydrologic complexity (Winter et al. 1998). Tóth (1963) developed a conceptual model for flow distribution in homogeneous substrates with undulating surface expression similar to that observed in ridge-swale systems. He identified three potential groundwater flow paths resulting from this topography-driven flow: local, intermediate, and deep. Local flow cells form due to the presence of individual ridges, and deep flow cells are a result of large-scale topographic change. In a seminal paper on groundwater-surface water interactions, Winter (1976) performed a numerical simulation analysis of the interactions between lakes and groundwater-flow systems that Winter (1989) and Winter and LaBaugh (2003), among others, applied to flow-through wetlands systems.

Where changes in surface topology are great and hydraulic conductivity values are low, flow-system dynamics can be ascertained by analysis of changes in hydraulic head as determined by piezometers and water-table wells (Tóth 1963, Freeze and Witherspoon 1979, Winter and Rosenberry 1995). In places underlain by sands with high hydraulic conductivity and low topographic relief, however, changes in water levels often do not occur even though flow cells exist (Winter, personal communication, October 24, 2005; Baedke, personal communication, July 2, 2006). In such cases, hydrochemical analysis can elucidate groundwater flow systems (Kehew et al. 1998, Marimuthu et al. 2005). In a review of the linkages between groundwater and coastal wetlands, Crowe and Shikaze (2004) identified a general lack of field studies of groundwater-wetland interactions in coastal areas of the Great Lakes. My study seeks to identify and define the mechanisms governing such groundwater-wetland interactions.

Hydrology and climate influence biological communities in important ways. Positive feedbacks between plants and water (a limiting resource) can lead to catastrophic shifts between states, such as a transition from a completely vegetated area to a mosaic of shrub communities dotting the landscape (Rietkerk et al. 2004, Ridolfi et al. 2006). In a model developed by Breshears and Barnes (1999) for semiarid landscapes, heterogeneity

in soil moisture constrains the relative proportions of trees, shrubs, and herbaceous vegetation, which in turn have an effect on patterns of soil moisture. Euliss et al. (2004) presented the concept of the wetland continuum, in which the interplay between hydrology and climate determine the biological community present in any given wetland. In the wetland continuum concept, wetlands are plotted in two-dimensional space according to their location on a drought-deluge (climate) axis and a recharge-discharge (hydrology) axis. By doing so, they hypothesized that predictions of the wetland's biological expression can be made at any point in time. While acknowledging that biological interactions can help determine the wetland community, they suggested in their model that the hydrological and climatologic factors constrain those interactions. Understanding feedbacks between these components may be important for understanding the overall ecohydrology of the system.

1.3 Contents

In this dissertation, I develop a conceptual model that describes the interactions of plants and hydrology in groundwater-fed wetland systems in which the only other major source of water is precipitation. The study site is a ridge-swale wetland system on Lake Huron consisting of an extensive chronosequence of former beach ridges and intervening swales that support a variety of wetland vegetation types.

In Chapter 2, I develop modifications to a method for determining sub-daily evapotranspiration and groundwater flow from diurnal fluctuations in the water table. The modifications were necessary to adapt a method developed for riparian zones in semiarid regions to the highly dynamic wetland site in this study, which lies in a rain-prone region of the Great Lakes.

My third chapter examines transient water-table dynamics resulting from interactions between groundwater hydrology and evapotranspiration using water-balance analysis. I explore how variation in swale hydrology arises through interactions between plants and site hydrology and discover interesting changes in hydrology over time based on physiographic context. I surmise how climate change will bring about wetland change given the water balance.

Chapter 4 investigates the ecohydrological dynamics among wetland vegetation, hydrology, and physiography. I examine feedbacks between plant water use, indexed by ET, and water availability, indexed by soil moisture. Using structural equation modeling to implement the conceptual model, as well as ordination techniques to describe variation in plant community structure, I am able to draw a more complete picture of the interconnectedness of plants and hydrology in wetlands. Fortuitously, the study period spanned both a wet year and a dry year, allowing discussion results in the context of pending global climate change.

I conclude by synthesizing the results to describe the system of interactions between plants, hydrogeology, physiography, and climate and discuss issues of scale relevant to all ecohydrologic studies. Finally, I suggest potential changes to coastal wetland hydrology and plant communities that may be expected in light of my findings.

REFERENCES CITED

Blöschl, G. 2001. Scaling in hydrology. Hydrological Processes 15:709–711.

Breshears, D. D. and F. J. Barnes. 1999. Interrelationships between plant functional types and soil moisture heterogeneity for semiarid landscapes within the grassland/forest continuum: a unified conceptual model. Landscape Ecology 14:465–478.

Caylor, K. K., P. D'Odorico, and I. Rodriguez-Iturbe. 2006. On the ecohydrology of structurally heterogeneous semiarid landscapes. Water Resources Research 24:W07424.

Crowe, A. S. and S. G. Shikaze. 2004. Linkages between groundwater and coastal wetlands of the Laurentian Great Lakes. Aquatic Ecosystem Health & Management 7:199–213.

Dacey, J. W. H. and B. L. Howes. 1984. Water uptake by roots controls water table movement and sediment oxidation in short *Spartina* marsh. Science 224:487–489.

Doss, P. K. 1993. The nature of a dynamic water table in a system of non-tidal, freshwater coastal wetlands. Journal of Hydrology 141:107–126.

Dwire, K. A., J. B. Dauffman, and J. E. Baham. 2006. Plant species distribution in relation to water-table depth and soil redox potential in montane riparian meadows. Wetlands 26:131–146.

Euliss, N. H., J. W. LaBaugh, L. H. Fredrickson, D. M. Mushet, M. K. Laubhan, G. A. Swanson, T. C. Winter, D. O. Rosenberry, and R. D. Nelson. 2004. The wetland continuum: a conceptual framework for interpreting biological studies. Wetlands 24:448–458.

Freeze, R. A. and P. A. Witherspoon. 1979. Theoretical analysis of regional groundwater flow: 2. Effect of water table configuration and subsurface permeability variation. Water Resources Research 3:623–634.

Gerla, P. J. 1992. The relationship of water-table changes to the capillary fringe, evapotranspiration, and precipitation in intermittent wetlands. Wetlands 12:91–98.

Hancock, P. J., R. J. Hunt, and A. J. Boulton. 2009. Preface: hydrogeoecology, the interdisciplinary study of groundwater dependent ecosystems. Hydrogeology Journal 17: 1–3.

Harris, S. W. and W. H. Marshall. 1963. Ecology of water-level manipulations on a northern marsh. Ecology 44:331–343.

Henszey, R. J., K. Pfeiffer, and J. R. Keough. 2004. Linking surface- and ground-water levels to riparian grassland species along the Platte River in central Nebraska, USA. Wetlands 24:665–687.

Huxman, T. E. , B. P. Wilcox, D. D. Breshears, R. L. Scott, K. A. Snyder, E. E. Small, K. Hultine, W. T. Pockman, and R. B. Jackson. 2005. Ecohydrological implications of woody plant encroachment. Ecology 86:308–319.

Kantrud, H. A., J. B. Millar, and A. G. van der Valk. 1989. Vegetation of wetlands of the Prairie Pothole Region, p. 132–187. *In* A. van der Valk (ed.) Northern Prairie Wetlands. Iowa State University Press, Ames, IA, USA.

Kehew, A. E., R. N. Passer, R. V. Krishnamurthy, C. K. Lovett, M. A. Betts, and B. A. Dayharsh. 1998. Hydrogeochemical interaction between a wetland and an unconfined glacial drift aquifer, southwestern Michigan. Ground Water 36:849–856.

Kirchner, J. W. 2006. Getting the right answers for the right reasons: linking measurements, analyses, and models to advance the science of hydrology. Water Resources Research 42:W03S04.

Laczniak, R. J., G. A. DeMeo, S. R. Reiner, J. L. Smith, and W. E. Nylund. 1999. Estimates of groundwater discharge as determined from measurements of evapotranspiration, Ash Meadows area, Nye County, Nevada. U.S. Geological Survey Water-Resources Investigations Report 99–4079.

Leyer, I. 2005. Predicting plant species' responses to river regulation: the role of water level fluctuations. Journal of Applied Ecology 42:239–250.

Loheide, S. P., J. J. Butler, and S. M. Gorelick. 2005. Estimation of groundwater consumption by phreatophytes using diurnal water table fluctuations: a saturated-unsaturated flow assessment. Water Resources Research 41:W07030.

Marani, M., S. Silvestri, E. Belluco, N. Ursino, A. Comerlati, O. Tosatto, and M. Putti. 2006. Spatial organization and ecohydrological interactions in oxygen-limited vegetation ecosystems. Water Resources Research 42:W06D06.

Marimuthu, S., D. A. Reynolds, and Le Gal La Salle, C. 2005. A field study of hydraulic, geochemical and stable isotope relationships in a coastal wetlands system. Journal of Hydrology 315:93–116.

McCune, B. and M. J. Mefford. 1999. PC-ORD. Multivariate Analysis of Ecological Data. Version 4.36. MjM Software, Gleneden Beach, OR, USA.

Meyboom, P. 1966. Unsteady groundwater flow near a willow ring in hummocky moraine. Journal of Hydrology 4:38–62.

Mitsch, W. J. and J. G. Gosselink. 2000. Wetlands. Third edition. John Wiley & Sons, Inc., New York, NY, USA.

Noest, V. 1994. A hydrology-vegetation interaction model for predicting the occurrence of plant species in dune slacks. Journal of Environmental Management 40:119–128.

Poiani, K. A., W. C. Johnson, G. A. Swanson, and T. C. Winter. 1996. Climate change and northern prairie wetlands: simulations of long-term dynamics. Limnology and Oceanography 41:871–881.

Reiner, S. R., R. J. Laczniak, G. A. DeMeo, J. L. Smith, P. E. Elliott, W. E. Nylund, and C. J. Fridrich. 2002. Ground-water discharge determined from measurements of evapotranspiration, other available hydrologic components, and shallow water-level changes, Oasis Valley, Nye County, Nevada. U.S. Geological Survey Water-Resources Investigation Report 01-4239.

Ridolfi, L., P. D'Odoric, and F. Laio. 2006. Effect of vegetation-water table feedbacks on the stability and resilience of plant ecosystems. Water Resources Research 42:W01201.

Rietkerk, M., S. C. Dekker, P. C. de Ruiter, and J. van de Koppel. 2004. Self-organized patchiness and catastrophic shifts in ecosystems. Science 305:1926–1929.

Rodriguez-Iturbe, I. 2000. Ecohydrology: a hydrologic perspective of climate-soil-vegetation dynamics. Water Resources Research 36:3–9.

Rodriguez-Iturbe, I., P. D'Odorico, F. Laio, L. Ridolfi, and S. Tamea. 2007. Challenges in humid land ecohydrology: interactions of water table and unsaturated zone with climate, soil, and vegetation, Water Resources Research 43:W09301.

Seyfried, M. S., S. Schwinning, M. A. Walvoord, W. T. Pockman, B. D. Newman, R. B. Jackson, and F. M. Phillips. 2005. Ecohydrological control of deep drainage in arid and semiarid regions. Ecology 86:277-287.

Tóth, J. 1963. A theoretical analysis of groundwater flow in small drainage basins. Journal of Geophysical Research 68:4795–4812.

Troxell, H. C. 1936. The diurnal fluctuation in the ground-water and flow of the Santa Ana River and its meaning. EOS Transactions, American Geophysical Union 17:496–505.

Ursino, N., S. Silvestri, and M. Marani. 2004. Subsurface flow and vegetation patterns in tidal environments. Water Resources Research 40:W05115.

van Geest, G. J., H. Coops, R. M. M. Roijackers, A. D. Buijse, and M. Scheffer. 2005. Succession of aquatic vegetation driven by reduced water-level fluctuations in floodplain lakes. Journal of Applied Ecology 42:251–260.

White, W. N. 1932. A method of estimating ground-water supplies based on discharge by plants and evaporation from soil. U.S. Geological Survey Water-Supply Paper 659-A, Washington, DC, USA.

Wilcox, D. A. and H. A. Simonin. 1987. A chronosequence of aquatic macrophyte communities in dune ponds. Aquatic Botany 28:227.

Winter, T. C. 1976. Numerical simulation analysis of the interaction of lakes and ground water. U.S. Geological Survey Professional Paper 1001.

Winter, T. C. 1989. Hydrologic studies of wetlands in the northern prairie, p. 16–54. *In* A. G. van der Valk (ed.) Northern prairie wetlands. Iowa State University Press, Ames, IA, USA.

Winter, T. C., J. W. Harvey, O. L. Franke, and W. M. Alley. 1998. Ground water and surface water – a single resource. U.S. Geological Survey Circular 1139.

Winter, T. C. and J. W. LaBaugh. 2003. Hydrologic considerations in defining isolated wetlands. Wetlands 23:532–540.

Winter, T. C. and D. O. Rosenberry. 1995. The interaction of groundwater with prairie pothole wetlands in the Cottonwood Lake area, east-central North Dakota, 1979 to 1990. Wetlands 15:193–211.

CHAPTER 2

Evapotranspiration and Groundwater Determined from Water-Table Fluctuations in a Dynamic Great Lakes Coastal Wetland System

2.1 Introduction

Diurnal fluctuations in wetland water levels are the result of direct uptake of groundwater by plants rather than soil-water use (Loheide et al. 2009) and long have been used to estimate groundwater and evapotranspiration (ET) rates empirically in riparian areas on a daily scale (e.g., White 1932, Troxell 1936, Meyboom 1967, Laczniak et al. 1999). More recently, researchers have begun examining high-resolution wetland hydrographs on a sub-daily basis to understand nutrient cycling (Schilling 2007, Schilling and Kiniry 2007), groundwater consumption (Loheide 2008), and ET effects on river baseflow (Gribovszki 2008).

The application of these methods is relatively straightforward in riparian areas of semi-arid and arid regions in which water levels are always below ground and precipitation events are infrequent. Under these conditions, the regularity with which the water table responds to transpirative demand facilitates ET calculation. In wetter regions, these methods are complicated by recurring precipitation, above-ground water storage (flooding), and highly variable climatic conditions.

In this chapter, I develop modifications to a method for calculating ET and shallow groundwater recovery developed by Loheide (2008) that extend its utility to rain-prone coastal, non-riparian wetlands. Applying the method to sub-daily hydrographs from a structurally and vegetatively complex ridge-swale wetland system in the Great Lakes region, I am able to estimate ET and shallow groundwater fluxes over two annual growing seasons for 15 wetland units in a ridge-swale wetland complex.

2.2 Method and Modifications

Diurnal water-table fluctuations associated with vegetation were reported in early work by White (1932), Troxell (1936), and Meyboom (1967). Many researchers since have used this method to calculate both ET and groundwater flow rates (e.g., Gerla 1992, Loheide et al. 2005, Butler et al. 2007, Hill and Neary 2007, Lautz 2008). Plants draw down water levels during daylight hours, and groundwater recharges the water table at night to replenish the water extracted by ET. The classic work by White (1932) empirically determined groundwater flow and ET rates from diurnal water-table fluctuations in the absence of precipitation using the following equation:

$$ET_G = S_y(G_{rec} + \Delta S \cdot t^{-1}), \quad (1)$$

where ET_G is evapotranspirative groundwater consumption [length per unit time, $l\ t^{-1}$], S_y is the "readily available specific yield" [dimensionless, dim.], which is the water released over the period of a diurnal cycle (Meyboom 1967, Loheide et al. 2005), G_{rec} is the net shallow groundwater inflow rate [$l\ t^{-1}$], ΔS is change in storage [l], and t is equal to the length of one day [t]. ET is considered negligible from 0000 h to 0400 h (pre-dawn), making groundwater inflow solely responsible for changes in water level for that period. Multiplying readily available specific yield, S_y [dim.], by the slope, m [$l\ t^{-1}$], of the line tangent to the pre-dawn portion of the water-level curve gives the rate of groundwater inflow per unit area (Figure 2.1). Summing this rate over a 24-hour period produces a daily rate of groundwater supply, $G_{rec} = 24m$ [$l\ t^{-1}$], which typically is adjusted for the net change in water-table elevation over the 24-hour period, ΔS [l]. By convention, a positive ΔS indicates a decrease in water-table elevation.

The White (1932) method assumes constant flow of groundwater over the 24-hour period. The recovery rate, however, is not constant; it changes over the course of the day with evapotranspirative demand (Troxell 1936). Gribovski et al. (2008) and Loheide (2008) used modifications of the empirical White (1932) method to resolve this problem by estimating ET as a function of time. In these methods,

$$G_{rec} = S_y(dh/dt), \quad (2)$$

where G_{rec} [l t^{-1}] is the net inflow rate and dh/dt represents the change in water-table elevation, h [l], over time, t [t]. The Loheide (2008) method assumes that a recovery source an arbitrary distance away supplies water to the unconfined aquifer at the location of the observation well. Furthermore, the rate of change in head at the recovery source is assumed equal to the overall water-table rate of change at the well. If this assumption is accurate, the net inflow rate, G_{rec} [l t^{-1}], can be estimated by detrending the water-level curve and then regressing it against the time rate of change in detrended water-table elevation for the pre-dawn hours of two consecutive nights. The regression is extended to predict time rate of change in detrended water-table elevation over the day, which is retrended and multiplied by specific yield to obtain the inflow rate. Once inflow rate is known, evapotranspiration, ET_G [l t^{-1}], is calculated as:

$$ET_G = G_{rec} - S_y(dh/dt). \quad (3)$$

2.2.1 Correcting for Above-Ground Storage

The White (1932), Gribovszki et al. (2008), and Loheide (2008) methods originally were developed to estimate ET_G from below-ground water-table fluctuations in riparian areas of semi-arid regions. When the water table elevation exceeds the topographic surface (i.e., the site is flooded), however, water-table head elevation shows a reduced response per unit change in storage even though the volumetric change is the same. This must occur because the above-ground void volume must equal the storage volume. For wider application to wetland scenarios when water-table elevations sometimes fluctuate above ground, a modification is required that involves adjusting the specific yield (S_y). Whereas the readily available specific yield ($0 < S_y < 1$) is appropriate when working with below-ground-surface (BGS) water levels (Loheide et al. 2005), a specific yield of 1.0 usually is used for the portion of water that is above ground surface (AGS) (e.g., Mitsch and Gosselink 2000, Hill and Neary 2007). To account for this, a weighted specific yield (S_{yc}) value can be used that is similar to the composite specific yield of Hill and Neary (2007) and accounts for the respective portions of the water column that are AGS and BGS. Whereas Hill and Neary (2007) accounted for actual wetland geometry, using a rectangular wetland geometry may be appropriate if ET and

groundwater fluxes are calculated as depths (rather than volumes) across a 1-m^2 cross-section of wetland and the slope of the bottom is minimal in relation to the side slopes (Figure 2.2A). Adopting the specific-yield notation of Hill and Neary (2007), a composite specific yield (S_{yc}) then can be calculated by Equation (4).

$$S_{yc} = S_{ya}\left(\frac{D_w}{D_w + D_s}\right) + S_{ys}\left(\frac{D_s}{D_w + D_s}\right) \quad (4)$$

In Equation (4), S_{ya} is the specific yield of air (standing water) of 1.0, S_{ys} is the specific yield of the soil and sediment derived from slug tests or the ratio of precipitation to water-table rise (described below), D_w is the water depth, D_s is the depth from soil surface to the impermeable predepositional surface, and $D_w + D_s$ represents the total depth over which the specific yield is estimated (Figure 2.2).

By convention, the naming scheme "ET_G" usually refers to direct groundwater withdrawal by phreatophytes. When considering AGS water levels, some of the ET is also due to free-water-surface evaporation. In this chapter, I maintain the ET_G notation to indicate calculation from water-level fluctuations even though I recognize implicitly that all ET is not due to direct groundwater withdrawal by plants when water levels are AGS.

2.2.2 Accounting for Daily and Seasonal Variability

As a part of his methodology, Loheide (2008) recommended defining the pre-dawn, groundwater-recovery period as 0000 h to 0600 h, when evapotranspiration is assumed to be zero. For the method to work for a given day, the slopes for corresponding time steps on the night before and the night after must overlap. When applying this method to more variable wetlands, it may be necessary to capture the portion of the groundwater inflow curve from 0000 h to the earlier of 0600 h or the time of peak water-table elevation for that day (Figure 2.1) for the incremental slopes for each time step to overlap. In this case, the pre-dawn hours for each day can be defined individually. Doing so accounts for seasonal changes in daylight as well.

2.2.3 Precipitation Events and Other Decoupling from the Recovery Source

The assumption that the water table and head at the recovery source fluctuate at similar rates also must be tested by regressing change in detrended water table over time against detrended water table in the pre-dawn hours of two sequential days, which is inherent to the general method. Applicable only for days when the regression is significant, the method fails when fluctuations are erratic or during rain events that cause a rapid water-table rise at the surface but a muted and lagged rise at the recovery source. Another modification is needed to estimate ET_G for days when the method fails.

For such days, hourly ET_G can be predicted using an appropriate linear or nonlinear regression relating ET_G to potential evapotranspiration (PET). The resulting time series, a composite of estimated ET_G from water-level fluctuations and ET values predicted from PET, is referred to henceforth as ET_C. Many forms of the Penman-Monteith equation have been used by researchers to calculate PET. I compared the original Penman-Monteith equation parameterized for this specific wetland scenario (PET_{PM}) (Souch et al. 1996, 1998) to the Penman equation (PET_P) (Penman 1948, Shuttleworth 1993), the FAO56 Penman-Monteith equation (PET_{FAO}) (Allen et al. 1998), the ASCE Penman-Monteith equation (PET_{ASCE}) (Allen et al. 2005), and the Paw and Gao (1988) quadratic solution to the Penman-Monteith equation (PET_{QUAD}). I also modified the PET_{FAO} and PET_{ASCE} equations to account for leaf area index (LAI) ($PET_{FAO\text{-}LAI}$, $PET_{ASCE\text{-}LAI}$), as described below, and included these in the comparison. For brevity, the PET_{PM}, PET_{ASCE}, PET_{QUAD} equations are described below along with a suggested method of accounting for LAI. The reader is referred to Shuttleworth (1993) for calculation of PET_P and to Allen et al. (1998) for PET_{FAO} calculation.

The hourly Penman-Monteith equation (Monteith 1965, Shuttleworth 1993, Souch et al. 1996, 1998, Allen et al. 2006) is as follows:

$$PET_{PM} = \frac{1000}{\lambda \rho_w}\left[\frac{\Delta(R_n - H_s) + \rho_a c_p (e_s - e_a)/r_a}{\Delta + \gamma(1 + r_s/r_a)}\right], \tag{5}$$

where λ [MJ kg^{-1}] is the latent heat of vaporization, ρ_w is the density of liquid water [kg m^{-3}], Δ [kPa $ºC^{-1}$] is the slope of the saturation vapor pressure curve at air temperature T_a [ºC], γ [kPa $ºC^{-1}$] is the psychometric constant, R_n [MJ m^{-2} h^{-1}] is the net radiation, H_s is

the soil heat flux [MJ m^{-2} h^{-1}], (e_s - e_a) is the vapor pressure deficit of the air [kPa], ρ_a is the density of air [kg m^{-3}], c_p is the specific heat of air at constant pressure [MJ kg^{-1} $^oC^{-1}$], r_a is the aerodynamic resistance [h m^{-1}], and r_s is the surface resistance [h m^{-1}]. The value 1000 converts PET units from m h^{-1} to mm h^{-1}.

The standardized ASCE Penman-Monteith equation for hourly reference ET (PET_{ASCE}) (Allen et al. 2005) is

$$PET_{ASCE} = \frac{0.408\Delta(R_n - H_s) + \gamma \frac{C_n}{T_a + 273} u(e_s - e_a)}{\Delta + \gamma(1 + C_d u)}, \quad (6)$$

where u is hourly wind speed at a height of 2 m [m s^{-1}], and coefficients C_n and C_d are 37 [K mm s^3 mg^{-1} h^{-1}] and 0.24 [s m^{-1}] or 0.96 [s m^{-1}] for daytime or nighttime periods, respectively.

Some researchers (e.g., Shi et al. 2008, Langensiepen et al. 2009) recommend accounting for variation in leaf area index (LAI) over time when calculating PET, as the amount of vegetated cover affects the rate of evapotranspirative demand by plants. A modification similar to that presented by Pereira et al. (2006) can be used that accounts for canopy and herbaceous ground cover as follows:

$$PET_{ASCE-LAI} = \left(\frac{LAI_c + LAI_g}{2.88} \right) ET_o, \quad (7)$$

where LAI_c [m^2 leaf m^{-2} ground] is the canopy leaf area index, LAI_g [m^2 leaf m^{-2} ground] is the herbaceous ground-cover leaf area, and 2.88 m^2 leaf m^{-2} ground is the hypothetical grass leaf area index assumed by the FAO56 and ASCE methods (Allen et al 1998, Allen et al. 2005).

One potential inaccuracy in the Penman-Monteith-type equations is in the linear approximation of the slope of the saturation vapor pressure curve, Δ. This parameter is dependent on both surface and air temperature but is approximated at air temperature in the Penman-Monteith-type equations. Paw and Gao (1988) proposed instead to use a second-order Taylor approximation of Δ, contending that less error is generated. A recent

study (Widmoser 2009) recommended the revival of Paw and Gao's (1988) work considering that technological developments have eased the calculations involved substantially.

The PET method chosen to predict ET_G on days when it cannot be calculated using the Loheide (2008) method should maximize the goodness of fit between PET and ET_G values. The regression chosen can be linear or nonlinear, depending on the behavior of the data and should, for example, maximize the coefficient of determination (R^2) and minimize the root mean squared error (RMSE) calculated as:

$$RMSE = \left[\frac{1}{N} \sum_{i=1}^{N} (o_i - e_i)^2 \right]^{1/2}, \quad (8)$$

where N is the number of observations, o_i are observed values of ET_G, and e_i are estimates of ET_G predicted from PET.

Daily groundwater values (G_{rec}) can be estimated for days when the Loheide (2008) method failed by linear regression of daily G_{rec} and daily ET_G. This relationship then can be used to predict a daily "composite groundwater" (G_C) from the composite ET_C in the absence of ET_G values (i.e., gaps in the ET_G time series when the Loheide method failed). The validity of this relationship is based on the assumption that ET draws groundwater to the swale, thereby relating ET and groundwater fluxes on a daily scale.

In summary, the Loheide (2008) method can be useful for calculating sub-daily ET and daily groundwater in dynamic, non-riparian wetlands in rain-prone, temperate climates provided that several modifications are applied. First, a weighted specific yield correction is needed to account for above-ground and below-ground water levels. Second, regression predictions of ET_G from PET are calculated for days when the method fails due to precipitation events. Finally, if a flexible window is allowed for defining the pre-dawn hours, the method is more likely to succeed for any given day. Below, to illustrate these modifications, I apply this method and modifications in a non-riparian wetland system in the Great Lakes region.

2.3 Example Application

2.3.1 Site Description

An undisturbed ridge-and-swale wetland is located along the western shore of Lake Huron (25 km south of Alpena, MI) within the boundaries of Negwegon State Park (Figure 2.3). Over the last 3500 years at this site, coastal processes in an embayment with high sediment supply have led to the preservation of approximately 90 beach ridges and intervening swales (Thompson, personal communication, May 30, 2005). Approximately half of the swales support wetland plant communities. Beach ridges bounding the swales represent local topographic highs that may drive shallow and intermediate groundwater-flow cells similar to those described by Tóth (1963), connecting the swales via groundwater flow.

Near-surface sediments are homogeneous fine- to medium-grained sands with some gravel. At approximately 3 m depth, a semi-continuous yet extensive diamicton (very poorly sorted sediment of low permeability) of glacial origin was detected in sediment cores and by ground-penetrating radar (GPR) (Thompson, unpublished data; Posner et al. 2005). Breaks in this layer may permit intermediate groundwater flow to the overlying wetlands. Water-chemistry data, however, suggest that this system has little or no deep, regional aquifer feeding it, as noted at similar sites (Baedke, personal communication, July 2, 2006; Wilcox et al. 2005).

2.3.2 Monitoring Wells and Sensors

Fifteen swales were selected for monitoring using a stratified random sample. Instrumentation in each swale included a relative-humidity and air-temperature sensor (Onset, HOBO H8 Pro Series, H08-032-08 RH/Temp) and a substrate temperature sensor (Onset, HOBO H8 Family, H08-001-02) located at the middle of a transect that crossed the swale. A pressure transducer (Solinst LT Levelogger Model 3001, F15/M5, 0.02-cm resolution) in a well slotted across the water table (Aquatic Eco-Systems, Inc.; 3.18-cm diameter, 1.52-m length, 0.0254-cm slotted PVC) was installed on the lakeward side of the swale, several meters from the base of the ridge. Wells were hand-driven into the ground such that no borehole was present and no backfill was needed. Wells were conditioned by pumping. Relative-humidity and air-temperature sensors with rain shields

were placed 2 m above the May 2006 water level. The substrate temperature sensors were submersed just below the water surface. When the water level fell below the soil surface, the sensor was buried in the top 6 cm of soil. A barometric pressure transducer (Solinst Barologger Model 3001, F5/M1.5) was installed in one swale. Data were recorded at five-minute intervals from May 20 to October 27 in 2006 and April 14 to October 12 in 2007.

Weather data—precipitation (0.25-mm accuracy) [mm], incoming solar radiation [MJ m^{-2} d^{-1}], air temperature [°C], dew point [°C], and wind speed [m s^{-1}]—were recorded every 15 minutes during the same period with a weather station (Davis Instruments Cabled Vantage Pro2 Plus with Standard Radiation Shield 6162C) located centrally at the site (Figure 2.3) and installed 2 m above May 2006 water levels.

2.3.3 Sediments

The soils at Negwegon State Park are of the Tawas-Au Gres complex (USDA 2008). Sediments underlying these hydric soils comprise a strand plain of sand with very little silt or clay fraction (Table 2.1). The strand plain sits atop a semi-continuous diamicton that represents a confining layer in the stratigraphy (Thompson, personal communication, July 2, 2006). Sand samples were collected from the C horizon of the 15 instrumented wetlands. Samples were refrigerated and sent moist to the Michigan State University Soil and Plant Nutrient Lab (East Lansing, MI), where texture analysis was performed.

Specific yield (S_y) estimates were determined in two ways: 1) as the ratio of infiltrated precipitation to recorded water-table rise (Gerla 1992) and 2) from slug tests (Bouwer 1989). Several researchers have supported the validity of the first method in wetlands (Gerla 1992, Rosenberry and Winter 1997, Loheide et al. 2005). I approximated S_y for each swale in the study using 2006 and 2007 precipitation events totalling more than 5 mm. Due to the saturated soils, shallow water table, and sandy soils, I assumed that infiltrated precipitation equalled recorded precipitation, although I recognize implicitly that some precipitation that falls does not reach the water table. Using rain events greater than 5 mm, however, reduced the error associated with infiltration and soil storage. Specific-yield values calculated from multiple rain events when the water table

was below ground were arithmetically averaged to obtain a single value for each swale (Table 2.1).

As an independent measure of S_y, I performed slug tests on October 11-12, 2007 to measure hydraulic properties of underlying sediments (Bouwer 1989). In swales 8, 14, 26, 55, and 78 (Figure 2.3), a capped length of PVC pipe was submersed below the water table in the well, and the water table was allowed to equilibrate before the PVC pipe was removed. Water-table recovery was recorded at 5-second intervals using a pressure transducer (Solinst LT Levelogger Model 3001, F15/M5). Five slug tests were performed at each site, but only one to three resulted in a water-table recovery that could be used to calculate hydraulic conductivity by the Bouwer and Rice method (Bouwer 1989); arithmetic averaging was used to obtain a single hydraulic conductivity for each swale. The top of the diamicton layer, as determined by sediment cores (Thompson, unpublished data), was considered the base of the unconfined aquifer. For swales where slug tests were not performed, water-table recovery of the nearest tested swale was used to calculate hydraulic conductivity, with the assumption that the underlying sands were fairly homogeneous. To estimate specific yield, I matched calculated hydraulic conductivity to representative values of specific yield (Johnson 1967) presented in Loheide et al. (2005) and interpolated linearly between values. As the slug tests were performed when the water table was near the lowest point observed in the study, and greater depth to water table generates higher specific yield (Duke 1972, Nachabe 2002, Loheide et al. 2005), the values obtained from slug tests were considered the upper limit.

Hydraulic conductivity (K) at the site, as determined by slug-test analysis, ranged from 1.81 to 4.70 m d^{-1} (Table 2.1), which was on the order of magnitude for silty sands and fine sands (Fetterer 2001). Swales in the middle of the sequence had greater K values than the younger and older swales on either side. Specific yield (S_y) values by the slug-test method ranged from 0.212 to 0.283. These values were significantly higher than the ratio-derived S_y values and tended to overpredict groundwater flow (G_{rec}) and evapotranspiration (ET_G), which are directly proportional to specific yield by the methodology used in this study. Therefore, I used the ratio-derived values, ranging from 0.100 to 0.156, but discarded erroneous values that were greater than the slug-test-derived values.

Depth to predepositional surface that underlies the strand plain was determined individually for each swale from core logs collected and described by T. Thompson of the Indiana Geological Survey.

2.3.4 Water-Level Data Processing

To filter the data of sensor noise, water-level and barometric-pressure data were smoothed using locally weighted, second-order polynomial regression (LOESS) that assigned lower weight to outliers (span = 0.005) (Cleveland 1979, Cleveland et al. 1988). The LOESS smoothing produces very similar results to a windowed-sinc, low-pass filter (unpublished data) but can be easier to execute. Caution was taken to avoid over-smoothing the data because this can artificially inflate ET and groundwater values by increasing the time base of the daily fluctuations. Minor gaps in the data (< 0.5 h) occurred when pressure transducers were downloaded; missing values were estimated by spline interpolation prior to smoothing.

Effects of barometric pressure on water levels must be taken into account when water-level fluctuations are used for calculating groundwater flow and ET. The simplest procedure involves subtracting the barometric pressure from the absolute head pressure of an unconfined aquifer (i.e., water-table elevation), which is valid when water levels are above ground surface (AGS). A time-lagged response of the water table to barometric-pressure change, however, often is observed when water levels are below ground surface (BGS) (Rasmussen and Crawford 1997, Spane 1999, Rasmussen and Mote 2007, Toll and Rasmussen 2007). A function describing the response of water level to barometric pressure change, termed barometric efficiency, can be calculated and used to extract water-table elevations from pressure-transducer data.

I assumed that barometric efficiency was zero, meaning an instantaneous transmission of atmospheric pressure through the vadose zone (i.e., no lag), because the aquifer underlying this wetland system was very shallow (< 0.60 m). Furthermore, I expected no skin or borehole storage effects due to the small diameter of the well (3.18 cm), the high transmissivity and storativity of sand aquifers, and the fact that the wells were hand-driven and conditioned by pumping rather than completed by borehole. The water-level data recorded by the pressure transducers represented total head (H_t), which is

the sum of water-surface elevation head (W) and barometric pressure (B) (Rasmussen and Crawford 1997, Spane 2002). Barometric efficiency is the ratio of change in water-surface elevation (ΔW) to barometric pressure change (ΔB) (BE = -ΔW/ΔB), where ΔB by convention is negative for an increase in barometric pressure. The assumption of zero barometric efficiency was tested in two ways: a slope method (Ferris et al. 1962) and a graphical method (Gonthier 2007). Using the slope method, median BE was 0.03 (mean = 0.06 ±0.11 SD), as determined by 28 barometric pressure change events. Using the graphical method of Gonthier (2007), BE was 0. The results of these tests indicated that barometric efficiency was negligible, and barometric pressure was subtracted from the water-level pressure-transducer data without modification.

Although barometric efficiency was determined to be negligible, regression deconvolution (Rasmussen and Crawford 1997, Rasmussen and Mote 2007, Toll and Rasmussen 2007) was used to investigate barometric-pressure lag and earth-tide effects using MATLAB code provided by T. Rasmussen. Even though Earth-tide effects would not be predicted in an unconfined aquifer such as this, some periodicity corresponding to tide-like frequencies (e.g., Halford 2006, Leaver and Unsworth 2007, Rasmussen and Mote 2007) was observed in ET rates and Fourier analysis of water levels. The observed signal likely is due to direct effects of tides rather than earth tides exerting a force on the aquifer skeleton (Halford, personal communication, May 1, 2009) or could be an artefact of the data resulting from an interaction between barometric pressure and storm events (Rasmussen, personal communication, May 18, 2009). A lag of one to three hours, depending on the swale, was estimated from the step loading response function in the regression deconvolution. This lag, however, may be erroneous if the method is not applicable without accounting for the precipitation-barometric pressure interaction. Such an analysis is outside the scope of this study, as further evidence suggests that the lag is minimal (<1 h).

The onset of precipitation resulted in a nearly instantaneous rise in water table over the entire growing season and is evidence that a barometric-pressure lag is minimal within this unconfined aquifer (Rasmussen, personal communication, May 18, 2009). Furthermore, removing barometric pressure from total head without accounting for a

lagged response produced a well-behaved diurnal signal of evapotranspiration during the day and groundwater inflow at night, whereas a lagged response confounded the signal.

To convert pressure-transducer data to water depth and water-table elevation, I directly measured water depths monthly using a water-level meter (Solinst Model 101). Water depths were converted to water-table elevation using surveyed well elevations. After removing barometric pressure effects, rating curves were generated linking observed water depths and water-table elevations to corresponding compensated pressure-transducer data at the time of measurement.

2.3.5 PET Parameterization

Of the many potential ET (PET) options, I pursued comparison of the original Penman-Moneith equation (PET_{PM}) [Equation (5)], the ASCE equation (PET_{ASCE}) [Equation (6)] without accounting for LAI, and the Paw and Gao (1988) quadratic equation (PET_{QUAD}). The PET_{PM} and PET_{QUAD} equations were parameterized similarly and, therefore, showed parallel results.

Parameterization of the PET_{PM} [Equation (5)] and PET_{QUAD} (Paw and Gao 1988) equations followed recommended methods in the literature (e.g., Shuttleworth 1993, Allen et al. 1998), including the air and surface resistance values (r_a, r_s) given by Souch et al. (1998) for a similar ridge-swale wetland system. For wind speeds below detection, I assigned a value of half the detection limit of the anemometer (0.22 m s^{-1}). I used a daily mean short-wave solar radiation reflection coefficient (albedo, α) of 0.11, estimated from Shuttleworth (1993) for tall forest. I followed Shuttleworth's (1993) equation for saturation vapor pressure, e_s [kPa]. The actual vapor pressure, e_a [kPa], was calculated from the measured relative humidity, RH [%], and the saturated vapor pressure, e_s at air temperature T [ºC], following Allen et al. (1998). The variables λ, Δ, and γ were calculated using methods outlined in Shuttleworth (1993). R_n is the difference between incoming net shortwave radiation, R_{ns} [MJ m^{-2} h^{-1}], and outgoing net longwave radiation, R_{nl} [MJ m^{-2} h^{-1}]. After Allen et al. (1998), I used the following components to calculate R_{ns} and R_{nl}: measured incoming shortwave radiation, R_s [MJ m^{-2} h^{-1}]; their Equation (28) for R_a [MJ m^{-2} h^{-1}]; their Equation (37) for clear-sky solar radiation, R_{so} [MJ m^2 h^{-1}]; and their Equation (39) for R_{nl} [MJ m^2 h^{-1}]. I used the R_s/R_{so} ratio that was calculated two to

three hours prior to sunset to estimate the ratio for nighttime hours (Allen et al. 1998). Allen et al. (1998) equations (45) and (46) were used to determine G_s. I used a value of 0 s m^{-1} for r_s for standing water levels and 5 s m^{-1} for below-ground water levels, following Souch et al. (1998) for similar ridge-swale wetlands. I used a plant height of 0.12 m and the standard FAO method for aerodynamic resistance, r_a (Allen et al., 1998). PET_{QUAD} parameterization matched that of PET_{PM}.

I used the ASCE Penman-Monteith Equation (6) with an albedo of 0.23 and plant height of 0.12 m to calculate the standardized potential ET (ET_o) [mm h^{-1}]. Other parameters matched those used in PET_{PM} and PET_{QUAD} calculations described above.

To relate hourly ET_G to PET, I used nonlinear regression analysis, which minimized the RMSE better than linear regression. A power function was fit by least squares in MATLAB R2007a v.7.4 (Seber 2003, Mathworks 2007). Negative and zero values were removed prior to analysis. A theoretical power relationship may exist between actual and potential evapotranspiration. As temperature and radiation increase, PET continues to increase. Actual ET, however, may decrease at midday due to photoinhibition, heat stress, or water limitation, resulting in an asymptotic relationship between actual and potential ET. When this is the case, a nonlinear relationship may be more appropriate than a linear one.

2.3.6 Composite ET and Groundwater

Evapotranspiration (ET_G) and shallow groundwater recovery (G_{rec}) at 15-min intervals were calculated using the Loheide (2008) method. Modifications to this method were used to calculate the composite sub-daily ET (ET_C) and daily groundwater (G_C) time series as described above. Programming was done in MATLAB R2007a v.7.4 (Mathworks 2007). After comparing the results of the various PET options, the ASCE-PM equation without LAI (PET_{ASCE}) (6) was chosen for subsequent analyses in this example application due to its goodness of fit with ET_G and its utility and widespread application.

Lag between ET and groundwater was calculated as the time difference of peak flux rate within a single day for empirically determined ET_G and G_{rec} (i.e., not predicted from PET).

2.4 Results

2.4.1 Water Levels

Water extracted by evapotranspiration provided a head differential that drew groundwater into the swales, as evidenced by the time lag between ET and groundwater peaks (Figure 2.4). Although precipitation events (Figure 2.5A) offset evapotranspirative losses, water supply to the swales was not sufficient to offset ET demand, resulting in water-level decline over the summer (Figure 2.5B). The additive effect of groundwater and precipitation, however, helped to maintain water levels within the rooting zone, as evidenced by diurnal fluctuations in the water table even when at its lowest elevation. In 2006, large storm events periodically raised the water table. In 2007, standing water levels were maintained until mid-summer by multiple small rain events and colder temperatures; the long period without a major rain event led to a significant drawdown in July and August of 2007. Whereas September and October rain in 2006 resulted in water-level recovery to May-June water levels, no such recovery occurred in 2007 prior to the end of the study.

Stage responses of the water table to precipitation varied depending on whether the water table was above ground surface (AGS) or below ground surface (BGS). Precipitation events (Figure 2.5A) resulted in a rapid rise in BGS water levels but had a muted effect when standing water was present (Figure 2.5B). For example, the ratio of water-table rise to precipitation ($1/S_y$) during flooded conditions in Swale 28 was 3.8 compared to 8.1 when the water table was below ground.

Minor differences were observed in the power regressions of ET_G against PET_{PM}, PET_{ASCE}, and PET_{QUAD} depending on whether water levels were AGS or BGS (Table 2.2). Regressions were significant ($\alpha = 0.05$) and performed slightly better for AGS conditions. No significant difference was observed, however, between above- and below-ground R^2 or RMSE values in two-tailed t-tests (t-critical = 2.05, $p > 0.05$). The Loheide method, applied to both AGS and BGS water levels simultaneously, corresponded favorably with the PET_{PM}, PET_{ASCE}, and PET_{QUAD} methods (Table 2.2, Figure 2.6).

2.4.2 Evapotranspiration

ET_C tended to be higher earlier in the summer and tapered off toward the end of July and August (Figure 2.5D, Figure 2.7). Average daily rates over the 2006 growing season ranged from 5.5 mm d^{-1} (SD 1.6) in Swale 8 to 8.1 mm d^{-1} (SD 2.5) in Swale 73 (Figure 2.7). The 2007 growing season showed average daily rates ranging from 5.5 mm d^{-1} (SD 1.3) in Swale 26 to 7.8 mm d^{-1} (SD 2.4) in Swale 73. Spatial and temporal variability in ET was observed across the chronosequence with highest rates generally observed in July of 2006 and June of 2007 (Figure 2.7).

ET values calculated by the Loheide (2008) method (ET_G) approximated the PET calculations in magnitude (Figure 2.6). Considering that a 1:1 relationship is not necessarily expected, the average ET_G rates corresponded favorably with calculated PET (Figure 2.6A, Figure 2.6B) for the growing-season days that ET_G could be calculated. Differences resulting from the PET calculation method (e.g., PET_{PM}, PET_{ASCE}, and PET_{QUAD}) were minimal and barely observable in Figure 2.6A. Predicted ET values (e.g., ET_{ASCE}) also showed good correspondence with empirically derived ET_G (Figure 2.6C). Although linear regression gave a higher R^2 value (unpublished data), a power function was used instead because it minimized the RMSE [mm h^{-1}] and described the data trend more realistically (Figure 2.6B). As all PET calculation methods produced very similar results, I used PET_{ASCE} in subsequent analyses due to its utility and widespread treatment in the literature.

Taking LAI into account in the PET_{ASCE} equation improved the regression between ET_G and PET slightly but was not enough of an improvement to warrant the extra effort need to obtain the LAI measurements.

2.4.3 Sources of Water

Groundwater was drawn into the wetland by a head differential created by evapotranspirative demand, as is demonstrated by the lag in peak ET_G and groundwater inflow rates in Figure 2.4; loss by ET was followed by a gain in groundwater. Mean lag times between the daily ET and groundwater peaks in 2006 ranged from 1.5 h (Swale 17) to 4.2 h (Swale 38) and from 2.4 h (Swale 17) to 4.0 h (Swale 30) in 2007 (Figure 2.8). In most swales, the lag time was greater in 2007 than 2006.

The linear regression used to predict groundwater (G_{rec}) from evapotranspiration (ET_G) performed well. Regressions for all swales were significant ($\alpha = 0.05$), and R^2 ranged from 0.73 to 0.96, with a mean of 0.88 (SD 0.06) across all swales in 2006 and 2007, suggesting that ET is a robust predictor of shallow groundwater at this site.

Shallow groundwater offset 69-82 % of the water loss by ET in 2006 and 72-81 % in 2007, with the greater percentage offsets occurring when ET rates were low in the spring and fall (Figure 2.5, Figure 2.7). Precipitation accounted for 30-44% of ET in 2006 but only 21-30 % in 2007. The sources of water calculated explicitly in the water budget (precipitation and groundwater inflow) were sufficient to account for loss due to evapotranspiration, but water levels still declined over the growing season (Figure 2.5B), likely due to percolation loss following rainstorms. This topic will be discussed in Chapter 3.

2.4.4 Specific Yield

Specific yield determined by slug-test analyses was higher than values determined by the ratio of precipitation to water-table rise (Table 2.1). The composite specific yield modeled using the relative weights of the water depth and the sediment depth [Equation (4)] compared favorably with observed specific yield values estimated by the ratio method (Figure 2.9).

2.5 Discussion

The Loheide (2008) method for calculating evapotranspiration and groundwater inflow using diurnal water-level fluctuations is a useful technique for obtaining sub-daily values of evapotranspiration (ET) and groundwater. It does not assume the constant recovery rate of the original White (1932) method, making it more accurate. Moreover, the fact that sub-daily values of ET and groundwater can be calculated makes it useful in water-resource management. Water-use due to groundwater development (e.g., agricultural pumping, municipal water use) may vary over the course of a day. Understanding how plants interact with hydrologic flow on a sub-daily basis may help water-resource managers predict effects of groundwater withdrawal not only on riparian wetlands but also in coastal and other wetland ecosystems. Of course, lysimeter

measurements of ET are superior to this water-table fluctuation method; in natural areas and wooded wetlands where lysimeter installation is not feasible, the Loheide (2008) method provides a good option for scaling potential to actual ET.

Applying the method to non-riparian wetlands with recurring precipitation and periodically flooded conditions requires modifications to the method, including 1) weighting the specific yield (S_y) during periods of standing water, 2) using regression analysis to predict ET_G from PET for days when the method is not applicable, and 3) allowing flexibility in defining the pre-dawn hours in which ET is negligible. Caution must be taken when filtering or smoothing data, as over-smoothing can lead to overestimation of ET and groundwater by increasing the time base of each daily fluctuation. Many wetlands, like those in this study, have standing water for some portion of the growing season (e.g., Figure 2.5B); without the first modification, the method would only be applicable for periods when water levels were below ground. If the interest is to extrapolate the wetland water budget to the entire growing season, including standing-water periods, this modification is needed. The second modification, predicting ET_G from PET, is required for days when the Loheide (2008) method does not apply. This generally occurs either in the case of a precipitation event or when atmospheric conditions are dissimilar from one pre-dawn time period to the next. The third modification regarding the pre-dawn period assignation, while not required in riparian systems, was critical to the ability to uphold the assumptions of the method in this wetland system. It also was useful for incorporating changes in seasonality; longer mid-summer days affected the timing of the night-time peak water-table elevation. Photosynthesis, and therefore ET, began earlier in the morning and lasted later into the evening hours in June, for example, than in October. With this modification, I could account for seasonal changes in daylight.

The nonlinear power regression I used to predict actual ET (ET_G) from potential (PET_{ASCE}) described the observed relationship with better goodness of fit than a linear regression. In most studies comparing meteorological methods to actual ET measurements, a linear relationship has been observed between actual and potential ET. The lack of linear relationship here is perplexing, but at least one instance of nonlinearity has been documented (Vaughan et al. 2007). Furthermore, the ratio of actual to potential

ET may vary nonlinearly with environmental water-limiting factors (Flint and Childs 1991, Stannard 1993). Because PM-type equations are highly sensitive to radiation and temperature (Beven 1979, Rosenberg et al. 1989), it is theoretically possible that PET would continue to increase while actual ET shows asymptotic decline due primarily to water limitation and perhaps to photoinhibition or heat stress as well. This is shown in Figure 2.6B, where the highest hourly PET values represent mid-day values, the lowest PET values represent dawn and dusk, and the points in the middle are mid-morning and mid-afternoon. Because these are hourly values, there also may be discordance between the actual timing of daily evapotranspiration onset and cessation and that predicted by meteorological methods, which assume an instantaneous response of the biology to atmospheric conditions. Instead, the stomatal opening and closing that governs the ET rate may proceed at a rate different than is predicted by the Penman-Monteith equation, thereby generating nonlinearity in the relationship between actual and potential ET. Considering the atmospheric and water-level variability at the site, the goodness of fit of the power function seems adequate. The correspondence between PET and ET_G is evidence of this (Table 2.2, Figure 2.6A).

2.5.1 Comparison of ET_G, PET, and Pan Evaporation

ET rates estimated from water-level fluctuations (ET_G) compared favorably with potential evapotranspiration (PET) rates (Figure 2.6A), as well as pan evaporation (676 mm at Lupton, MI from 1976 to 2000) (NOAA 2009), although ET_G generally was greater than pan evaporation by a factor of 1.32 on average in 2006 and 1.37 in 2007. I recognize that the amount of water transferred to the atmosphere by transpiration cannot exceed PET determined by atmospheric capacity for absorbing water vapor. The meteorological methods (Penman-Monteith-type equations) for calculating PET, however, were developed primarily for use in agricultural applications. Some simplifying assumptions inherent to these methods may not apply as well to wetlands and may have led to underestimation of PET. For example, the meteorological methods assume homogeneous airflow over a plant community of uniform height. In the wetlands in this study, non-uniform vegetation height and morphology likely led to greater turbulence, which would have increased advective exchange across the boundary layer. Similarly,

Lott and Hunt (2001) observed higher wetland ET rates directly measured from water levels and lysimeters than by the Penman equation. Actual ET at rates greater than pan evaporation previously have been observed at multiple wetland sites. For example, Rushton (1996) observed actual ET rates nearly twice that of pan ET in a freshwater marsh. Dolan et al. (1984) found actual ET rates that were 10% greater than pan evaporation in the hot, dry parts of the year. Additionally, the effect of trees, both in wetlands and on the ridges, on ET rate is not taken into account in the PM-type equations. Greater ET rates have been observed in wetlands with woody vegetation than in sedge-dominated wetlands (Lafleur and Rouse 1988). I used the standard height for collecting meteorological data of 2 m; as such, the tree canopy was not taken into account, which also may have led to underprediction of PET. Although these explanations describe why the PET rates in this study were sometimes lower than actual ET rates, the method of scaling PET to directly measured ET rendered these concerns inconsequential.

I thought that taking vegetation into account would improve the regression of ET_G on PET noticeably. Since transpiration generally is positively related to biomass, I expected times of the year when the leaf area index (LAI) was high to have more ET than would not otherwise be accounted for in the PET_{ASCE} calculation. My results suggested that LAI had little effect, perhaps because the temporal resolution of the LAI data was insufficient. Although I used modeled change in LAI over time (Pereira et al. 2006, Allen et al. 2008), I only measured LAI twice during the growing season (leaf on and leaf off). The $PET_{ASCE\text{-}LAI}$ equation might perform better if canopy and understory vegetation data were taken at regular intervals over the growing season (Shi et al. 2008, Langensiepen et al. 2009). More likely, the relationship between PET and LAI is more complex than can be estimated by a simple ratio like in Equation (7), as demonstrated by Rosenberg et al. (1989) and more recently by Zhou et al. (2006), among others. In any case, since $PET_{ASCE\text{-}LAI}$ [Equation (7)] for available data was only a marginal improvement on PET_{ASCE} [Equation (6)], I used the simpler PET_{ASCE} calculation.

2.5.2 Potential Sources of Error

Uncertainty in the method primarily is associated with its sensitivity to specific yield (S_y). For example, a 10% reduction in S_y would yield an average change in ET_G of

1.66 mm d^{-1} over the growing season for Swale 28. First pointed out by Meyboom (1967) and then by Nachabe (2002), this sensitivity was described in depth by Loheide et al. (2005), who addressed using readily available S_y (water released over the period of a diurnal cycle) rather than classically defined S_y (saturation water content minus residual water content). Since the wells were developed in sand, classically defined S_y closely approximates readily available S_y (Loheide et al. 2005). The hydraulic-conductivity (K) values derived from field slug tests likely were more accurate than laboratory-derived values would have been, but the spatial and temporal resolution were insufficient to describe the actual specific yield. When compared to the specific yield as determined by the ratio of precipitation to water-table rise, which seems to be a more accurate test, especially due to the temporal resolution, the slug tests overestimated growing-season S_y by a factor of two or more (Table 2.1). I performed slug tests in October of 2007 when water levels were near the lowest in the study (Figure 2.5B). Specific yield has been shown to increase with increasing depth to water table (Duke 1972, Nachabe 2002, Loheide et al. 2005). Therefore, the slug-test S_y values can be interpreted as the uppermost limit of specific yield. Using the depth to predepositional surface (D_s) and water depth (D_w) to weight the soil and air components of specific yield provided a reasonable estimate for the composite specific yield when water levels were above ground, as shown in Figure 2.9. If anything, the method appears to underestimate S_y in that the modeled trend of the composite specific yield (S_{yc}) against water depth matches the slope but underestimates the intercept in comparison to the observed trend.

Additionally, ET calculated from water levels is subject to overestimation because the daily decline in water table also can include percolation loss when the change in water level at the well is decoupled from the change in head at the recovery source. A check for such decoupling is inherent in the method (Loheide 2008). My results suggest that regular pattern of groundwater influx for two subsequent nights following a rainstorm can bypass the safety check of the method and overestimate ET by including percolation loss. Therefore, care must be taken to ensure that ET by this method is not estimated for several days following rain events until the water table has re-equilibrated with the recovery source. Days when ET calculation may include percolation are readily evident from the hydrograph (Figure 2.5B) as an exaggerated decline in the water table

following a rainstorm and are easily removed from the data set. At the same time, it is possible that ET rates are actually higher after rainstorms due to saturation of the soil. This is less likely in wetlands, however, than in more arid regions where water limitation is paramount and rain events produce a marked increase in ET (Sanderson and Cooper 2008).

Although the differences I observed between AGS and BGS water-level scenarios were minimal, several errors may have been introduced when combining ET and groundwater calculations for flooded and non-flooded conditions. First, in all swales, there were fewer observations in the ET regression when water levels were AGS than BGS, which may have led to reduced accuracy in the AGS data set. Moreover, flooded conditions occurred early in the growing season when atmospheric variability could have led to more erratic water-level fluctuations and reduced accuracy in ET_G calculation.

Second, the modification of the Loheide for AGS water levels presented here involved weighting the specific yield (S_y). Since detailed swale surveying was not performed, I assumed that each swale had a rectangular cross-sectional geometry with a much larger width than depth (Figure 2.2A). Rather than having a circular planform shape, the swales extend longitudinally for more than 1 km (Figure 2.3). As a result, I chose to examine a rectangular portion with dimensions of 1 m (x), the lateral width of the swale (y), and the distance from the water surface to the predepositional surface (z). I assumed a uniform wetland surface area for all changes in stage but also accounted for above- and below-ground specific yield (S_{ya}, S_{ys}) using a weighted ratio, as described above. Hill and Neary (2007) showed that assuming a columnar (similar to a rectangular) geometry can lead to overestimation of ET in flooded conditions if an S_{ya} of 1.0 is used for the entire wetland. Conversely, the composite S_y method used in this study would lead instead to underestimation of ET. Since the water-level recorders were located on the lakeward side of each swale (Position 1 in Figure 2.2), the portion of the water column representing standing water (S_{ya}=1.0) would be less than the bulk of the wetland if a more conic geometry were the case, as argued by Hill and Neary (2007) (Figure 2.2B). Other configurations, however, could lead to overestimation of S_{yc} and, therefore, ET. In cross-section, the swales in this study were relatively flat in the middle and steep on the sides, as in Figure 2.2C (personal observation). Overestimation was possible but was probably

minimal, as storage near the edges represented a minor part of the overall water budget. A more substantial overestimate could occur if the configuration was steep on the lakeward side and graded gradually upward (Figure 2.2D). In this case, the water levels would be weighted more heavily to the S_{ya} than would be applicable to the bulk of the wetland. While some of the wetlands tended toward this geometry, ET rates for days when water levels were BGS were higher than for flooded conditions, suggesting that gross overestimation did not occur (Figure 2.5D).

Third, bank storage or water-table mounding near the edges of the swales might have affected water-level fluctuations as well (Winter and Rosenberry 1995), thereby affecting ET_G calculations. As noted by Healy et al. (2007), however, the magnitude of fluctuation in non-riparian wetlands is not great enough to lead to significant bank storage observed in riparian wetlands.

Finally, uncertainties in PET calculation when water levels were AGS might have occurred due to parameterization error, such as estimation of the surface resistance (r_s) in PET calculations. Nonetheless, the Loheide method, applied to both AGS and BGS water levels simultaneously, corresponded favorably with the PET_P, PET_{PM}, and PET_{FAO} methods (Figure 2.6), supporting findings by Loheide (2008) for this method and Gribovszki et al. (2008) for a similar empirical method.

2.5.3 ET Losses in a Unique Great Lakes Coastal Wetland

Wetland ET depends on the specific short- and long-term climatic and vegetative conditions at a site. Therefore, it is no surprise that wetland ET rates vary considerably from site to site and even within a single wetland complex. Despite their geographic proximity to one another, the wetlands in this study showed variability in ET, both spatially and temporally (Figure 2.7). Averaging 6.3 mm d^{-1} across all swales over the 2006 and 2007 growing seasons (May 20–October 11) and ranging from 5.5 (Swale 8) to 7.8 mm d^{-1} (Swale 73), mean daily ET was similar to previously reported rates. For example, Souch et al. (1996, 1998) used eddy covariance techniques to describe the energy balance of a ridge-swale system similar to the one in this study. They reported a June mean latent heat flux rate of 8.14 MJ m^{-2} d^{-1}, which converted to equivalent evaporation is 3.3 mm d^{-1} (Allen et al. 1998), but reported maximum latent heat flux rates

of close to 26 MJ m^{-2} d^{-1} (10.6 mm d^{-1}). For comparison, mean daily June ET rates in this study ranged from 6.0 (Swale 8) to 9.3 mm d^{-1} (Swale 73) and averaged 7.3 mm d^{-1} across all swales in both years. The maximum observed ET rate in this study was 17.5 mm d^{-1} in Swale 73 on June 24, 2007. Other wetlands have produced high ET rates as well. In a cattail- and bulrush-dominated wetland, Allen et al. (1992) observed rates of 69 MJ m^{-2} d^{-1} (28 mm d^{-1}), and Hill and Neary (2007) reported 18.7 mm d^{-1} in a sinkhole wetland. In this study, the regular pattern of upland sandy ridges with narrow intervening swales and a water table that infrequently fell below the rooting depth of phreatophytes facilitated high rates of evapotranspirative loss in this system. Plants were rarely, if ever, water-limited and continued to transpire throughout the growing season. Deeper rooted trees on the ridges (e.g., birch, maple) also used groundwater and no doubt contributed to these high ET rates. The proximity of the site to Lake Huron likely provided an atmospheric regime (e.g., high net radiation, lack of cumulus cloud formation, high vapor pressure deficit) conducive to high ET. Wind generation off the lake during the day and from land at night further contributed to ET loss.

This study captured ET rates across two growing seasons in a unique Great Lakes coastal wetland. More studies of diverse wetland types that span the growing season are needed to capture the full range of ET and provide a better description the water balance of wetlands.

Table 2.1. Hydraulic and texture properties of the soils and sediments at the 15 swales and representative values for similar texture classes. The hydraulic conductivity (K) and specific yield (Slug S_y) were determined by slug tests on October 11-12, 2007 and represent the upper limit. The more accurate S_y calculated as the ratio of precipitation to water-table rise (Ratio S_y) was estimated for the number of precipitation events listed for each swale, and the arithmetic mean was used to calculate groundwater and ET rates in Equations (2) and (3). Representative S_y values for sand, loamy sand, and sandy loam are also shown, as determined by Johnson (1967) and presented in Loheide (2005), along with percent sand, silt, and clay for the three texture classes and the 15 swales. Soil depths also are shown. Values in parentheses represent standard deviation.

	K [m d^{-1}]	Slug S_y [dim.]	Slug tests	Ratio S_y [dim.]	Precip. Events	Sand [%]	Silt [%]	Clay [%]	Soil Depth [m]
Texture									
Sand	7.1	S_y = 0.34				92.7	-	2.9	
Loamy sand	3.5	S_y = 0.26				80.9	-	6.4	
Sandy loam	1.1	S_y = 0.19				63.4	-	11.1	
Swale									
8	2.26	0.223 (0.28)	3	0.124 (0.03)	18	98.3	1.0	0.7	0.66
14	1.89	0.213 (-)	1	0.150 (0.05)	29	98.4	0.0	1.6	0.37
17	1.81	0.212 (-)	1	0.119 (0.06)	16	95.9	0.9	3.2	0.15
26	4.47	0.278 (0.35)	3	0.120 (0.07)	19	97.7	0.6	1.7	0.35
28	4.63	0.282 (0.36)	3	0.100 (0.04)	19	97.8	1.5	0.7	0.60
29	4.63	0.281 (0.36)	3	0.124 (0.06)	20	98.2	1.1	0.7	0.53
30	4.62	0.281 (0.36)	3	0.108 (0.06)	20	98.1	0.2	1.7	0.42
32	4.57	0.280 (0.36)	3	0.127 (0.05)	26	97.8	1.5	0.7	0.72
37	4.64	0.282 (0.36)	3	0.153 (0.05)	25	93.2	4.1	2.7	0.26
38	4.70	0.283 (0.37)	3	0.121 (0.05)	12	97.3	0.5	2.2	0.20
55	3.03	0.242 (0.23)	3	0.120 (0.06)	27	97.9	0.4	1.7	0.56
73	2.46	0.228 (0.29)	2	0.156 (0.06)	31	96.9	1.9	1.2	0.42
78	2.43	0.227 (0.29)	2	0.113 (0.05)	23	98.1	1.5	0.4	0.69
81	2.43	0.227 (0.29)	2	0.136 (0.06)	30	97.5	1.1	1.4	0.14
82	2.43	0.227 (0.29)	2	0.116 (0.06)	26	97.8	0.0	2.2	0.18

Table 2.2. Across-swale mean coefficient of variation (R^2) and root mean squared error (RMSE) for the power regressions between ET_G and potential ET (PET). PET was calculated by the Penman-Monteith equation (PM), the ASCE-PM equation (ASCE), and the Paw and Gao (1988) quadratic solution to the PM equation (QUAD). For comparison of flooded and non-flooded conditions, regressions were run for above-ground-surface (AGS) and below-ground-surface (BGS) water levels individually and combined. Only the combined AGS and BGS regressions were used for predictive purposes.

PET Equation	R^2	RMSE [mm h^{-1}]
AGS		
PM	0.353	0.155
ASCE	0.356	0.154
QUAD	0.351	0.155
BGS		
PM	0.336	0.176
ASCE	0.337	0.175
QUAD	0.337	0.176
All		
PM	0.311	0.183
ASCE	0.313	0.183
QUAD	0.311	0.184

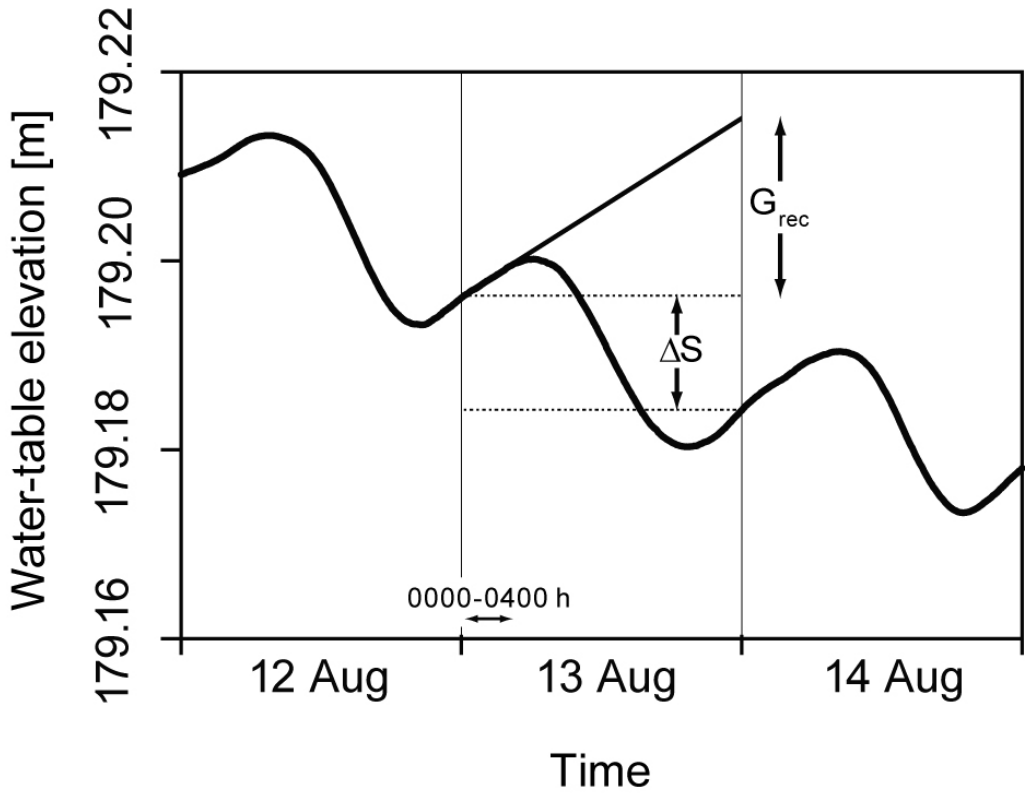

Figure 2.1. Water-level curve at Swale 28 from 12-14 August 2006 showing the White (1932) method for empirically calculating daily ET (after Gribovszki et al. 2008). G_{rec} represents the net groundwater flow over a 24-hour period as extrapolated from the slope of the water-level curve from 0000 h to 0400 h. Change in storage is depicted by ΔS. As shown in Equation (1), ET is the sum of G_{rec} and ΔS multiplied by the specific yield, S_y.

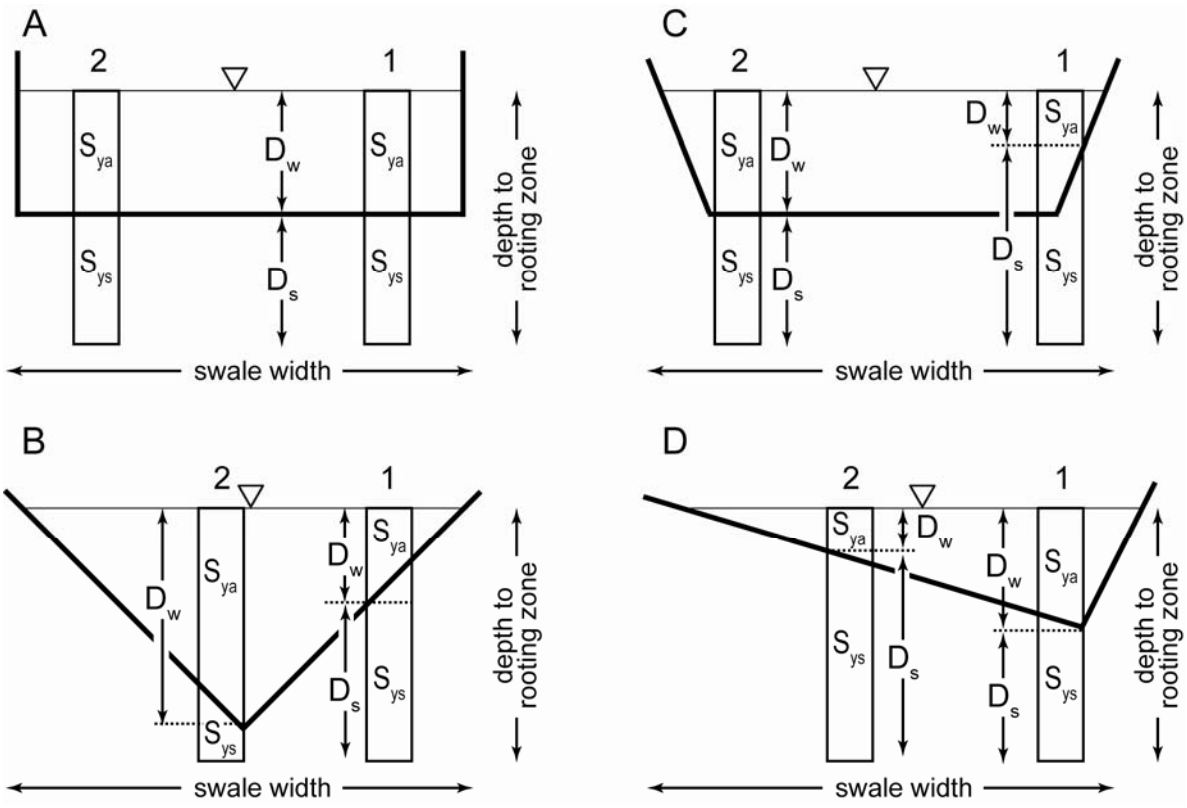

Figure 2.2. Various wetland geometries in cross-section showing effect of the weighted specific yield (S_{yc}) when the water-level gage is placed at two positions. Position 1 represents the location of the wells in this study, which were installed on the lakeward side of each swale. Position 2 is an alternate location for comparison. The shape of C is most similar to actual swale geometry (personal observation). S_{ya} is the specific yield of air applied to flooded conditions and is assigned a value of 1.0; S_{ys} is the soil and sediment specific yield for below-ground water levels, as determined by the ratio of precipitation to water-level rise. D_w represents the depth of standing water. D_s is the distance from the soil surface to the predepositional surface of the strand plain. Diagrams are not drawn to scale.

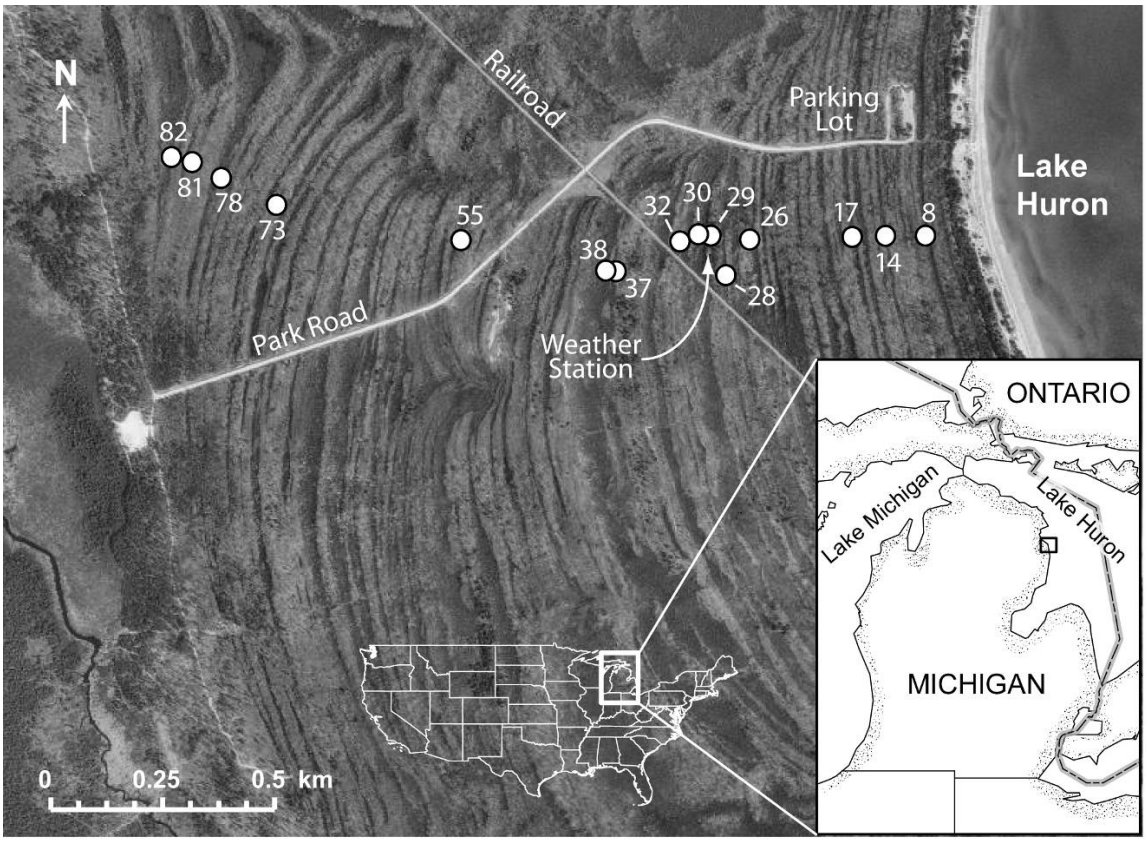

Figure 2.3. Location (inset) and air photo of the ridge-and-swale chronosequence at Negwegon State Park showing hydrologic sampling sites. The lighter linear features in the photo represent the ridges, and darker features are the swales.

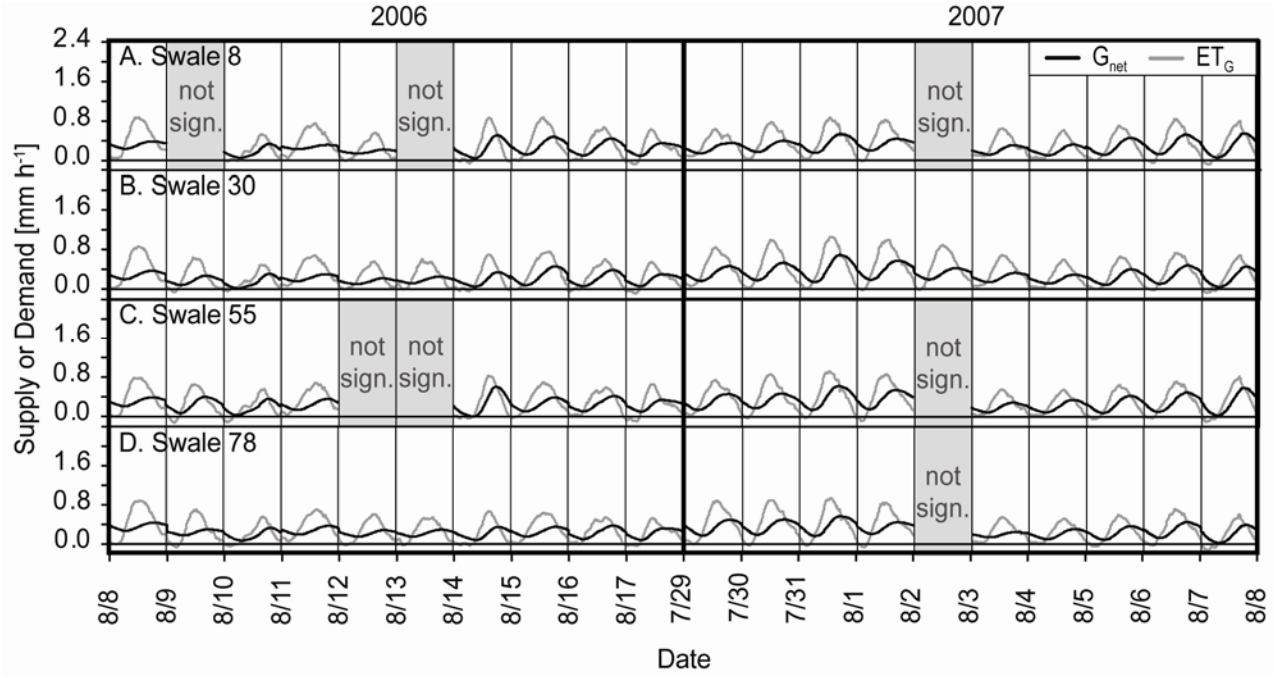

Figure 2.4. Estimated shallow groundwater recovery (G_{rec}) and evapotranspirative demand (ET_G) calculated by the modified Loheide (2008) method over two ten-day periods (July 8 to 18, 2006 and July 29 to August 8, 2007) for four of the 15 swales. A three- to four-hour lag was observed between the ET_G and groundwater peaks. On some days, test statistics used to evaluate the Loheide (2008) method were not significant, as noted (not sign.).

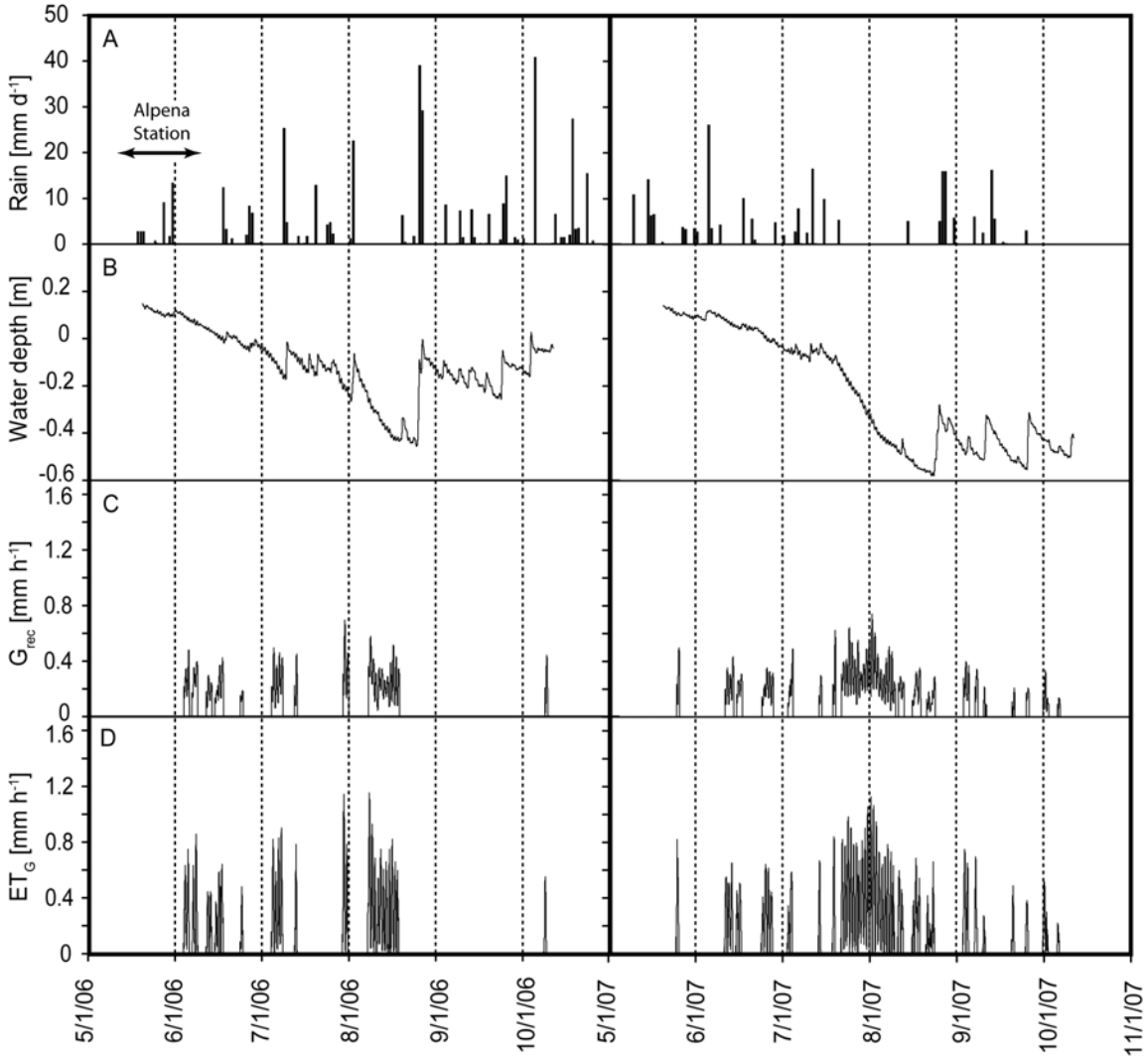

Figure 2.5. Precipitation (A), observed water depth (B), estimated shallow groundwater inflow (G_{rec}) (C), and estimated evapotranspiration (ET_G) (D) for Swale 30 for the 2006 and 2007 growing seasons. Groundwater and ET were calculated using the Loheide (2008) variation of the empirical White (1932) method. Gaps in groundwater and ET records indicate days in which the Loheide method was not applicable (i.e., rainfall occurred or the slopes of the detrended water-table curves for sequential nights were not uniform). A short-term gap in the 2006 precipitation record due to instrument failure was populated with data from the Alpena, MI weather station approximately 20 km north of the study site (NOAA 2008). Extreme values on August 2-3, 2007 were due to high temperatures (max 34°C), incoming solar radiation (peak 3.2 MJ m^{-2} h^{-1}), and sustained winds averaging 4.1 m s^{-1} (max 7.5 m s^{-1}).

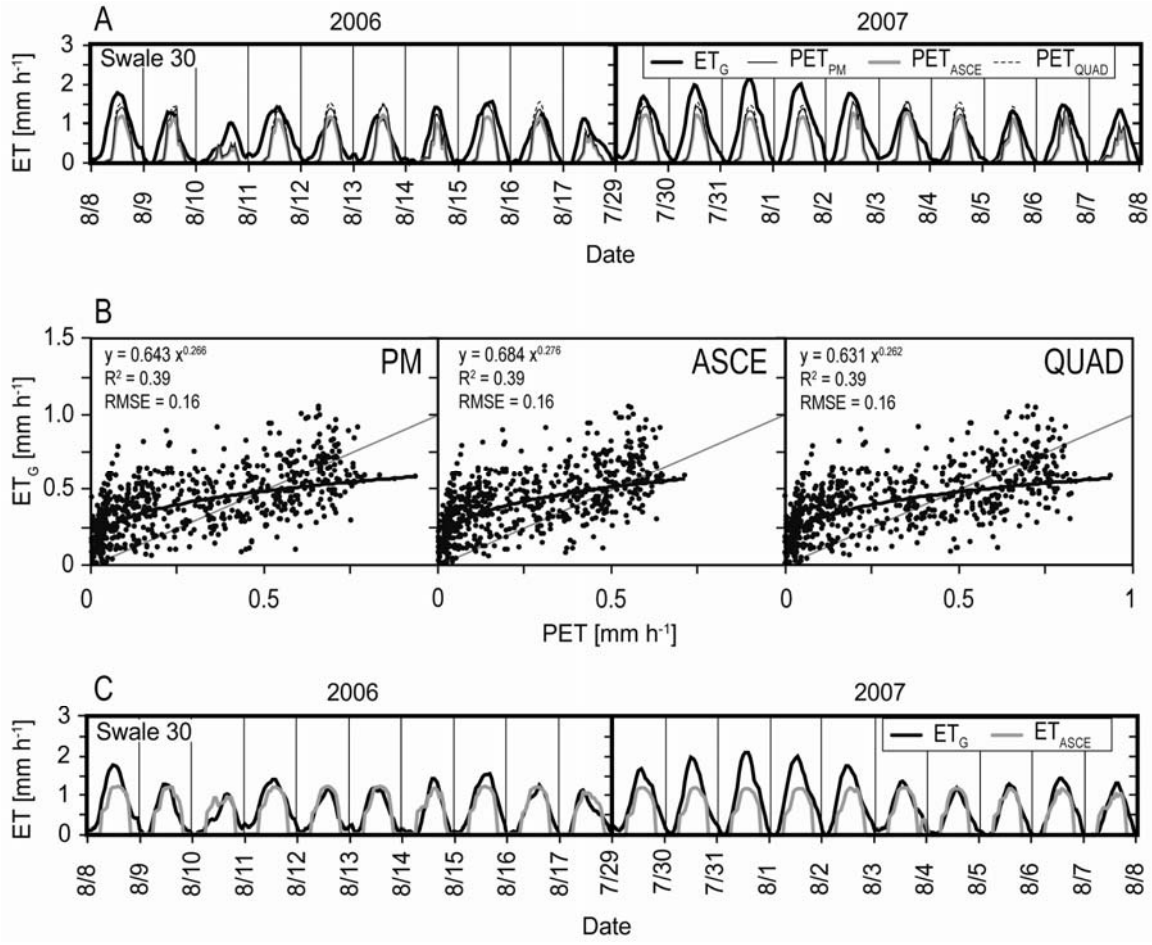

Figure 2.6. Comparison of estimated evapotranspiration (ET_G) and potential evapotranspiration calculated by the Penman-Monteith equation (PET_{PM}), the ASCE equation (PET_{ASCE}), and the quadratic equation of Paw and Gao (1988) over two ten-day periods (July 8-18, 2006 and July 29-August 8, 2007) at Swale 30 (A). Estimated ET (ET_G) plotted against potential ET (PET) at Swale 30 for the 2007 growing season (B). ET_G (black line) and ET predicted by the power relationship between PET_{ASCE} and ET_G (gray line) (C) at Swale 30.

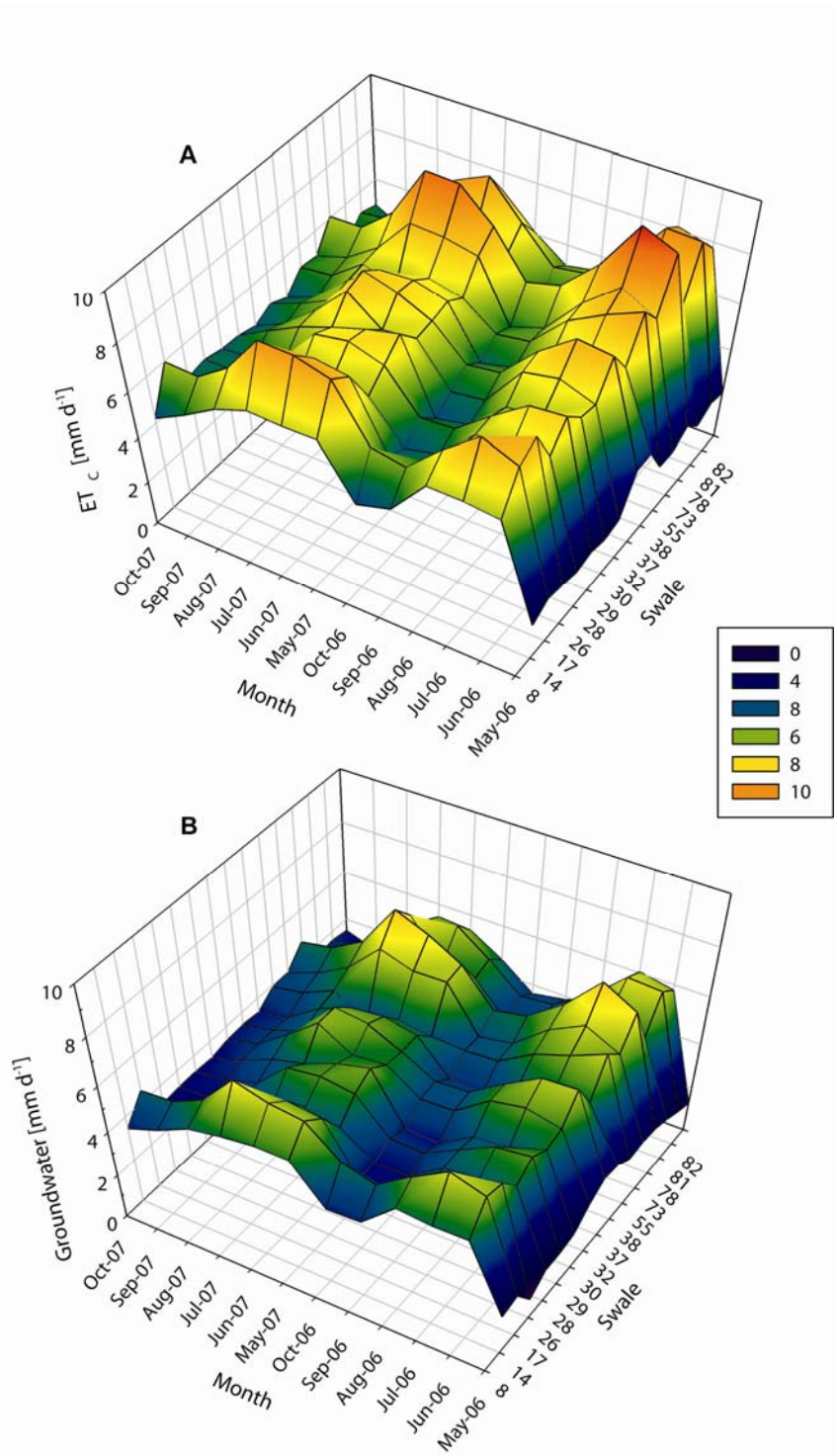

Figure 2.7. Mean daily evapotranspiration (ET_C) (A) and groundwater inflow (G_C) (B) by month of the growing season in 2006 and 2007 for each of the 15 swales in the study.

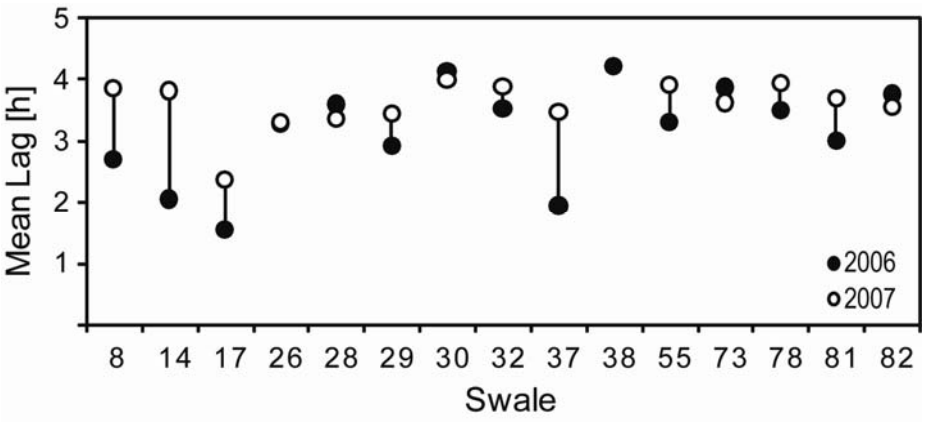

Figure 2.8. Mean lag time between the daily peaks of ET and groundwater inflow for the 15 swales in the study in 2006 and 2007. Lines between points connect 2006 and 2007 data points for each swale. A value for Swale 38 in 2007 was not available due to instrument failure.

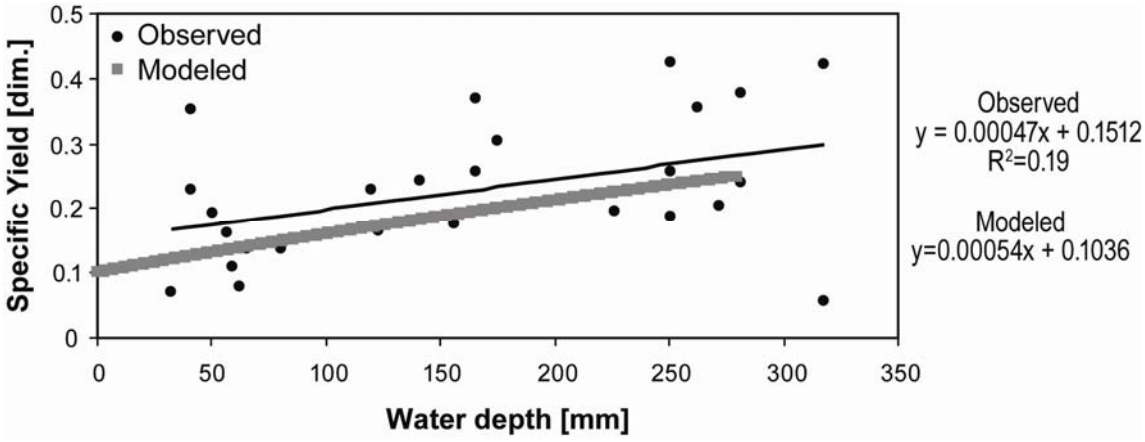

Figure 2.9. Plot of above-ground specific yield against water depth for the observed values (ratio of precipitation to water-table rise) and the values modeled using Equation (4) for Swale 28, as an example. At greater water depths, the specific yield of air (S_{ya} = 1.0) is weighted higher in the equation than the specific yield of soil and sediment (S_{ys}), resulting in a greater composite specific yield (S_{yc}). The modeled relationship appears to be a relatively accurate description of the observed trend.

REFERENCES CITED

Allen, R.G., J. H. Prueger, and R. W. Hill. 1992. Evapotranspiration from isolated stands of hydrophytes: cattail and bulrush. Transactions of the American Society of Agricultural Engineers 35:1191–1198.

Allen, R. G., L. S. Pereira, D. Raes, and M. Smith. 1998. Crop evapotranspiration - guidelines for computing crop water requirements. FAO Irrigation and Drainage Paper 56, FAO - Food and Agriculture Organization of the United Nations, Rome, Italy.

Allen, R.G., I. A. Walter, R. L. Elliott, T. A. Howell, D. Itenfisu, M. E. Jensen, M. E., and R. L. Snyder. 2005. The ASCE Standardized Reference Evapotranspiration Equation, American Society of Civil Engineers, Reston, VA, USA.

Allen, R. G., W. O. Pruitt, J. L. Wright, T. A. Howell, F. Ventura, R. Snyder, D. Itenfisu, P. Steduto, J. Berengena, J. B. Yrisarry, M. Smith, L. S. Pereira, D. Raes, A. Perrier, I. Alves, I. Walter and R. Elliott. 2006. A recommendation on standardized surface resistance for hourly calculation of reference ET_o by the FAO56 Penman-Monteith method. Agricultural Water Management 81:1–22.

Beven, K. 1979. A sensitivity analysis of the Penman-Monteith actual evapotranspiration estimates. Journal of Hydrology 44:169–190.

Bouwer, H. 1989. The Bouwer and Rice slug test - an update. Ground Water 27:304–309.

Butler, J. J., G. J. Kluitenberg, D. O. Whittemore, S. P. Loheide, W. Jin, M. A. Billinger, and X. Zhan. 2007. A field investigation of phreatophyte-induced fluctuations in the water table. Water Resources Research 43:1–12.

Cleveland, W. S. 1979. Robust locally-weighted regression and smoothing scatterplots. Journal of the American Statistical Association 74:829–836.

Cleveland, W. S., S. J. Devlin, and E. Grosse 1988. Regression by local fitting: methods, properties, and computational algorithms. Journal of Econometrics 37:87–114.

Dolan, T. J., A. J. Hermann, S. E. Bayley, and J. Zoltek. 1984. Evapotranspiration of a Florida, U.S.A., freshwater wetland. Journal of Hydrology 74:355–371.

Duke, H. R. 1972. Capillary properties of soils—Influence upon specific yield. Transactions of the American Society of Agricultural Engineers 15:688–691.

Ferris, J. G., D. B. Knowles, R. H. Brown, and R. W. Stallman. 1962. Geological Water-Supply Paper 1536-E. United States Government Printing Office, Washington, DC, USA

Fetterer, C. W. 2001. Applied Hydrogeology. Fourth edition. Prentice Hall, Upper Saddle River, NJ, USA.

Flint, A. L. and S. W. Childs. 1991. Use of the Priestly-Taylor evaporation equation for soil water limited conditions in a small forest clearcut. Agricultural and Forest Meteorology 56:247–260.

Gerla, P. J. 1992. The relationship of water-table changes to the capillary fringe, evapotranspiration, and precipitation in intermittent wetlands. Wetlands 12:91–98.

Gonthier, G. J. 2007. A graphical method for estimation of barometric efficiency from continuous data: concepts and application to a site in the Piedmont, Air Force Plant 6, Marietta, Georgia. Scientific Investigation Report 2007-5111, U.S. Geological Survey, Reston, VA, USA.

Gribovszki, Z., P. Kalicz, J. Szilagyi, and M. Kucsara. 2008. Riparian zone evapotranspiration estimation from diurnal groundwater level fluctuations. Journal of Hydrology 349:6–17.

Halford, K. J. 2006. Documentation of a spreadsheet for time-series analysis and drawdown estimation, USGS Scientific Investigations Report 2006-5024, Carson City, NV, USA.

Healy, R. W., T. C. Winter, J. W. LaBaugh, and O. L. Franke. 2007. Water budgets: foundations for effective water-resources and environmental management. U.S. Geological Survey Circular 308, Reston, VA, USA.

Hill, A. J. and V. S. Neary. 2007. Estimating evapotranspiration and seepage for a sinkhole wetland from diurnal surface-water cycles. Journal of the American Water Resources Association 43:1373–1382.

Johnson, A. I. 1967. Specific yield – compilation of specific yields for various materials. Geological Water Supply Paper 1662-D, United States Government Printing Office, Washington, DC, USA.

Laczniak, R. J., G. A. DeMeo, S. R. Reiner, J. L. Smith, and W. E. Nylund. 1999. Estimates of groundwater discharge as determined from measurements of evapotranspiration, Ash Meadows area, Nye County, Nevada. Water-Resources Investigation Report 99–4079, U.S. Geological Survey, Reston, VA, USA.

Lafleur, M. and W. R. Rouse. 1988. The influence of surface cover and climate on energy partitioning and evaporation in a subarctic wetland. Boundary Layer Meteorology 44:327–347.

Langensiepen, M., M. Fuchs, H. Bergamaschi, S. Moreshet, Y. Cohen, P. Wolff, S. C. Jutzi, S. Cohen, L. M. G. Rosa, Y. Li, and T. Fricke. 2009. Quantifying the uncertainties of transpiration calculations with the Penman-Monteith equation under different climate

and optimum water supply conditions. Agricultural and Forest Meteorology 149:1063–1072.

Lautz, L. 2008. Estimating groundwater evapotranspiration rates using diurnal water-table fluctuations in a semi-arid riparian zone. Hydrogeology Journal 16:483–497.

Leaver, J. D. and C. P. Unsworth. 2007. Fourier analysis of short-period water level variations in the Rotorua geothermal field, New Zealand. Geothermics 36:539–557.

LI-COR. 1992. LAI-2000 Plant Canopy Analyzer Instruction Manual. LI-COR, Inc., Lincoln, NE, USA.

Loheide, S. P. 2008. A method for estimating subdaily evapotranspiration of shallow groundwater using diurnal water table fluctuations. Ecohydrology 1:59–66.

Loheide, S. P., J. J. Butler, and S. M. Gorelick. 2005. Estimation of groundwater consumption by phreatophytes using diurnal water table fluctuations: a saturated-unsaturated flow assessment. Water Resources Research 41:1–14.

Loheide, S. P., R. S. Deitchman, D. J. Cooper, E. C. Wolf, C. T. Hammersmark, J. D. Lundquist. 2009. A framework for understanding the hydroecology of impacted wet meadows in the Sierra Nevada and Cascade Ranges, California, USA. Hydrogeology Journal 17:229–246.

Mathworks. 2007. MATLAB R2007a, Version 7.4. Mathworks, Inc., Natick, MA, USA.

Meyboom, P. 1967. Groundwater studies in the Assiniboine River drainage basin—Part II: Hydrologic characteristics of phreatophytic vegetation in south-central Saskatchewan. Bulletin – Geological Survey of Canada, 139.

Mitsch, W. J. and J. G. Gosselink. 2000. Wetlands. Third edition. John Wiley & Sons, Inc., New York, NY, USA.

Monteith, J. 1965. Evaporation and environment. p. 205–234. *In* G. Fogg (ed.) The State and Movement of Water in Living Organisms, 19th Symposium of the Society of Experimental Biologists. Cambridge University Press, Cambridge, MA, USA.

Nachabe, M. H. 2002. Analytical expressions for transient specific yield and shallow water table drainage. Water Resources Research 38:1193.

National Oceanographic and Atmospheric Administration National Climate Data Center (NOAA). 2008. Annual Climatological Summary (Alpena County Regional Airport). http://www4.ncdc.noaa.gov/cgi-in/wwcgi.dll?wwDI~StnSrch~StnID~20010361.

National Oceanographic and Atmospheric Administration National Climate Data Center (NOAA). 2009. Annual Climatological Summary (Lupton 1S Station). http://www4.ncdc.noaa.gov/cgi-win/wwcgi.dll?wwDI~StnSrch~StnID~20010297.

Paw U, K. T. and W. Gao. 1988. Applications of solutions to nonlinear energy budget equations. Agricultural and Forest Meteorology 43:121–145.

Penman, H. L. 1948. Natural evaporation from open water, bare soil and grass. Proceedings of the Royal Society of London 193:120–145.

Pereira, A. R., S. Green, and N. A. Villa Nova. 2006. Penman-Monteith reference evapotranspiration adapted to estimate irrigated tree transpiration. Agricultural Water Management 83:153–161.

Posner, R. N., J. M. Bell, S. J. Baedke, T. A. Thompson, and D. A. Wilcox. 2005. Aqueous geochemistry as an indicator of subsurface geology and hydrology of a beach-ridge/wetland complex in Negwegon State Park, MI. Geological Society of America Abstracts with Programs 37:300.

Rasmussen, T. C. and L. A. Crawford. 1997. Identifying and removing barometric pressure effects in confined and unconfined aquifers. Groundwater 35:502–511.

Rasmussen, T. C. and T. L. Mote. 2007. Monitoring surface and subsurface water storage using confined aquifer water levels at the Savannah River Site, USA. Vadose Zone Journal 6:327–335.

Rosenberg, N. J., M. S. McKenney, and P. Martin. 1989. Evapotranspiration in a greenhouse-warmed world: a review and a simulation. Agricultural and Forest Meteorology 47:303–320.

Rosenberry, D. O. and T. C. Winter. 1997. Dynamics of water-table fluctuations in an upland between two prairie-pothole wetlands in North Dakota. Journal of Hydrology 191:266–289.

Rushton, B. 1996. Hydrologic budget for a freshwater marsh in Florida. Water Resources Bulletin 32:13–21.

Sanderson, J. S. and D. J. Cooper. 2008. Ground water discharge by evapotranspiration in wetlands of an arid intermountain basin. Journal of Hydrology 351:344–359.

Schilling, K. E. 2007. Water table fluctuations under three riparian land covers, Iowa (USA). Hydrological Processes 21:2415–2424.

Schilling, K. E. and J. R. Kiniry. 2007. Estimation of evapotranspiration by reed canarygrass using field observations and model simulations. Journal of Hydrology 337:356–363.

Seber, G. A. F. and C. J. Wild. 2003. Nonlinear Regression. Wiley-Interscience, Hoboken, NJ, USA.

Shi, T., D. Guan, A. Wang, J. Wu, C. Jin, and S. Han. 2008. Comparison of three models to estimate evapotranspiration for a temperate mixed forest. Hydrological Processes 22:3431–3443.

Shuttleworth, W. J. 1993. Evaporation. p. 4.1–4.53. *In* D. R. Maidment (ed.) Handbook of Hydrology. McGraw-Hill, Inc., New York, NY, USA.

Souch, C., C. S. B. Grimmond, and C. P. Wolfe. 1998. Evapotranspiration rates from wetlands with different disturbance histories: Indiana Dunes National Lakeshore. Wetlands 18:216–229.

Souch, C., C. P. Wolfe, and C. S. B. Grimmond. 1996. Wetland evaporation and energy partitioning: Indiana Dunes National Lakeshore. Journal of Hydrology 184:189–208.

Spane, F. A. 1999. Effects of barometric fluctuations on well water-level measurements and aquifer rest data. Department of Energy Report PNNL-13078, Richland, WA, USA.

Stannard, D. I. 1993. Comparison of the Penman-Monteith, Shuttleworth-Wallace, and modified Priestley-Taylor evapotranspiration models for wildland vegetation in semiarid rangeland. Water Resources Research 29:1379–1392.

Toll, N. J. and T. C. Rasmussen. 2007. Removal of barometric pressure effects and Earth tides from observed water levels. Groundwater 45:101–105.

Tóth, J. 1963. A theoretical analysis of groundwater flow in small drainage basins. Journal of Geophysical Research 68:4795–4812.

Troxell, H. C. 1936. The diurnal fluctuation in the groundwater and flow of the Santa Ana River and its meaning. EOS Transactions, American Geophysical Union 17:496–505.

United States Department of Agriculture Natural Resources Conservation Service (USDA). 2008. Web Soil Survey. http://websoilsurvey.nrcs.usda.gov/app/WebSoilSurvey.aspx.

Vaughan, P. J., T. J. Trout, and J. E. Ayars. 2007. A processing method for weighing lysimeter data and comparison to micrometeorological ET_o predictions. Agricultural Water Management 88:141–146.

White, W. N. 1932. A method of estimating groundwater supplies based on discharge by plants and evaporation from soil. Water-Supply Paper 659-A, U.S. Geological Survey. Washington, DC, USA.

Widmoser, P. 2009. A discussion on and alternative to the Penman–Monteith equation. Agricultural Water Management 96:711–721.

Wilcox, D. A., S. J. Baedke, and T. A. Thompson. 2005. Groundwater contribution to hydrology-driven development of wetland plant communities. Geological Society of America Abstracts with Programs 37:244.

Winter, T. C. and D. O. Rosenberry. 1995. Evaluation of 11 equations for determining evaporation for a small lake in the north central United States. Water Resources Research 31:983–993.

Zhou, M. C., H. Ishidaira, H. P. Hapuarachchi, J. Magome, A. S. Kiem, and K. Takeuchi. 2006. Estimating potential evapotranspiration using Shuttleworth-Wallace model and NOAA-AVHRR NDVI data to feed a distributed hydrological model over the Mekong River basin. Journal of Hydrology 327:151–173.

CHAPTER 3

The water balance of wetlands: Interactions of groundwater loading and evapotranspiration

3.1 Introduction

In a process integral to wetland ecology, wetland plants interact with site hydrology directly through transpiration and indirectly through shading and temperature regulation affecting surface evaporation (Mitsch and Gosselink 2000). The water available to plants, in turn, is controlled by the local water balance which drives wetland maintenance and soil development (Carter 1986, Erwin 1989, Winter et al. 1999), biogeochemical cycling (Mitsch and Gosselink 2000, Brady and Weil 2002), and ultimately plant composition and distribution (Mitsch and Gosselink 2000). In some wetlands, the availability of water may be governed by site hydrogeology irrespective of the vegetation; plants persist there that can withstand the prevailing hydrologic conditions. In other situations, plants may themselves strongly influence water availability by reducing soil evaporation and by root uptake and transpiration.

Coastal ridge-swale wetlands, in particular, are sensitive to changes in climate and drought (Doss 1993, Winter 1999). This sensitivity is apparent in the paleoecological record, in which climate-driven vegetation change has been preserved in sediment cores only in the absence of constant groundwater discharge (Booth et al., unpublished data; Burkett et al. 2005). When local groundwater loading greatly exceeds the transpiration rate of plants, it is likely to buffer climate-change effects on the structure of wetland plant communities; despite changes in temperature and precipitation, water availability in a groundwater-fed wetland will remain the same, and plant community change will be slowed. If plant water use becomes greater than groundwater can supply, however, wetlands may become drier, and changes in climate are likely to lead to more drastic changes in vegetation. Understanding the current hydrologic balance of wetlands will

give us a baseline for comparison to future climate scenarios (Restrepo et al. 1998, Sun et al. 1998).

In this chapter, I examine transient water-table dynamics resulting from interactions between groundwater hydrology and evapotranspiration in a structurally and vegetatively complex Great Lakes coastal wetland system. I am interested in the system of feedbacks that link water-balance dynamics and vegetation. My specific objectives were to 1) explore how variation in swale hydrology arises through interactions between plants and site physiography and 2) examine how inter-annual climatic variability affects these interactions. Results are discussed in the context of pending global climate change.

3.2 Site Description

An undisturbed ridge-swale chronosequence located along the western shore of Lake Huron (25 km south of Alpena, MI) within the boundaries of Negwegon State Park is a site suited particularly well for examining transient water-table dynamics (Figure 2.3). Over the last 3500 years, coastal processes in an embayment with high sediment supply have led to preservation of a strand plain comprised of approximately 90 former beach ridges and their intervening swales (Thompson, personal communication, May 30, 2005). The beach ridges represent local topographic highs that drive shallow and intermediate groundwater-flow cells such as those described by Tóth (1963), thereby connecting the swales hydrologically (Baedke, personal communication, July 2, 2006). Deeper, regional flow is impeded by an impermeable layer, as described below. Hydric soils and wetland plant communities have developed in 37 of the swales.

Swale vegetation falls into three main categories: sedge meadow/emergent marsh (henceforth, herbaceous), seasonally flooded forested overstory with emergent wetland plants in the understory (henceforth, forested), and seasonally flooded scrub-shrub (henceforth, shrub). Swales in the herbaceous category are dominated by sedges and grasses [e.g., Northwest Territory sedge, *Carex utriculata* Boott; bluejoint, *Calamagrostis canadensis* (Michx.) P. Beauv.]. Swales in the forested category show a dominant overstory of hydromesophytic trees such as black ash [*Fraxinus nigra* Marsh.] and green ash [*Fraxinus pensylvanica* Marsh.]. The emergent areas in the forested type are mostly devoid of vegetation, save a few species [e.g., small floating mannagrass,

Glyceria borealis (Nash) Batchelder; hemlock waterparsnip, *Sium suave*Walter] but transition to emergent marsh (see above) or herbaceous forest-floor cover [e.g., dwarf red blackberry, *Rubus pubescens* Raf.; sensitive fern, *Onoclea sensibilis* L.] later in summer. The scrub-shrub wetlands are dominated by gray alder [*Alnus incana* (L.) Moench] and common winterberry [*Ilex verticillata* (L.) A. Gray], along with ash [*Fraxinus*] saplings.

Near-surface sediments are homogeneous fine- to medium-grained sands with some gravel. Beneath the strand plain at approximately 3 m depth, the predepositional surface consists of a diamicton (very poorly sorted sediment of low permeability) of glacial origin that acts as an aquiclude or aquitard. Detected in sediment cores and by ground-penetrating radar (Thompson, unpublished data; Posner et al. 2005), this layer may permit intermediate groundwater flow to and from the overlying wetlands. Water-chemistry data suggest that more permeable areas of the diamicton allowed intermediate flow paths described by Tóth (1963) to interact with the unconfined aquifer above (Baedke, unpublished data; Posner et al. 2005). Deeper, regional flowpaths, however, do not appear to feed the site (Baedke, personal communication, July 2, 2006; Wilcox et al. 2005).

Hydraulic conductivity of the strand plain sediments, as determined by slug-test analyses I estimated in Chapter 2, range from 1.81 to 4.70 m d^{-1}, which is within the typical range for silty sands and fine sands (Fetterer 2001). Swales in the middle of the sequence have greater hydraulic conductivity than the younger and older swales on either side.

An on-site weather-station (Davis Instruments Cabled Vantage Pro2 Plus with Standard Radiation Shield 6162C) was installed centrally at a height of 2 m above May 2006 water levels (Figure 2.3). Recorded weather data—precipitation [mm], incoming solar radiation [MJ m^{-2} d^{-1}], air temperature [ºC], dew point [ºC], and wind speed [m s^{-1}]—spanned 145 days of the growing season (May 20 to October 11) for each year of the study, 2006 and 2007 (Figure 3.1). In north temperate regions, the growing season generally extends from May to October and ends at the first frost. In 2006, this occurred on the night of October 12 but much earlier in 2007 on September 23. The growing season was defined arbitrarily as May 20 to October 11 for this study because these were the days for which water-level data were recorded in both 2006 and 2007. Total

precipitation over the growing season was 337.1 mm in 2006 and 240.8 mm in 2007. Mean temperature also was greater in 2006 (17.1 °C) than 2007 (12.2 °C). Wind speed [m s^{-1}], relative humidity [%], and incoming solar radiation [MJ m^{-2} d^{-1}] did not vary greatly between years.

3.3 Methods

3.3.1 Monitoring Wells and Water-Level Data

Fifteen swales were selected for hydrologic monitoring using a stratified random sampling design. Five wells were allocated to each of three vegetation strata: forested, shrub, and herbaceous (Figure 2.3). Instrumentation in each swale included a relative-humidity and air-temperature sensor (Onset, HOBO H8 Pro Series, H08-032-08 RH/Temp) placed 2 m above May water levels, a substrate temperature sensor (Onset, HOBO H8 Family, H08-001-02), and a pressure transducer (Solinst LT Levelogger Model 3001, F15/M5, 0.02 cm resolution) in an unlined well (slotted across the water table) (Aquatic Eco-Systems, Inc.; 3.18 cm diameter, 1.52 m length, 0.0254 cm slotted PVC). Wells were hand-driven to a depth of 1 m and conditioned by pumping. The substrate temperature sensors were submersed just below the water surface until water levels fell below ground, at which point the sensor was buried in the top 6 cm of soil. A barometric pressure transducer was installed centrally at Swale 29. Data were recorded at five-minute intervals from May 20 to October 27 in 2006 and April 14 to October 12 in 2007.

Water-level and barometric-pressure data at five-minute intervals were smoothed using locally weighted, second-order polynomial regression (LOESS) that assigned lower weight to outliers (span = 0.005) (Cleveland 1979, Cleveland et al. 1988). Minor gaps in the data (< 0.5 h) occurred when pressure transducers were downloaded; missing values were estimated by spline interpolation prior to smoothing. I compensated for barometric pressure by subtracting it from the absolute pressure recorded by the pressure transducers and calculated zero barometric efficiency by slope (Ferris et al. 1962) and graphical methods (Gonthier 2007). Fifteen-minute intervals were extracted from the five-minute smoothed time-series data. I directly measured water-table elevation monthly using a

water-level meter (Solinst Model 101) and converted pressure-transducer data to water-table elevation using linear regression rating curves.

3.3.2 Underlying Geology and Soils

To estimate specific yield for soils at each swale, I used the ratio of precipitation to associated water-table rise for multiple rain events greater than 5 mm. This method is considered adequate for application to wetlands where water levels are near the surface (Gerla 1992, Rosenberry and Winter 1997, Loheide et al. 2005). As an independent measure of specific yield, I performed slug tests using the Bouwer and Rice method (Bouwer 1989). In October, 2007, five slug tests were performed at each of five swales (8, 14, 26, 55, and 78), but only one to three of the tests showed a clear water-level recovery and could be used to calculated hydraulic conductivity. Arithmetic averaging of valid tests was used to obtain a single hydraulic conductivity for each swale. As determined by sediment core descriptions by T. Thompson (Indiana Geological Survey), the top of the diamicton confining layer was considered the base of the unconfined aquifer. I matched calculated hydraulic conductivity to representative values of specific yield (Johnson 1967) presented in Loheide et al. (2005) and interpolated linearly between known values. For swales where slug tests were not performed, water-table recovery of the nearest tested swale was used to calculate hydraulic conductivity, with the assumption that the underlying sands as described in core logs were fairly homogeneous. Because the slug tests for the first method were performed when water levels were at a maximum depth to water table, and specific yield increases within increasing depth (Loheide et al. 2005), the ratio method proved to be more accurate, both spatially and temporally, and was used in subsequent calculations. The slug-test-derived specific yields, however, were used to constrain the maximum allowable specific yield and thereby justify the deletion of outliers produced by the ratio method.

When water levels were below ground, the estimated specific yield was used directly. For flooded conditions, a composite specific yield was used that weighted the relationship between the specific yield of air (1.0) for the depth of standing water and the specific yield estimated by the ratio method for the depth of sediment to the predepositional surface (see Section 2.3.3).

For further sediment description, sand samples were collected from the C horizon of the 15 instrumented wetlands and sent to the Michigan State University Soil and Plant Nutrient Lab (East Lansing, MI), where they were processed for texture analysis.

3.3.3 Water Budget Estimation

In the water balance for individual swales, [Figure 3.2, Equation (1)], no surface-water flows (e.g., overspill) were observed between swales during the growing season; therefore, the losses must have been due to ET and groundwater flow. Changes in storage (ΔS) inferred from measured head elevation changes in a shallow well were estimated as the difference in water depths between midnight and midnight on subsequent days.

$$\pm \Delta S = P - ET \pm G_{net} \pm \xi \,, \qquad (1)$$

In Equation (1), a positive ΔS represents an increase in unit storage (rise in water level), and water level was used to represent change in storage. P represents precipitation, a positive G_{net} represents net input to the swale, and ξ is an error term. G_{net} was estimated as the sum of two components: measured groundwater recovery at the root zone (G_{rec}) and unmeasured deep percolation gains and losses at the swale level (G_{perc}). Groundwater recovery (G_{rec}) occurs when evaporative consumption by plants creates a head differential between the root zone and the recovery source of water, generating flow toward the root zone (e.g., White 1932, Loheide 2008). Deep groundwater gains and losses (G_{perc}) were not estimated directly due to the difficulty in measuring groundwater flow in highly porous unconfined sand aquifers such as this; rapid re-equilibration of head pressures can occur, which often renders traditional methods (i.e., piezometer nests) inadequate for describing groundwater flow (Baedke, personal communication, May 30, 2005; Winter, personal communication, October 24, 2005). Instead, percolation gains and losses (G_{perc}) were inferred by difference in the mass balance of the water budget but also contain the error term (ξ). Daily estimates for ΔS, P, ET, and G_{rec}, G_{perc}, and G_{perc} were summed over monthly and growing-season time periods.

3.3.4 Evapotranspiration and Groundwater

Evapotranspiration (ET) and groundwater recovery (G_{rec}) at 15-min intervals were estimated using a modification to Loheide's (2008) method based on diurnal changes in water level at the location of the well in each swale. Most studies of diurnal water-table fluctuations (e.g., White 1932, Troxell 1936, Meyboom 1967, Laczniak et al. 1999, Gribovszki et al. 2008) have been applied to riparian areas where water levels were below ground. For application to a wider variety of wetland ecosystems, including rain-prone regions, I made the following three modifications: 1) varying the specific yield to account for above- and below-ground water levels as described above, 2) using regression analysis to relate measured ET to Penman-Monteith potential ET for days when the method failed due to precipitation events, and 3) flexibly defining the pre-dawn hours in which ET was negligible. This method and modifications, described in detail in Chapter 2, were programmed in MATLAB R2007a v.7.4.

Gaps in the ET and G_{rec} data were due to inapplicability of the method on days following rain events. To construct a water budget, estimates for those days were needed. For ET, I used a nonlinear power regression to predict actual ET from ASCE reference ET (Allen et al. 2005) (see Chapter 2). To obtain estimates for G_{rec}, I used a linear regression between G_{rec} and ET.

Instrument failure in the form of vandalism occurred at Swale 38 in August 2007. Missing water-budget data for this swale were predicted from regression relationships between 2006 and 2007 data.

3.3.5 Comparisons among Swales

To help understand variability in the water budget among the 15 swales, I performed hierarchical cluster analysis with the Euclidean distance measure and Ward's method using PCORD (McCune and Mefford 1999). I examined growing-season net groundwater flux (G_{net}), groundwater recovery (G_{rec}), net groundwater percolation gains and losses (G_{perc}), evapotranpsiration (ET), change in storage (ΔS), mean July water depth, and the ratio of sources to losses [(G_{net} + precipitation) / ET].

3.4 Results

Total precipitation over the growing season was 337.1 mm in 2006 and 240.8 mm in 2007. Total ET losses over both years averaged 6.3 mm d^{-1}, and groundwater replaced 69-82 % of the water lost by ET (Table 3.2), with greater offset occurring when ET rates were low in the spring and fall (Figure 3.3). ET exceeded annual precipitation by 2.3 to 3.3 times in 2006 and 3.3 to 4.7 times in 2007 and represented evaporative groundwater consumption, as evidenced by the high degree of correlation between ET and G_{rec}, the groundwater recovery in the root zone (Figure 3.4A, Table 3.3).

The net groundwater flux (G_{net}) showed variability between the two years. In 2006, a wet year, the net groundwater flux was positive in all cases, indicating that all swales received more groundwater than they lost. The wetland complex as a whole also gained overall (Table 3.2). In 2007, however, swales had either a net positive or net negative groundwater flux, indicating a discharge or recharge nature, respectively (Table 3.2); discharge swales gained water with respect to the water table, whereas recharge swales lost water over the annual growing season. The integrated effect over the entire wetland complex was a net zero groundwater flux in 2007 (Table 3.2). Net groundwater percolation losses (G_{perc}) were generally smaller for the discharge swales than the recharge swales (Table 3.4), matching a similar pattern in change in storage (ΔS) (Figure 3.4B). The groundwater recovery (G_{rec}), on the other hand, did not show a clear pattern, as it was closely tied to ET (Figure 3.4A).

Greater ET in relation to the sum of precipitation and net groundwater over the growing season was reflected in a source-to-loss ratio [(G_{net} + P)/ET] less than 1.0 in all cases (Table 3.4), which led to a decline in water levels over the growing season for all swales. The 2007 growing season showed smaller source to loss ratios than 2006. The degree of loss in storage was significantly related to the ratio of net groundwater to ET (G_{net}/ET) (Figure 3.4B) and varied between swales (Figure 3.3).

Peak ET occurred earlier in the summer in recharge units with lesser net groundwater flux (G_{net}) such as 17 and 81 (Figure 3.5A, Figure 3.5B) than in discharge swales such as 32 and 73 (Figure 3.5C, Figure 3.5D). Lesser net groundwater and earlier maximum ET rates reflected drier conditions in 2007, resulting in slightly lower ET rates toward the end of the growing season in 2007 than in 2006 (Figure 3.6). Discharge

swales (e.g., 8, 29, 30, 32, 38, 55, 73) experienced less relative change in excess groundwater between the 2006 and 2007 growing seasons (Table 3.4, Figure 3.7).

Furthermore, of the 15 swales studied, those with aquatic vegetation showed less fluctuation in water level over the growing season. Where shrubs or trees dominated, greater drawdowns were observed with a few exceptions. Water levels were maintained nearer the surface in swales 30, 32, and 38, which also were discharge swales (Table 3.3, Table 3.4).

3.5 Discussion

3.5.1 Underlying Geology

Spatial variability in the details of the water balance was observed across the chronosequence reflecting the structural complexity of the site, in terms of underlying stratigraphy, basin morphology, and vegetation. The underlying glacial deposits at this site are particularly complex. The predepositional surface of the strand plain (former beach ridges and intervening swales) consists of areas in which an aquicludal diamicton was detected and areas where it was not (Figure 3.8; T. Thompson, unpublished data). Consequently, the structure consists of areas that impede groundwater flow and conduits that assist it, setting up the potential for a unique hydrologic setting in each swale. For example, swales 30, 32, 38 and 55 showed high groundwater inflow (Table 3.2, Table 3.4) despite variable specific yield and hydraulic conductivity rates (Table 2.1). The diamicton was detected below swales 30 and 32 but was not detected immediately upslope beneath Swale 33 (Figure 3.8, d). The groundwater loading to Swale 38 probably results both from a conduit between impermeable lenses (Figure 3.8, d) and topographically driven flow from the series of upslope swales (Figure 3.8, a).

Conditions of discharge potential similar to Swales 28, 30, and 32 likely provided a groundwater source to Swale 55 as well. Swale 55 lies above what is probably a topographic high on the predepositional surface, as evidenced by diamicton detection directly below the swale (Figure 3.8, e) but much lower along the GPR line (Figure 3.8, b) (Thompson, unpublished data). Topographic highs of the subterranean surface likely drive water up toward the surface at the locations of swales 55 and 73 (Figure 3.8, e, f).

Further evidence for elevated subsurface in these locations is found in the air photo (Figure 2.3). Arcuate ridges contemporaneous with the deposition of ridges near swales 55 and 73 bend toward a single point (to the left of the words "Weather Station" in the figure, in the case of Swale 55). Another high point was located directly north of Swale 55. These points represent former islands around which the ridges formed (Thompson, personal communication, July 2, 2006) and probably extended beneath Swale 55, though at a lower elevation at the location of the sampling site (Figure 3.8).

The moderately large groundwater flow to Swale 8 likely is due to the break in water-table slope that occurred between swales 8 and 14 (Figure 3.8). Also, due to its lower elevation and subsequent proximity to the predepositional surface, flowpaths through the diamicton may reach Swale 8 while not reaching swales 14 and 17, which ranked lowest in groundwater among the swales studied.

The geologic conditions beneath swales 81 and 82 are less clear, as the strand plain thickens considerably progressing away from the lake (Figure 3.8).

Swale morphology and proximity to conduits also play a role in determining the water balance. Interestingly, 37 and 38 are close to one another but have very different water balances. Swale 37 is very narrow (Figure 3.8), whereas Swale 38 is wide with more trees than the other swales in the study (unpublished data). Groundwater comes from shallow flow paths from the upslope ridges and from below in Swale 38. Discharge probably occurs primarily on the upslope side of the swale, however, and little of the groundwater reaches 37.

3.5.2 ET and Water Storage

The complexity of the substrata led to variability in groundwater contribution to the various swales, allowing examination of the effects of groundwater on water storage and evapotranspiration (ET). My results suggest that plants, by evaporative consumption, assist in drawing water to the swales (Figure 3.4B), but groundwater delivery in excess of that drawn by plants increases the amount of ET that can occur (Figure 3.4A). This is evidenced by the plot of net percolation (G_{perc}) against change in storage (ΔS) (Figure 3.4A), which suggests that more supplemental groundwater (i.e., not due to evaporative consumption) results in less change in storage, thereby maintaining wetter conditions

throughout the growing season. This trend was observed for most months, with the exception of July, suggesting that groundwater influence is decoupled from storage due to the greater effect of ET in July (Table 3.3).

Conversely, in swales that recharged the water table, plants drove water levels down over the summer, likely leading to self-reduction in ET. Even though the water table did not fall below rooting zone (Figure 2.5B), lowering the water table decreased soil moisture (unpublished data) and limited ET over the growing season (Figure 3.6). Peak ET occurred earlier in the summer in recharge swales such as 17 and 81 (Figure 3.5A, Figure 3.5B) than in discharge swales such as 32 and 73 (Figure 3.5C, Figure 3.5D).

3.5.3 Vegetation Types

Prior to this study, I expected the water balance to be similar for swales with similar dominant vegetation (e.g., herbaceous, shrub, forested), but this was not the case. For example, both high and low ET rates occurred in all swale vegetation types, (Table 3.3). Within the respective hydrogeologic constraints of the swales, however, differences in vegetation structure (forested, shrub, herbaceous) appeared to affect water–balance dynamics. For example, reduced storage loss generally occurred in herbaceous swales than shrub or forested types with one notable exception, Swale 55. More trees in this swale than in other herbaceous aquatic swales (unpublished data) may have contributed to higher ET rates and greater storage loss there (Table 3.2, Table 3.4). The results of this analysis suggest that the mechanisms governing the interactions between ET and hydrogeology cannot be described by the vegetation class alone. Rather, they are influenced by both the biology and the hydrogeologic setting. The relative influences and interactions between these drivers is the topic of my next chapter.

3.5.4 Temporal variation

Temporal distribution in ET and groundwater was very similar for all swales in 2006 when climatic conditions were wetter than in 2007; peaks occurred at about the same time and gradually tapered off before and after (Figure 2.7). On the other hand, drier conditions in 2007 (NOAA 2009) led to greater temporal variability in both ET and

groundwater. Specific unit response reflected the relative contribution of groundwater; where groundwater in excess of evaporative consumption was more plentiful, greater ET proceeded later into the summer.

The water-table rebound that was observed in 2006 but not in 2007 was related to climate conditions as well. As ET decreased and eventually ceased in October of 2006, fall rains led to a rise in the water table. The water table rebounded in 2006 due to a very moist spell tending toward extremely wet conditions according to the Palmer Drought Severity Index (NOAA 2009). Conversely, a moderate drought occurred in September and October of 2007, and the precipitation necessary for bringing water levels back up did not occur.

In addition to seasonal variability, annual differences in the water budget were observed between 2006 and 2007. ET and groundwater recovery (G_{rec}) showed an increase or decrease depending on the specific biological and hydrogeological conditions of the particular swale. Drier conditions in 2007 led to lesser net groundwater fluxes (G_{net}) (Figure 3.7, Table 3.2). Swales that had greater net groundwater fluxes, however, experienced less change between years (Figure 3.7). As a result, plants were less water limited in these groundwater-supplemented swales, and higher ET rates proceeded later into the growing season (Figure 3.5).

3.5.5 Groundwater Terms

Net percolation gains and losses (G_{perc}), calculated by difference in the water balance, included percolation losses after rains as well as any other fluxes (e.g., lateral fluxes, error terms) not accounted for by the Loheide (2008) method, which is applicable only in the absence of precipitation when the water table declines in a regular diurnal pattern. Following rain events, water infiltrated the sandy soil and moved by shallow groundwater flow reflecting percolation loss, as evidenced by a rapid decrease in water table immediately following rainstorms (Figure 2.5B). Some of the loss could be due to increased ET resulting from more soil water availability to plants. For example, Cooper et al. (2006) observed highest ET rates following summer rains. In this study, high ET rates during August and September of 2007 when soil conditions were driest also occurred following rain events (Figure 3.5). Nonetheless, most of the water represented

by the rapid decline in water table directly following rainstorms is likely due to deeper percolation. Lateral fluxes may also be incorporated into the net percolation groundwater term (G_{perc}). The Loheide (2008) method assumes that the rate of change at the well fluctuates in the same manner as the rate of change of the recovery source that supplies water to the location of the well. When this is not the case, the groundwater percolation term includes any deviation from that. Some indication exists to suggest that for the most part, except following rain events, the assumption holds; time rate of change of the water table at the top of the ridge-swale sequence (i.e., deep well at Ridge 87) is similar to time rate of change of nearby swales (e.g., 81 and 82). Whether this is true for all swales is undocumented, though, and the definition of the recovery source is somewhat ambiguous in this setting due to the complexity of the underlying geology.

Nonetheless, the net percolation term (G_{perc}) accounts for these types of unknowns. Furthermore, it can be used as an indication of deep groundwater influx. In all swales, G_{perc} was a negative value, but a greater value (i.e., less negative) is an indication that deep groundwater may be discharging in that zone.

3.5.6 Inter-Annual Variability and Implications for Climate Change

Climate predictions indicate that the Great Lakes will become warmer and wetter overall, but drier in the summer months (Wuebbles and Hayhoe 2004). Daily high temperatures are predicted to increase by 3 to 6 °C compared to the 1961-1990 normal. Longer growing seasons will begin 15-35 days earlier in the spring and extend 35 days later in the fall. A thirty-percent increase in winter-spring precipitation likely will be matched by a similar decrease in summer-fall precipitation (Wuebbles and Hayhoe 2004), with heavier precipitation events likely (Solomon et al. 2007).

Overall, climate effects on wetlands are complicated, as warmer temperatures have a positive effect on ET rates, but drier soil conditions lead to a decrease in ET and lower water tables in general. Increased annual precipitation, especially if concentrated in the winter and spring months when groundwater recharge occurs, will lead to more groundwater availability. Greater spring rains may also result in higher water tables at the start of the growing season, but less rain in the summer and fall, coupled with a longer

growing season, could lead to greater water-table depression by the end of the growing season.

Fortuitously, the two years of this study encompassed a wet year (2006) and a dry year (2007). If the climate of the Great Lakes region maintains a trajectory toward drier conditions in summer and fall as predicted by many climate models (Wuebbles and Hayhoe 2004), the second year of this study, being drier than normal, is an indication of that climatic shift. Under drier conditions, the results of this study suggest that some swales (i.e., recharge swales) will lose what groundwater buffers they had, and ET will drive water levels even lower, whereas the discharge swales may be unaffected. A net flux into the wetland complex as a whole occurs in wet years that does not appear to occur in dry years (Table 3.2). This may be due to greater regional groundwater head pressures from below the confining layer forcing water toward the surface in wet years but not in dry. This could occur if there was greater recharge in the larger landscape due to heavy spring rains or greater snowmelt in that year. A net flux into the wetland complex also could also be due to higher water-table elevations in the immediate vicinity at the top of the ridge-swale sequence providing increased flux to the wetland complex downslope. Higher water levels in this area would be due to local recharge by precipitation. This effect may or may not be significant, depending on elevational and head pressures of the upslope area relative to the swales, but the source water body is limited, as the groundwater divide that partitions the ridge-swale complex from a river watershed to the west is only about 250 m from the uppermost swale (Swale 82).

The drier growing season conditions probably will result in more differentiation between swales in terms of the vegetation; some swales not fed by groundwater will receive supplemental groundwater, and ET rates may increase. Groundwater should mediate climate change effects in these swale wetlands as well by slowing vegetation change associated with long-term soil drying, which proceeds in ridge-swale wetlands on a trajectory toward drier conditions in the absence of groundwater (Shedlock et al. 1993, Burkett et al. 2005). If the swales currently receiving high discharge become further inundated, flooded conditions could inhibit ET, and overall unit losses could conceivably be somewhat reduced. On the other hand, the increase in groundwater may not offset

higher ET rates, increasing the role of ET in the water balance. These and related system dynamics will be addressed further in the next chapter.

3.5.7 Site Individuality

Differences in the fluxes controlling the water balance give interesting spatial and temporal variability to this wetland complex. The individuality of each swale's water budget reflects mechanisms that govern both site hydrology and biology. This research supports theory arising from the hydrogeomorphic classification literature (e.g., Brinson, 1993) that site-specific factors affecting the water balance of wetlands are important for understanding wetland development, maintenance, and succession. Spatial variation in the underlying stratigraphy ultimately leads to differences in groundwater flux. The absolute flux rates are strongly influenced by climatic variability. Nonetheless, some swales always receive greater groundwater loading than others (designated discharge and recharge swales in Table 3.2). Evapotranspiration by plants both brings water to the swale and removes it (Figure 3.4B). In this sense, plants help determine the water supply available to them. Where water availability in the rooted zone is higher, however, ET generally proceeds at higher rates, although there is some hint of ET suppression in very wet swales (Figure 3.9). In this manner, water availability controls ET by plants. Where groundwater availability is relatively low (in dry years and especially in recharge swales), plant ET has a greater control over water availability (Figure 3.10). The type of plant community appears to have a secondary effect on ET, explaining some variance among swales having similar water availability, but the relationship is not well-defined (Figure 3.11). This topic will also be addressed in more detail in my next chapter.

Table 3.1. Weather data from the on-site weather station at Negwegon State Park at the location shown in Figure 2.3.

Variable	2006			2007		
Length of record [d]	144	(May 20 - Oct 11)		144	(May 20 - Oct 11)	
Total precipitation, P_T [mm, growing season]	337.1			240.8		
	Mean	Min	Max	Mean	Min	Max
Precipitation, P [mm d^{-1}]	2.3	0.0	40.9	1.7	0.0	26.2
Air temperature, T_a [ºC]	17.1	-1.9	36.3	12.2	-17.9	34.2
Wind speed, u [m s^{-1}]	1.9	0.0	15.7	1.9	0.0	17.9
Relative humidity, RH [%]	78.4	0.0	97.0	77.1	20.0	98.0
Incoming solar radiation, R_a [MJ m^{-2} day^{-1}]	15.0	0.0	88.7	16.5	0.0	88.2

Table 3.2. Water balance results over the growing season (May 20 to Oct. 11, 145 days) for the entire wetland complex and the 15 study swales. Units are in mm. The net groundwater flux (G_{net}) represents the sum of the groundwater recovery in the root zone (G_{rec}) and the percolation gains and losses (G_{perc}) to the unit. Physiographic character is determined from the direction of net groundwater flux (G_{net}) in 2007 (R = recharge, negative G_{net}; D = discharge, positive G_{net}). Due to instrument failure, data were unavailable for Swale 38 in 2007; values listed for Swale 38 are estimates predicted from regression between 2006 and 2007 data among all swales.

	Wetland	Swale														
Component	Complex	8	14	17	26	28	29	30	32	37	38	55	73	78	81	82
2006																
Precipitation	337	337	337	337	337	337	337	337	337	337	337	337	337	337	337	337
Groundwater																
Recovery (G_{rec})	681	613	763	594	580	632	584	685	747	612	732	746	846	674	742	671
Percolation (G_{perc})	-399	-374	-560	-458	-353	-347	-342	-372	-369	-339	-346	-323	-479	-440	-465	-421
Total flux (G_{net})	282	239	203	136	227	286	241	313	377	273	387	424	367	234	277	250
ET	894	766	955	864	787	866	775	839	956	831	946	930	1128	832	1011	921
Change in storage	-275	-190	-415	-391	-223	-244	-197	-189	-242	-221	-222	-169	-424	-262	-397	-334
2007																
Precipitation	241	241	241	241	241	241	241	241	241	241	241	241	241	241	241	241
Groundwater																
Recovery (G_{rec})	705	673	820	627	584	647	653	689	697	672	752	790	891	727	727	632
Percolation (G_{perc})	-703	-595	-887	-727	-677	-698	-597	-609	-593	-694	-655	-688	-813	-737	-788	-783
Total flux (G_{net})	3	79	-68	-100	-93	-51	56	81	104	-22	97	102	78	-10	-61	-151
ET	924	836	1073	871	809	859	891	881	924	898	963	973	1133	902	984	856
Change in storage	-680	-516	-900	-731	-661	-670	-594	-559	-579	-678	-626	-630	-814	-672	-804	-766
Physiographic Character	-	D	R	R	R	R	D	D	D	R	D	D	D	R	R	R

Table 3.3. Pearson correlations between storage loss (ΔS) and groundwater recovery (G_{rec}), net groundwater percolation (G_{perc}), and net groundwater fluxes ($G_{net} = G_{rec} + G_{perc}$), for months of the growing season and overall. A positive correlation indicates a smaller storage loss associated with a greater G_{rec}, G_{perc}, or G_{net}.

	Correlation		
Time Interval	ΔS and G_{rec}	ΔS and G_{perc}	ΔS and G_{net}
2006			
May	-0.480	0.97	0.961
Jun	-0.802	0.992	0.951
Jul	-0.217	0.98	0.734
Aug	-0.086	0.985	0.912
Sep	0.421	0.969	0.927
Oct	0.197	0.996	0.987
Growing season	-0.441	0.898	0.343
2007			
May	-0.195	0.995	0.947
Jun	-0.671	0.995	0.956
Jul	0.092	0.979	0.712
Aug	0.306	0.993	0.931
Sep	0.036	0.954	0.805
Oct	-0.563	0.998	0.936
Growing season	-0.424	0.973	0.599

Table 3.4. Groups of swales identified by hierarchical cluster analysis based on net growing-season groundwater (G_{net}), shallow groundwater recovery (G_{rec}), net deep percolation flux (G_{perc}), evapotranspiration (ET), ratio of sources (groundwater, $G_{rec} + G_{perc}$; precipitation, P) to losses (ET), change in storage (ΔS), and two-year (2006 and 2007) mean July depth to water table (L = large, ML = moderate-large, M = moderate, MS = moderate-small, S = small). A negative depth indicates a below-ground water table. A large groundwater value (G_{net}, G_{rec}) indicates greater groundwater flow or less net percolation loss (more deep groundwater influx), in the case of G_{perc}. Physiographic character (D = discharge, R = recharge) was determined for each unit by 2007 G_{net} values. Vegetation types by which swales were stratified also are shown (H = herbaceous aquatic/emergent marsh, S = scrub-shrub, F = forested).

							(G_{net} + P) / ET					Mean July Depth to Water Table [mm]		
Group	Swale	Physiography	G_{net}	G_{rec}	G_{perc}	ET	2006	2007	Cluster	2007/ 2006	ΔS	Depth	Cluster	Vegetation Type
1	55	D	L	L	M	L	0.82	0.35	L	L	S	-305	deep	H
	38	D	L	M	M	L	0.76	0.34	L	L	S	-170	moderate	F
	32	D	L	M	L	L	0.74	0.37	L	L	S	-187	moderate	S
	73	D	L	L	S	L	0.62	0.28	M	L	L	-362	deep	S
2	30	D	ML	M	L	M	0.77	0.36	L	L	S	-115	shallow	S
	8	D	ML	S	L	S	0.75	0.38	L	L	S	-77	shallow	H
	29	D	ML	S	L	M	0.74	0.33	L	L	S	-55	shallow	H
3	37	R	MS	S	M	M	0.73	0.24	M	S	MS	-210	moderate	S
	28	R	MS	S	M	M	0.72	0.22	M	M	MS	-93	shallow	H
	78	R	MS	M	S	M	0.68	0.25	M	S	MS	-181	moderate	F
	81	R	MS	M	S	L	0.61	0.18	S	M	L	-365	deep	S
4	26	R	S	S	M	S	0.71	0.18	M	M	MS	-51	shallow	H
	14	R	S	L	S	L	0.56	0.15	S	M	L	-309	deep	F
	82	R	S	S	S	M	0.64	0.10	S	S	ML	-299	deep	F
	17	R	S	S	M	M	0.55	0.16	S	M	ML	73	shallow	F

Figure 3.1. Field site at Swale 28 in May (top) and August (bottom) of 2007 showing variation in water depth and vegetation over the growing season.

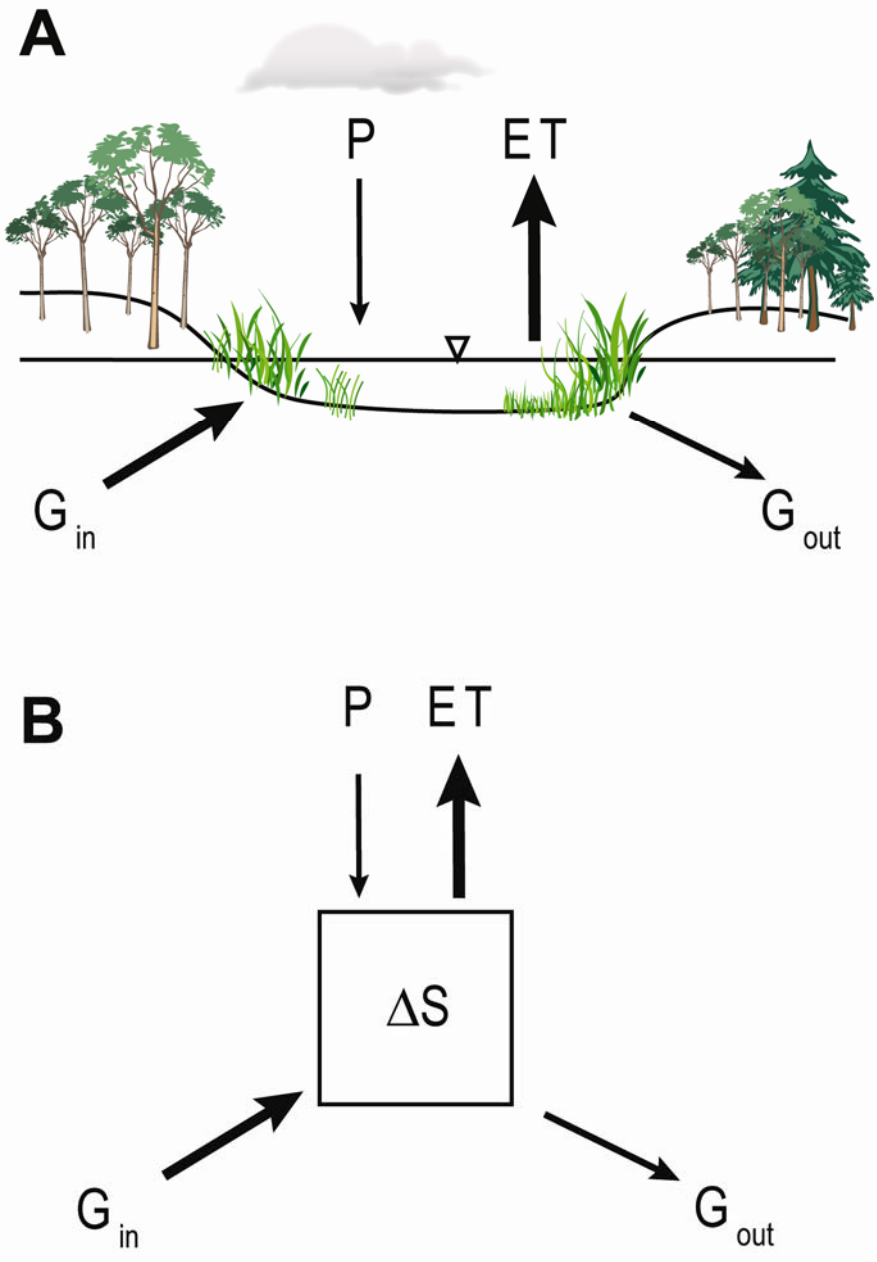

Figure 3.2. Conceptual schematic of the natural wetland in cross-section (A) and box-and-arrow diagram (B) of the growing-season wetland water balance (P = precipitation, ET = evapotranspiration, G_{in} = groundwater inflow, G_{out} = groundwater outflow, ΔS = change in storage). Difference in size of arrow indicates conceptual idea of the relative magnitudes of fluxes in and out of the wetlands in this study.

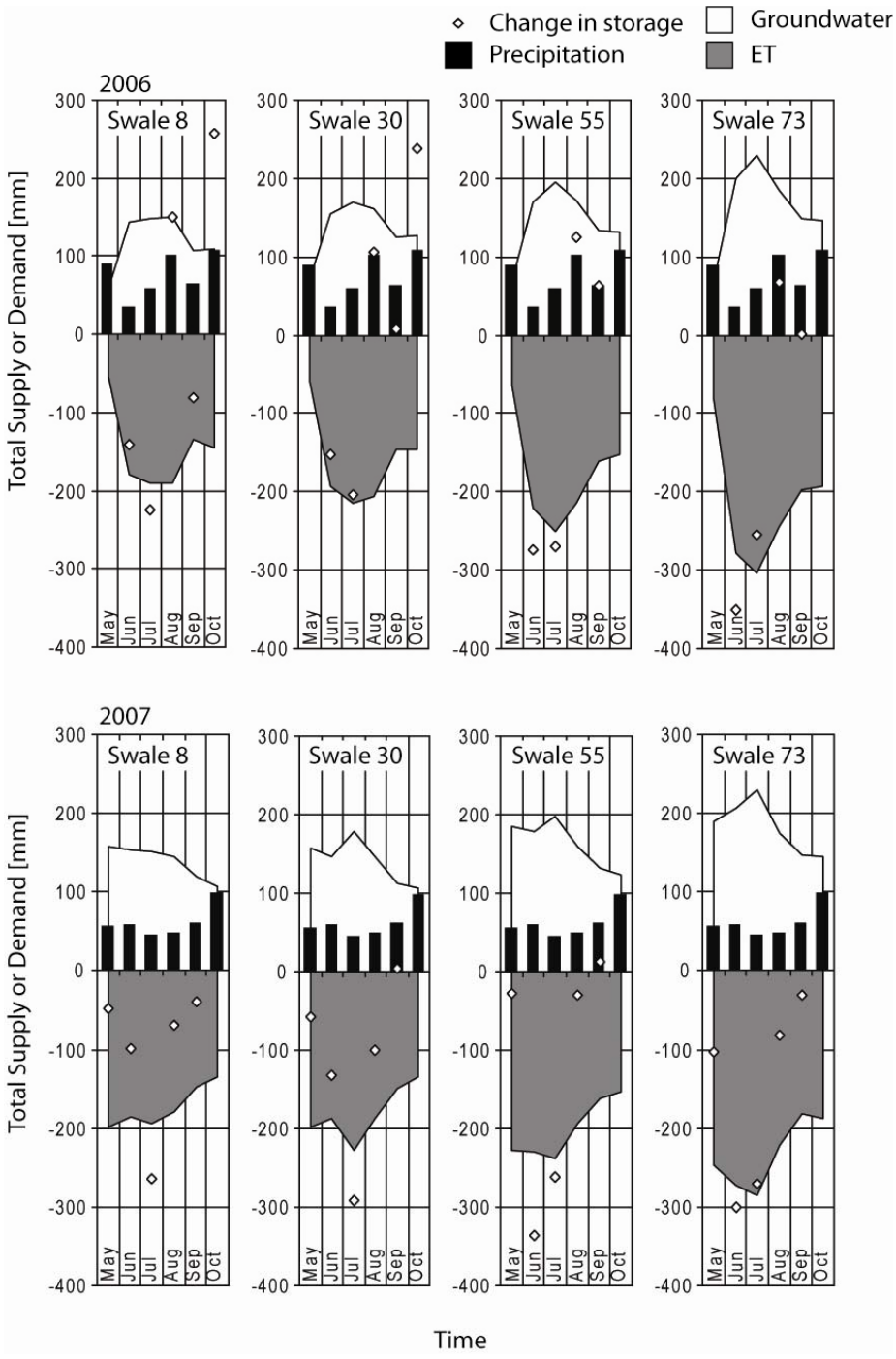

Figure 3.3. Total monthly groundwater supply (G_{rec}) (white), ET demand (ET) (gray), precipitation (black bars), and measured change in storage (white dots) over the growing season for four of the 15 swales studied. May and October values were extrapolated from mean values that were based on 11 and 10 days of the month, respectively, whereas June-September values were based on the entire month.

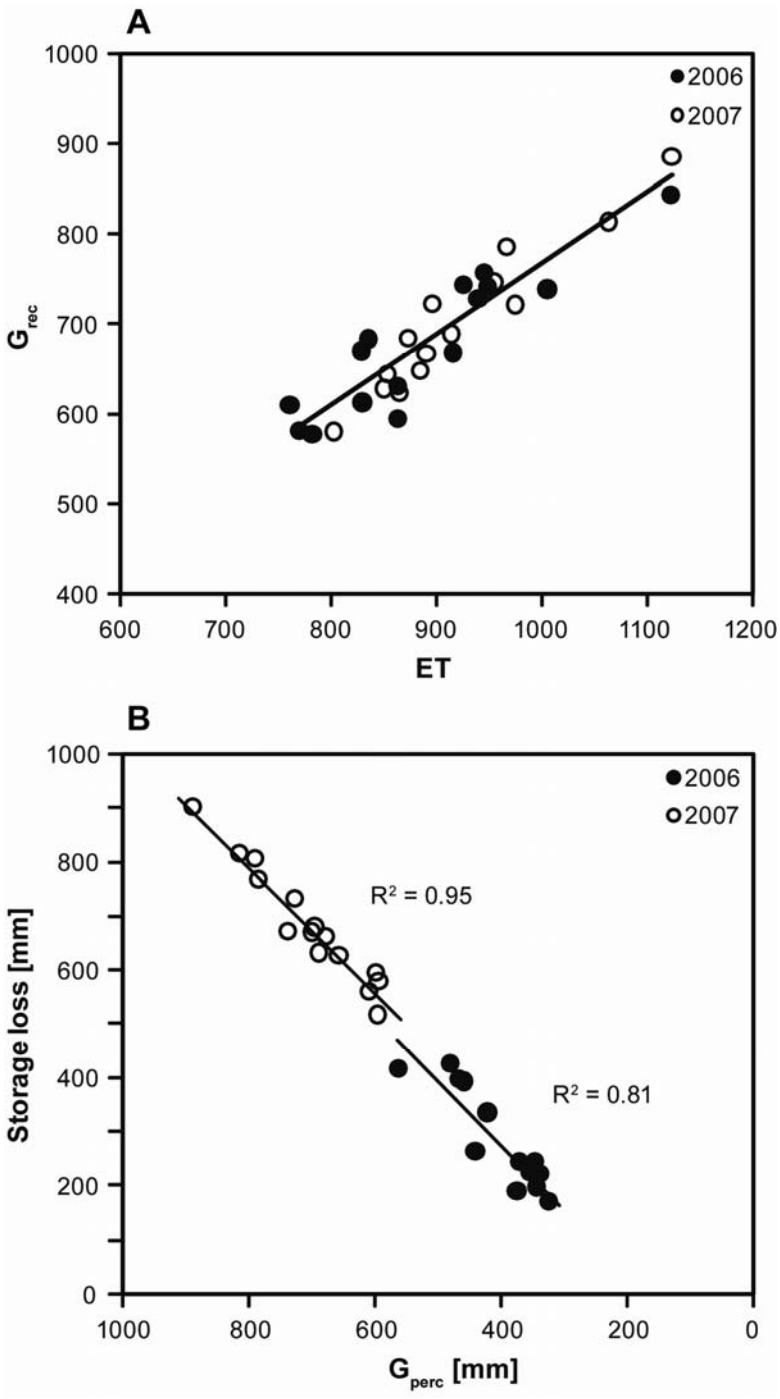

Figure 3.4. Growing-season groundwater (G_{rec}) [mm] plotted against evapotranspiration (ET) [mm] for all swales in 2006 and 2007 (A), demonstrating evaporative groundwater consumption (R^2 for 2006 and 2007 = 0.86). Storage loss [mm] plotted against net groundwater percolation G_{perc} [mm] over the 2006 and 2007 growing seasons (B), showing that where net percolation loss is less (i.e., in discharge swales), storage loss is reduced.

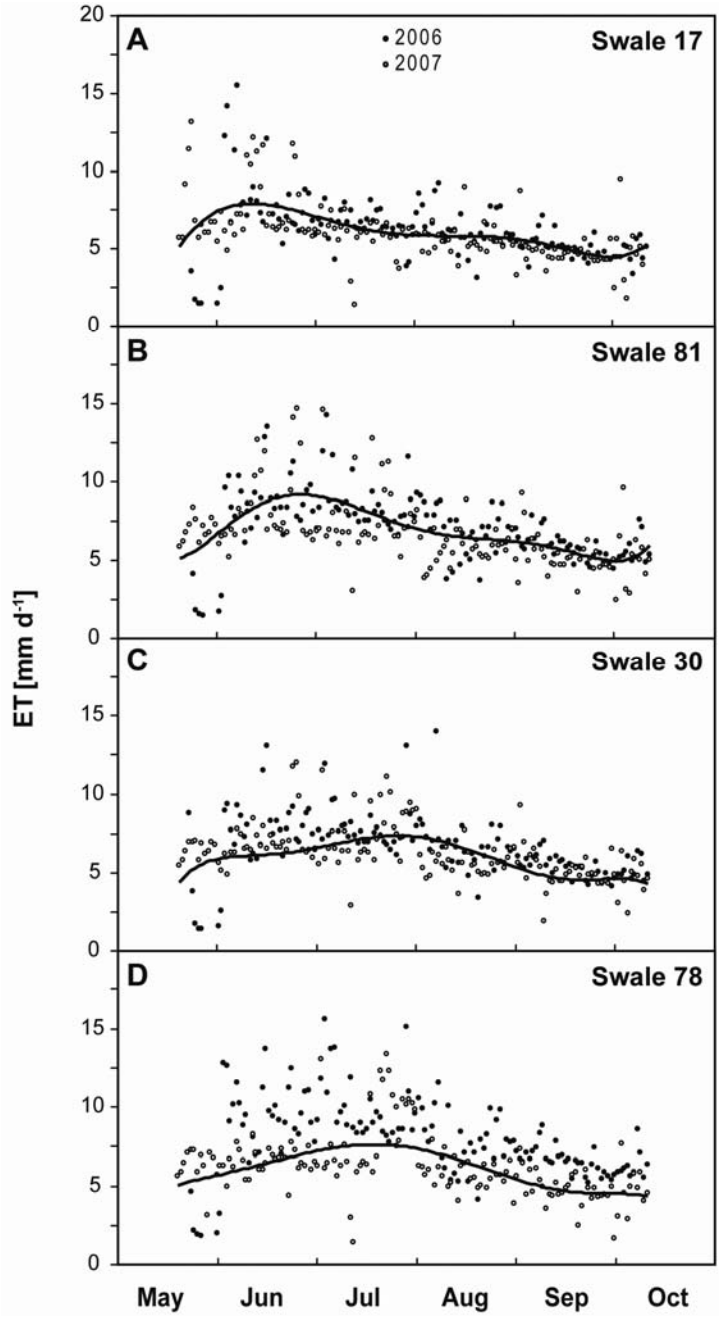

Figure 3.5. Plot of daily ET [mm] against time [d] displayed by month and overlaying 2006 and 2007 data. Trend lines represent sixth-order polynomial of 2006 and 2007 combined data. Swales 17 (A) and 81 (B) showed a recharge character and peaked earlier than swales 32 (C) and 73 (D), both discharge swales, which sustained higher ET rates later into the summer.

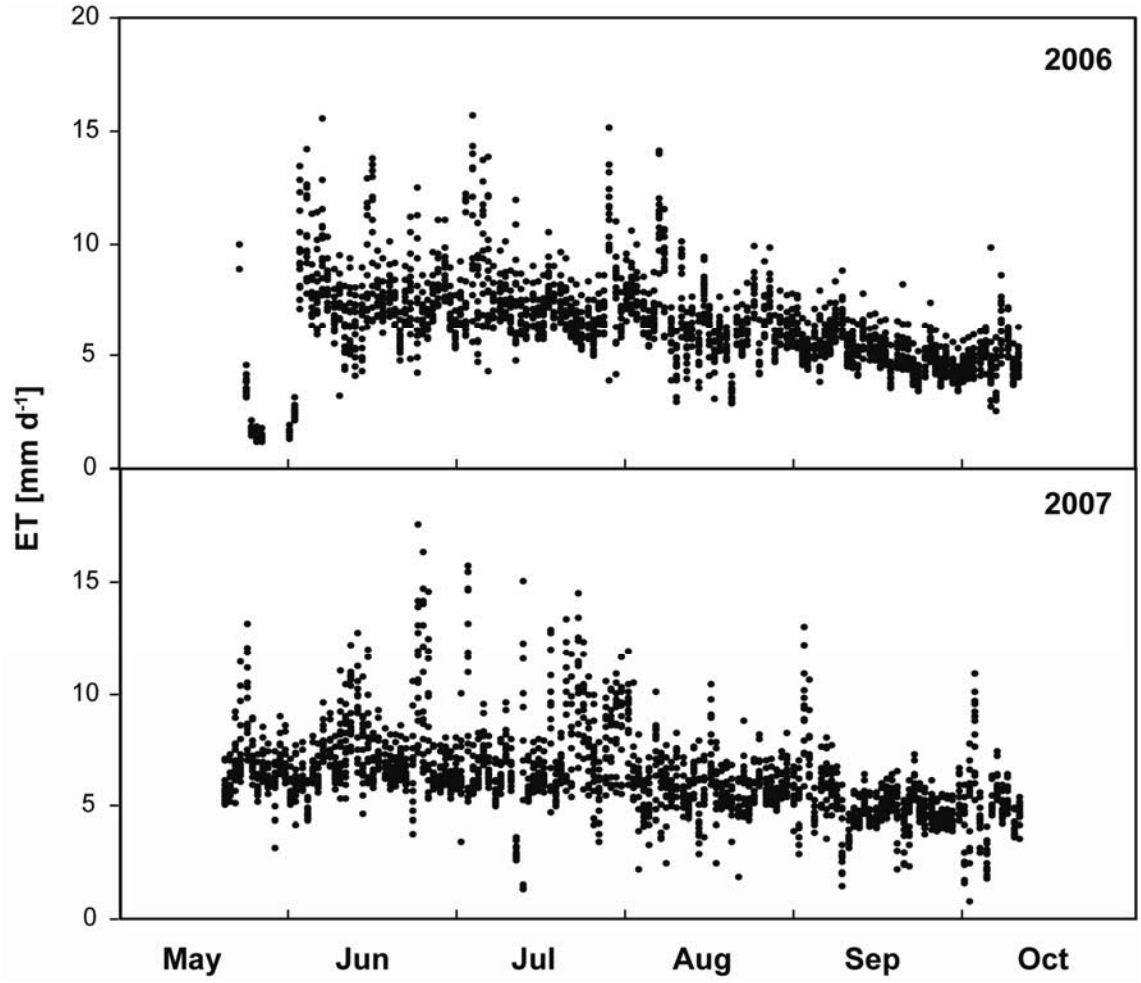

Figure 3.6. Daily ET rates [mm] for all swales in 2006 (A) and 2007 (B) showing a reduction in ET rate toward the end of the growing season as water became slightly more limiting relative to the early months.

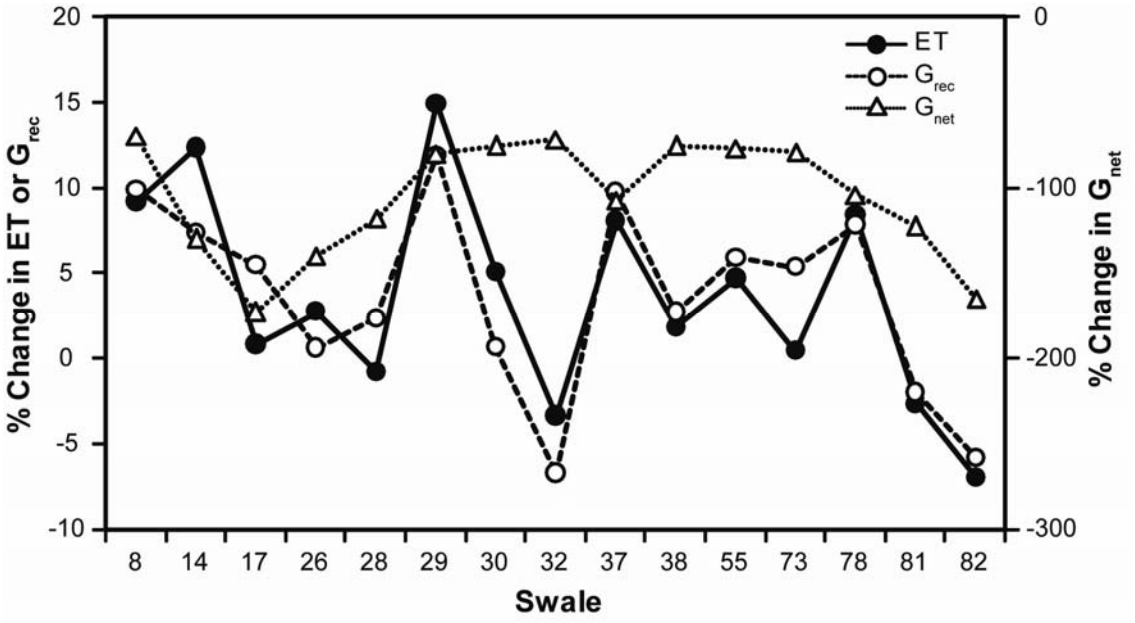

Figure 3.7. Percent change from 2006 to 2007 plotted by swale for evapotranspiration (ET), groundwater due to evaporative consumption (G_{rec}), and net groundwater flux (G_{net}). Changes in ET and G_{rec} varied in tandem depending on the specific biological and hydrogeologic setting of the particular swale. Swales having a discharge character in 2007 ($G_{net} > 0$) (e.g., 8, 29, 30, 32, 38, 55, 73) experienced less relative change between 2006 and 2007 than did recharge swales (e.g., 14, 17, 26, 37, 78, 81, 82).

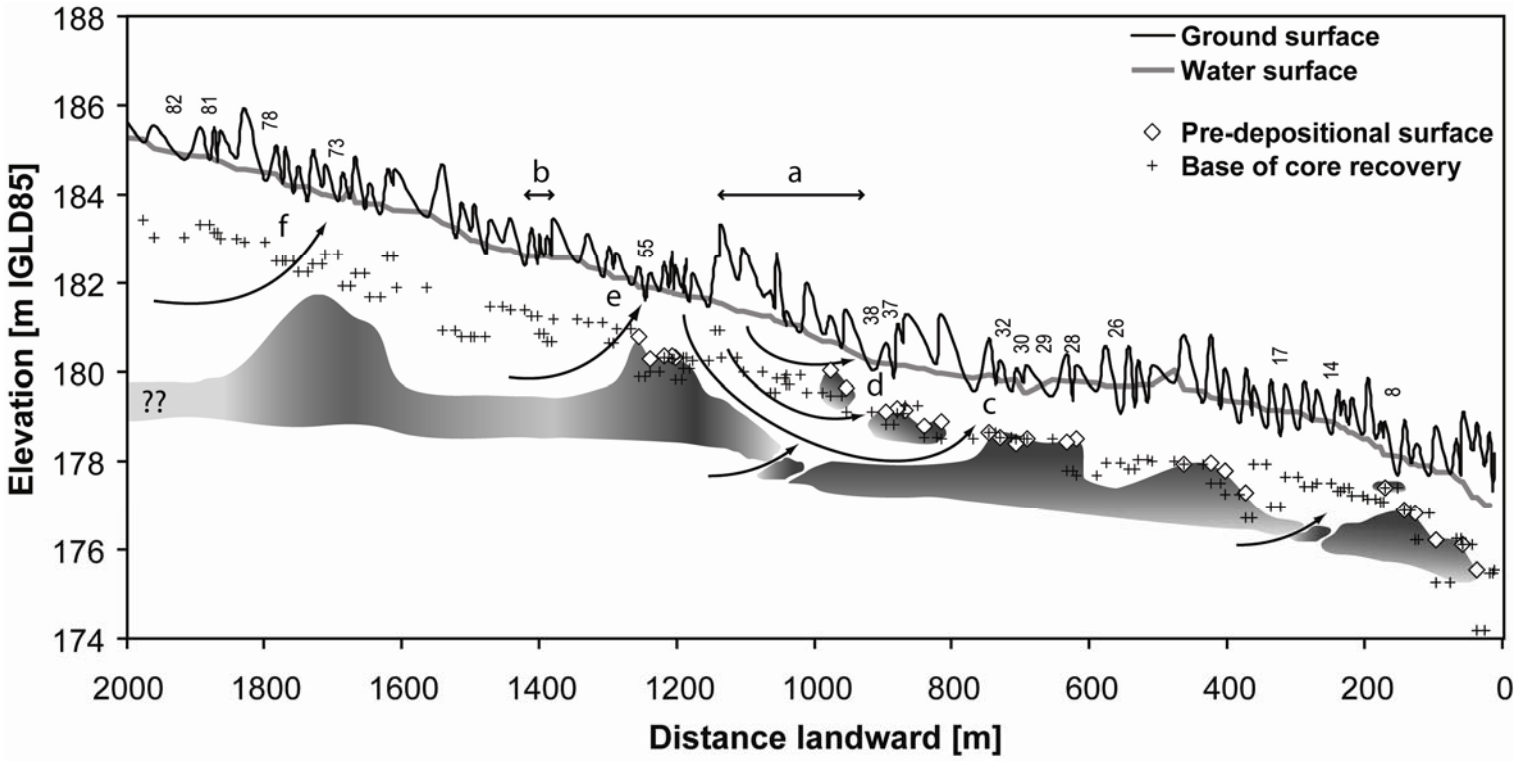

Figure 3.8. Cross-section of the ridges and swales at the study site. Studied swales are marked with numbers that correspond to sites in Figure 2.3. Ground surface and water surface (circa June, 2004) were provided by T. Thompson of the Indiana Geological Survey, as well as sediment cores and ground-penetrating-radar data from which the pre-depositional surface was estimated. Diamonds show cores in which the diamicton was observed. Gray areas indicate locations of the diamicton layer, as interpolated from cores and groundwater-flow data. Curved arrows depict possible groundwater flow paths.

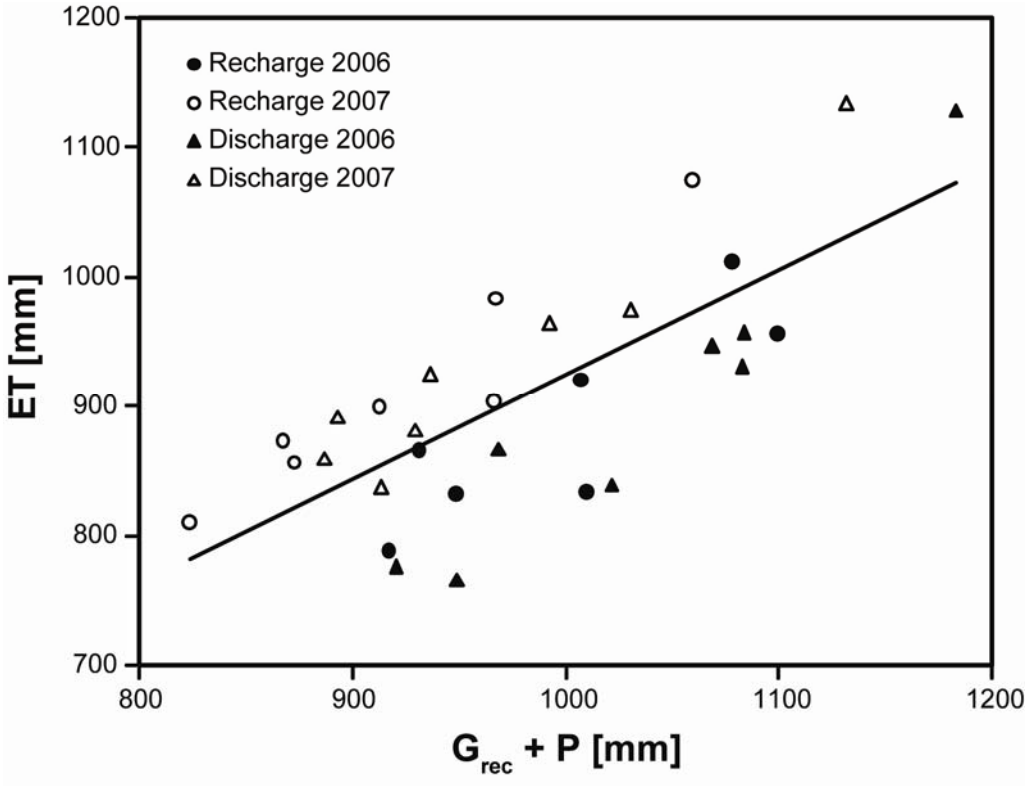

Figure 3.9. Plot of ET against groundwater recovery (G_{rec}) plus precipitation (P), as an indicator of water that may be available in the rooted zone. ET generally proceeds at a high rate for greater G_{rec} + P, although some indication of ET suppression in very wet swales is apparent.

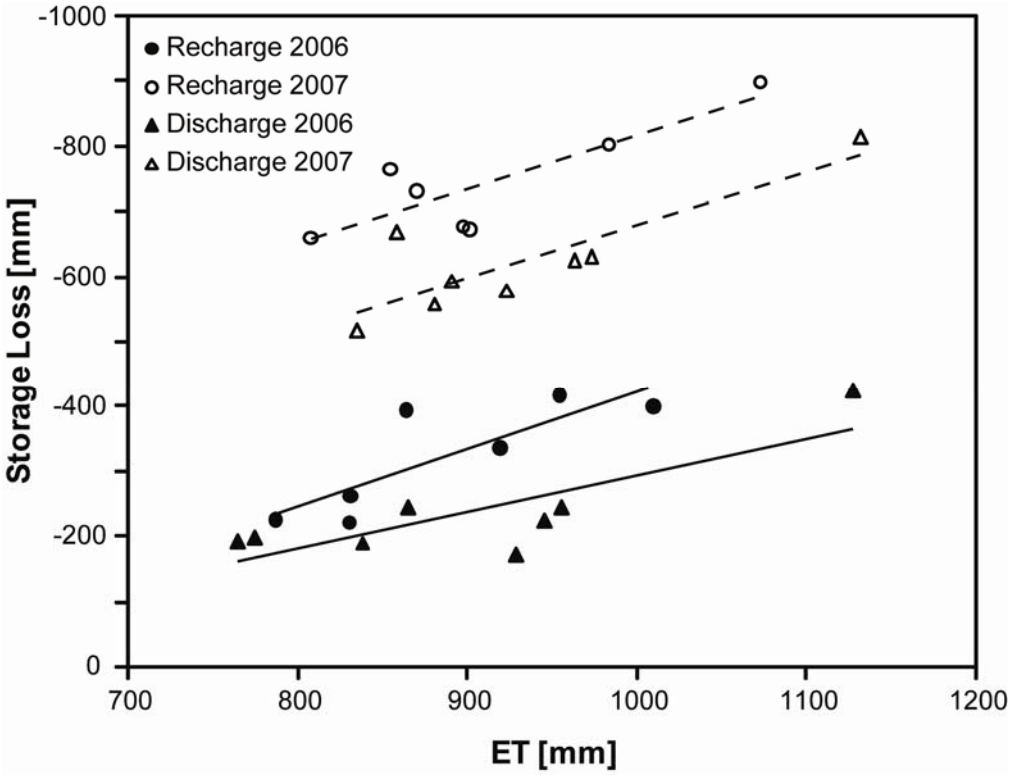

Figure 3.10. Plot of storage loss against ET for the recharge and discharge swales in 2006 (wet year) and 2007 (dry year).

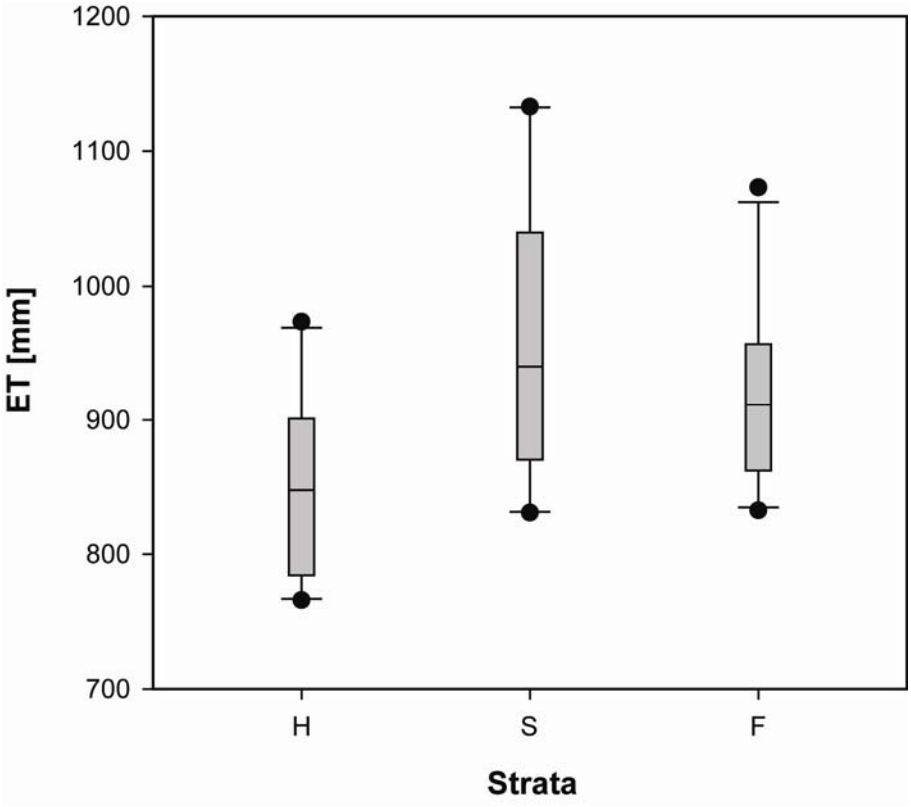

Figure 3.11. Box plot of ET by swale vegetation strata (H = herbaceous ground cover, S = scrub-shrub understory, F = forested understory), showing the possible effect of differences in vegetation on ET.

REFERENCES CITED

Allen, R. G., I. A. Walter, R. L. Elliott, T. A. Howell, D. Itenfisu, M. E. Jensen, and R. L. Snyder. 2005. The ASCE Standardized Reference Evapotranspiration Equation. American Society of Civil Engineers, Reston, VA, USA.

Bouwer, H. 1989. The Bouwer and Rice slug test - an update. Ground Water 27:304–309.

Brady, N. C. and R. R. Weil. 2002. The Nature and Property of Soils. Thirteenth edition. Prentice-Hall, Upper Saddle River, NJ, USA.

Brinson, M. M. 1993. Hydrogeomorphic classification for wetlands. Wetlands Research Program Technical Report WRP-DE-4. U.S. Army Corps of Engineers, Washington, DC, USA.

Burkett, V. R., D. A. Wilcox, R. Stottlemyer, W. Barrow, D. B. Fagre, J. Baron, J. Price, J. L. Nielson, C. Allen, D. L. Peterson, G. Ruggerone, and T. Doyle. 2005. Nonlinear dynamics in ecosystem response to climatic change: case studies and management implications. Ecological Complexity 2:357–394.

Carter, V. 1986. An overview of the hydrologic concerns related to wetlands in the United States. Canadian Journal of Botany 64:364–374.

Cleveland, W. S. 1979. Robust locally-weighted regression and smoothing scatterplots. Journal of the American Statistical Association 74:829–836.

Cleveland, W. S., S. J. Devlin, and E. Grosse. 1988. Regression by local fitting: methods, properties, and computational algorithms. Journal of Econometrics 37:87–114.

Cooper, D. J., J. S. Sanderson, D. I. Stannard, and D. P. Groeneveld. 2006. Effects of long-term water table drawdown on evapotranspiration and vegetation in an arid region phreatophyte community. Journal of Hydrology 325:21–34.

Doss, P. K. 1993. The nature of a dynamic water table in a system of non-tidal, freshwater coastal wetlands. Journal of Hydrology 141:107–126.

Erwin, K. L. 1989. Wetland evaluation for restoration and creation. p. 239–254. *In* J. A. Kusler and M. E. Kentula (eds.) Wetland creation and restoration: the status of the science, Vol. 1. USEPA EPA 600/3–89/038b, USEPA, Washington, DC, USA.

Ferris, J. G., D. B. Knowles, R. H. Brown, and R. W. Stallman. 1962. Geological Water-Supply Paper 1536-E. United States Government Printing Office, Washington, DC, USA.

Fetterer, C. W. 2001. Applied Hydrogeology. Fourth edition. Prentice Hall, Upper Saddle River, NJ, USA.

Gerla, P. J. 1992. The relationship of water-table changes to the capillary fringe, evapotranspiration, and precipitation in intermittent wetlands. Wetlands 12:91–98.

Gonthier, G. J. 2007. A graphical method for estimation of barometric efficiency from continuous data: concepts and application to a site in the Piedmont, Air Force Plant 6, Marietta, Georgia. Scientific Investigation Report 2007-5111, U.S. Geological Survey, Reston, VA, USA.

Gribovszki, Z., P. Kalicz, J. Szilagyi, and M. Kucsara. 2008. Riparian zone evapotranspiration estimation from diurnal groundwater level fluctuations. Journal of Hydrology 349:6–17.

Johnson, A. I. 1967. Specific yield - compilation of specific yields for various materials. Geological Water Supply Paper 1662-D, United States Government Printing Office, Washington, DC, USA.

Laczniak, R. J., G. A. DeMeo, S. R. Reiner, J. L. Smith, and W. E. Nylund. 1999. Estimates of groundwater discharge as determined from measurements of evapotranspiration, Ash Meadows area, Nye County, Nevada. Water-Resources Investigation Report 99-4079, U.S. Geological Survey, Reston, VA, USA.

Loheide, S. P. 2008. A method for estimating subdaily evapotranspiration of shallow groundwater using diurnal water table fluctuations. Ecohydrology 1:59–66.

Loheide, S. P., J. J. Butler, and S. M. Gorelick. 2005. Estimation of groundwater consumption by phreatophytes using diurnal water table fluctuations: a saturated-unsaturated flow assessment. Water Resources Research 41:1–14.

McCune, B., and M. J. Mefford. 1999. Multivariate Analysis of Ecological Data Version 4.0. MjM Software, Gleneden Beach, OR, USA.

Meyboom, P. 1967. Groundwater studies in the Assiniboine River drainage basin—Part II: Hydrologic characteristics of phreatophytic vegetation in south-central Saskatchewan, Bulletin – Geological Survey of Canada, 139.

Mitsch, W. J. and J. G. Gosselink. 2000. Wetlands. Third edition. John Wiley & Sons, Inc., New York, NY, USA.

National Oceanographic and Atmospheric Administration National Weather Service Climate Prediction Center (NOAA). 2009. Drought Monitoring. http://www.cpc.noaa.gov/products/monitoring_and_data/drought.shtml.

Posner, R. N., J. M. Bell, S. J. Baedke, T. A. Thompson, and D. A. Wilcox. 2005. Aqueous geochemistry as an indicator of subsurface geology and hydrology of a beach-ridge/wetland complex in Negwegon State Park, MI. Geological Society of America Abstracts with Programs 37:300.

Restrepo, J. I., A. M. Montoya, and J. Obeysekera. 1998. A wetland simulation module for the MODFLOW groundwater model. Groundwater 36:764–770.

Rosenberry, D. O. and T. C. Winter. 1997. Dynamics of water-table fluctuations in an upland between two prairie-pothole wetlands in North Dakota. Journal of Hydrology 191:266–289.

Shedlock, R. J., D. A. Wilcox, T. A. Thompson, and D. A. Cohen. 1993. Interactions between groundwater and wetlands, southern shore of Lake Michigan, USA. Journal of Hydrology 141:127–155.

Solomon, S., D. Qin, M. Manning, Z. Chen, M. Marquis, K. B. Averyt, M. Tignor, and H. L. Miller (eds.). 2007. Climate change 2007: the physical science basis. Contribution of Working Group I to the Fourth Assessment Report of the Intergovernmental Panel on Climate Change. Cambridge University Press, Cambridge, UK and New York, NY, USA.

Sun, G., H. Riekerk, and N. B. Comerford. 1998. Modeling the forest hydrology of wetland-updand ecosystems in Florida. Journal of the American Water Resources Association 34:827–841.

Tóth, J. 1963. A theoretical analysis of groundwater flow in small drainage basins. Journal of Geophysical Research 68:4795–4812.

Troxell, H. C. 1936. The diurnal fluctuation in the groundwater and flow of the Santa Ana River and its meaning. EOS Transactions, American Geophysical Union 17:496–505.

White, W. N. 1932. A method of estimating groundwater supplies based on discharge by plants and evaporation from soil. Water-Supply Paper 659-A, U.S. Geological Survey, Washington, DC, USA.

Wilcox, D. A., S. J. Baedke, and T. A. Thompson. 2005. Groundwater contribution to hydrology-driven development of wetland plant communities. Geological Society of America Abstracts with Programs 37:244.

Winter, T. C. 1999. Relation of streams, lakes, and wetlands to groundwater flow systems. Hydrogeology Journal 7:28–45.

Wuebbles, D. J. and K. Hayhoe. 2004. Climate change projections for the United States Midwest. Mitigation and Adaptation Strategies for Global Change 9:335–363.

CHAPTER 4

Interactions among vegetation, hydrogeology, and climate in a Great Lakes ridge-swale wetland system

4.1 Introduction

The interaction of vegetation with the water table is a key relationship in wetland ecosystem dynamics (Harris and Marshall 1963, Wilcox and Simonin 1987, Kantrud et al. 1989, Noest 1994, Poiani et al. 1996, Mitsch and Gosselink 2000, Henszey et al. 2004, Leyer 2005, van Geest et al. 2005, Dwire et al. 2006). Although soil saturation often controls vegetation pattern and structure, plants also can drive local hydrology through transpiration effects on the water table (Meyboom 1966, Doss 1993). In a process identified in early work by White (1932) and Troxell (1936) and further studied by many others (e.g., Gerla 1992, Laczniak 1999, Hill and Neary 2007, Gribovski et al. 2008, Loheide 2008), daily water-table fluctuations are driven by evapotranspiration (ET) that moves water from ground to atmosphere and sets up a head differential drawing groundwater toward the source of loss. These daily fluctuations often can be superimposed on longer-term trends in water-table elevation (Loheide 2005), implying that evapotranspiration is a potentially important driver of groundwater loss, along with deep percolation and other subsurface flow paths. Presumably, large transpiration losses can be self-limiting. If the recovery source (water table or nearby surface storage) cannot deliver flow at the same rate that ET removes it, water-table elevation will permanently fall (Loheide 2008). Soil moisture, then, can decrease as a result of disconnection between the water table and the soil profile (Tamea et al. 2009), thereby influencing vegetation patterns in the landscape (Loheide et al. 2009).

In a given wetland, six configurations for the interactions between plant water use (indexed by ET) and available water in the soil (indexed by volumetric soil moisture, Θ) are possible. The hypotheses are stated in terms of the net (total) effect (in Wright's 1921 path analytic sense) of plants (ET) on available water (Θ) and, conversely, of soil

moisture on plant metabolism (Figure 4.1). In water-limited environments, Θ generally increases the rate at which ET occurs, representing a positive effect of Θ on ET (e.g., Hale and Orchutt 1987) (Figure 4.1A). If soils are inundated so that oxygen levels are sufficiently low, a negative effect of soil moisture on plant productivity can result, which limits evapotranspiration (e.g., Wilde et al. 1953; Roy et al. 2000, and references therein; Chang 2002) (Figure 4.1B). The corresponding effect of ET on Θ could also be negative or positive. Generally, the process of evapotranspiration removes water from soil and releases it to the atmosphere, thereby decreasing soil moisture (Figure 4.1C and Figure 4.1F). On the other hand, transpiration by phreatophytic vegetation can create a local head pressure differential that results in groundwater flow toward the root zone and net accrual from a nearby recovery source, such as adjacent storage in an aquifer or river valley (Figure 4.1D and Figure 4.1E) (Gerla 1992, Laczniak 1999, Gribovski et al. 2008, Loheide 2008). In this manner, ET can have a positive effect on Θ. The existence of potential feedback loops are of ecological interest, as they may lead to dramatic shifts in vegetation communities, depending on the relative magnitudes and initial conditions of water-table fluctuation, evapotranspiration, and resulting soil aeration (Ridolfi et al. 2006).

Plant community composition, especially the presence or absence of trees also plays a role in shaping wetland water balance. Greater fluctuations in the water table have been observed in forested wetlands than in nearby wetlands without woody plants (Lafleur and Rouse 1988). Furthermore, deforestation of forested wetlands generally leads to a dramatic rise in water table, in a process termed “watering-up” (e.g., Wilde et al. 1953, Trousdell and Hoover 1955, Williams and Lipscomb1981, Peck and Williamson 1987, Borg et al. 1988, Riekerk 1989, Dubé et al. 1995, Sun et al. 2000, Marcotte et al. 2008). Conversely, planting vegetation in areas with a shallow water table has been shown to lower water levels (e.g., Wilde et al. 1953, Chang 2002); this is usually attributed both to transpiration and rainfall interception by vegetation reducing recharge (Wilde et al. 1953, Borg et al. 1988, Riekerk 1989, Dubé et al. 1995) but can also be due to direct uptake by tap roots of trees (e.g., Le Maitre 1999). Wet-meadow sedges and grasses also have been shown to use groundwater directly (Loheide et al. 2009). Therefore, species composition of the vegetative community can be both a cause and a

result of local water-table dynamics, again pointing to the potential importance of feedback loops in understanding ecohydrologic interactions.

In this chapter, I examine how the complex hydrology of a coastal ridge-swale wetland system in the Laurentian Great Lakes region is related to the structure and function of its plant community. Consisting of a series of nearly 40 wetland units without surface flows, the site is particularly suited for examining ecohydrologic interactions in a humid, phreatophytic system, a research need recently identified by Rodriguez-Iturbe et al. (2007). My primary objective was to examine the nature of the dynamic interaction between plant water use (as indexed by ET) and water availability (as indexed by soil moisture). By instrumenting a series of 15 adjacent swales, I use a path analytic approach to estimate interaction effects empirically during the growing season of two sequential wet and dry climate years. Building on that analysis, I then explore the relationships between vegetation structure (primarily abundance of large trees) and variations in the hydrogeologic setting.

4.2 Methods

4.2.1 Study Site

Located along the western coast of Lake Huron, approximately 25 km south of Alpena, MI and within the boundaries of Negwegon State Park, the site consists of an undisturbed set of 87 former beach ridges of lake-deposited sand comprising a strand plain formed over the past 3500 years (Figure 4.2). The ridges bound linear swale depressions, and hydric soils and wetland plant communities developed where wet conditions allowed. Climate is temperate, and the 20-year (1987-2007) average growing-season precipitation is 41.0 cm (72.1 cm annual). Growing-season precipitation in 2006 was well above average (50.5 cm), and 2007 was drier than normal (40.4 cm) (20-year range: 28.4 cm in 1989 to 60.4 cm in 1991).

Swale vegetation falls into three main categories: sedge meadow/emergent marsh (henceforth, herbaceous), seasonally flooded forested overstory with emergent wetland plants in the understory (henceforth, forested), and seasonally flooded scrub-shrub (henceforth, shrub). Swales in the herbaceous category are dominated by sedges and

grasses [e.g., Northwest Territory sedge, *Carex utriculata* Boott; bluejoint, *Calamagrostis canadensis* (Michx.) P. Beauv.]. Swales in the forested category have a dominant overstory of hydromesophytic trees such as black ash [*Fraxinus nigra* Marsh.] and green ash [*Fraxinus pensylvanica* Marsh.]. The open-water areas in the forested type are mostly devoid of vegetation, save a few species [e.g., small floating mannagrass, *Glyceria borealis* (Nash) Batchelder; hemlock waterparsnip, *Sium suave*Walter] but transition to emergent marsh (see above) or herbaceous forest-floor cover [e.g., dwarf red blackberry, *Rubus pubescens* Raf.; sensitive fern, *Onoclea sensibilis* L.] later in summer. The scrub-shrub wetlands are dominated by gray alder [*Alnus incana* (L.) Moench] and common winterberry [*Ilex verticillata* (L.) A. Gray], along with ash [*Fraxinus*] saplings.

Near-surface sediments are homogeneous, fine- to medium-grained sands with some gravel. Beneath the strand plain at approximately 3 m depth, the predepositional surface consists of a diamicton (very poorly sorted sediment of low permeability) of glacial origin that acts as an aquiclude or aquitard. Detected in sediment cores and by ground-penetrating radar (T. Thompson, unpublished data; Posner et al. 2005), this layer may permit groundwater flow from an intermediate aquifer to the overlying wetlands. Water-chemistry data suggest that more permeable areas of the diamicton allowed intermediate flow paths, as described by Tóth (1963), to interact with the unconfined aquifer above (Baedke, unpublished data; Posner et al. 2005). Deep, regional flowpaths, however, do not appear to feed the site (Baedke, personal communication, July 2, 2006, Wilcox et al. 2005).

4.2.2 Field Methods

Non-destructive vegetation sampling was performed in July 2005 in the 37 swales that sustained wetland plant communities and were greater than 10 m in width. In each swale sampled, five transects were established at 20-m intervals, and 1-m^2 quadrats were sampled at random in each quarter-transect. Percent cover of understory (to 1.5-m height) was determined by ocular estimation by one-percent intervals to 10 percent and five-percent intervals thereafter. To describe the overstory, all trees within 20 m on either side of the center transect were identified, counted, and measured for DBH. Plant area index of the tree canopy was measured every meter along the middle of the five transects using

a LI-COR LAI-2000 Plant Canopy Analyzer (LI-COR 1992) with a 45º view cap in the early morning or late afternoon in August 2007. Wood area index was measured in April 2008 and subtracted from plant area index to obtain a single direct measurement of leaf area index (LAI). Seasonal changes in understory vegetation and LAI were modeled using seasonal time-course plots of LAI presented by Allen et al. (1998) (their Figure 8) for understory and Breda (2003) (their Figure 6) for canopy.

Of the 37 swales sampled, 15 were chosen at random for hydrologic analysis from a sample stratified by the three vegetation categories described above (five swales in each stratum). Evapotranspiration (ET) and shallow groundwater recovery (G_{rec}) caused by evaporative demand by plants were determined from water-table fluctuations using an adaptation to the Loheide (2008) method described in detail in Chapter 2. Water-table fluctuations were recorded over the 2006 and 2007 annual growing seasons using pressure transducers installed in 0.0254-cm slotted PVC wells driven to 1 m depth and screened across the water table. Barometric-pressure effects were removed from the water-level data by simple subtraction, as barometric efficiency and time lag were determined to be minimal in this shallow sand aquifer.

In the same 15 swales, volumetric soil water content (henceforth, soil moisture) data were collected from the top 10 cm of soil using a volumetric soil moisture probe (Dynamax ThetaProbe type ML2x) on five days during the 2007 growing season (Jul. 11, Aug. 8, Aug. 28, Sep. 22, Oct. 12). Three measurements were taken by haphazard sampling (i.e., chosen without intentional bias but not randomly), one on either side of the swale and one near the middle. A single measurement for each swale was obtained by arithmetic average. The soil moisture in cases of standing water, including all of June, was assigned 1.0. For August, an average of the two sampling periods was used. A regression was developed from the 2007 data that predicted soil moisture from water depth and was used to predict soil moisture for 2006.

Water-budget analyses were performed on each of the 15 swales individually and for the wetland complex as a whole. Water-budget components (change in storage, groundwater, ET, and precipitation) were summed on a monthly time step from June to September. In this study, change in water level was used to represent change in storage, although I recognize implicitly that these are not identical phenomena. Precipitation

recorded at a weather station centrally located at the study site was summed and included in the water budget. An adaptation to a method presented by Loheide (2008), described in detail in Chapter 2, was used to obtain estimates from water-table fluctuations for ET and groundwater recovery (G_{rec}) associated with ET demand. G_{rec} represents the groundwater resulting from evaporative consumption and does not include percolation loss or gain following rain events (G_{perc}). Therefore, G_{perc} was determined by difference in the mass balance and added to G_{rec} to obtain total groundwater flux (G_{net}), as described fully in Chapter 3.

4.2.3 Vegetation Analysis

Non-metric multidimensional scaling (NMS) was performed on species presence and absence of understory and canopy species using PC-ORD v.4.0 (McCune and Mefford 1999). I also performed an NMS analysis of mean understory vegetation dominance data and found similar results. The Sorensen (Bray-Curtis) distance measure was used, and the autopilot was set to slow and thorough. Swales were plotted in species space. Proximity of swales in species space was used to determine groupings. Axes were rotated to maximize the relationship between the variable G_{perc} and Axis 1 (McCune and Grace 2002). Species plotted in species space are not presented here, as I was interested in the relationship between overall community patterns and hydrology rather than the responses of individual species.

4.2.4 Structural Equation Model Development

To evaluate the alternate hypotheses described above for this ridge-swale system, I used structural equation modeling (SEM *sensu* Bollen 1989) and path analysis (Wright 1921) to parameterize a basic conceptual model of wetland water-balance dynamics (Figure 4.3). My model asserts that changes in soil moisture (Θ) directly affect canopy and understory vegetation and control ET rates. ET can in turn drive groundwater flux and change in swale water storage, which affects Θ directly. The justifications for the model proposed lay in the theoretical and empirical basis for the causality implied by each direct causal path in Figure 4.3 and Figure 4.4, which I will describe in detail here.

Diurnal fluctuations in the water table are driven by evapotranspiration drawing down the water table (Loheide 2005), creating a head differential in the flow system, and drawing groundwater toward the source of loss (White 1932, Troxell 1936, Gerla 1992, Laczniak 1999, Loheide 2008). This results in an apparent nighttime groundwater recovery of the water table (Gribovszki et al. 2008), although this groundwater flux is continuous (Gribovszki et al. 2008, Loheide 2008). Thus, the direct effect of evapotranspiration on groundwater recovery is positive when groundwater is not limiting. Likewise, an influx of groundwater due to evapotranspirative loss must serve to increase water storage for mass balance to hold. For the same reason, precipitation also must act to increase water storage. In my model, the linkage between the hydrologic and biological components of the model occurs primarily through soil moisture, which is driven by changes in water level (Tamea et al. 2009). When the water table is near the surface, soil moisture is maintained by capillary action in the root zone (Laio et al. 2009). Water loss in excess of groundwater inputs leads to a lowering of the water table and a decrease in soil moisture. Soil moisture can be replenished by rain. If, however, precipitation fails to rebound the water table to within the capillary fringe, the effects of precipitation on soil moisture will be short-lived [see Sanderson and Cooper (2008) for an example of this phenomenon]. In my model, the effect of precipitation on soil moisture was determined indirectly through its effect on change in storage. Although precipitation falling on a unit of soil can increase the soil moisture without a change in storage at the water table, this effect likely was minimal comparatively, and the discrepancy in time between soil moisture and precipitation precluded the inclusion of a direct effect; whereas the soil-moisture data were collected at mid-month, precipitation represented a sum over the entire month and could not be related directly to soil moisture. Because the time period of observations in this model is by month, as described in Section 4.2.5, water depth at the beginning of the month sets the initial conditions for soil moisture and was used to predict observed mid-month soil moisture as a result. Additionally, beginning water depth influences change in storage. Higher water-surface elevations generate greater elevational heads, thereby increasing the rate at which storage loss occurs due to the increased head differential.

Water depth and soil moisture can have positive or negative effects on vegetation. Wetland plants are well-adapted to live in hydric soils (Mitch and Gosselink 2000b). Depending on the type of plant and its hydroperiod preferences, however, extended flooding can limit growth. Similarly, abundant soil moisture during dry periods can maintain understory or canopy vegetation, whereas extremely wet conditions in which aeration of the soil occurs infrequently can lead to waterlogged conditions and salt accumulation (van der Kamp and Hayashi 2009), thereby inhibiting plants and decreasing understory or canopy cover. In the case of canopy cover, high soil moisture content may preclude the persistence of trees at a particular site, and canopy cover will be reduced simply due to the presence of fewer trees.

Included in the model was a measure of canopy density, represented by leaf area index (LAI), which can have a positive or negative effect on ground cover. Increased canopy cover may inhibit understory growth by blocking light, or it may help to sustain ground cover during dry conditions due to the cooling properties of shade. Furthermore, shade-tolerant species may thrive with greater canopy cover.

Finally, tree canopy and understory vegetation drive transpiration losses, thereby closing the loop. The expected relationship between ET and understory vegetation clearly could be positive, indicating that more vegetation evapotranspires more water. On the other hand, a negative correlation of vegetation on ET could be due to the shading effects. More leaf cover reduces soil evaporation by reducing solar radiation to the surface (Mitsch and Gosselink 2000b). Furthermore, shading effects of the overstory canopy may reduce transpiration of ground cover by light limitation. Conversely, shade-tolerant plants in the understory may be photoinhibited by direct sunlight or may be better adapted to cooler temperatures (Lambers et al. 1998). As a result, more transpiration could also result by shading.

Climate and hydrogeologic context comprise overarching outside influences on the internal dynamics of each swale. Climate affects vegetation type and evapotranspiration rates (Lambers et al. 1998). Higher ET rates can occur in warmer, drier areas that experience more sunlight, given sufficient soil moisture, and plants are adapted to the climate in which they live. These effects were not explicitly included in the SEM, but model parameterizations for individual years (wet year in 2006 and dry year in

2007) and hydrogeologic context (recharge and discharge character as determined by net groundwater flux in 2007, described in next section) were used to elucidate some effects of climate and physiography.

4.2.5 Structural Equation Model Parameterization and Fit

I implemented a structural model (Figure 4.4) using path analytic techniques in Amos 17.0 (Arbuckle 2008). Structural equation modeling, of which path analysis is a special case, fits the specified model to the observed data using constraints of the expected patterns in covariance. Terms and concepts utilized in structural equation modeling can be found in Kline (1998), Maruyama (1998), and Hershberger et al. (2003); a brief but useful descriptive summary of the terms is provided by Grace and Pugesek (1997).

To describe the system of interactions across various conditions (wet and dry years, wetter and drier places, tree abundance), the model was parameterized for the 2006-2007 combined data set (number of data points, n = 87) and for each year's data (n = 45, n = 42) independently. The data for Swale 38 in 2007, which were missing data due to well vandalism and had been predicted by regression analysis, were identified as outliers and removed. I also fit the same structural model to interesting subsets of the data representing contrasting hydrologic "types" identified in Chapter 3: recharge swales (n = 48) and discharge swales (n = 39), and to the group of swales with abundant large trees (n = 33) or without (n = 54). I was most interested in recharge swales and swales with abundant large trees and present the fit results of those subsets along with the combined data set and annual subsets. The recharge character of a swale was used to describe a physiographic context in which a swale had a net negative groundwater flux (G_{net}) observed in the 2007 drier-than-average year; total groundwater flux in 2007 in particular was a good descriptor of the physiographic character of the swale due to dry conditions that differentiated gaining swales from those that lose water to the water table. The number and size of trees within 40 m of the center transect (see Section 4.2.2) were used to determine swales that had abundant large trees (summed DBH for all trees > 100 cm).

Maximum likelihood (ML) is the estimation method used most widely in SEM (Tomer and Pugesek 2003) and was used in this analysis. In an exploratory fashion,

modification indices (Sorbom 1989), constrained by theory, in ML were used to respecify the SEM model from the conceptual model until a "best-fitting" model was chosen.

My data set in these analyses consisted of monthly summaries for July, August, and September of years 2006 and 2007. I constrained my data set to these six periods for two somewhat different reasons. First, the complete inundation of swales early in June precluded the model's ability to resolve properly for both flooded and non-flooded states. Much of the ability of the model to solve seemed to hinge on soil-moisture effects on vegetation (LAI and ground cover). During flooded conditions (i.e., all sites in June), the soil moisture was assigned a value of 1.0 which led to strong non-linearities. Second, while multiple time points can be used in structural equation modeling to examine longitudinal trends over time for multiple variables at once, only five or six time points are recommended (MacCallum et al. 1997, Fuller et al. 2003), and using the June values would have generated a data set with eight time points. For example, Fuller et al. (2003) used SEM with multiple time points to describe effects of flooding and canopy cover on the growth of wetland trees and showed its utility in comparison to more traditional multivariate methods. MacCallum et al. (1997) suggested that there is no "rule of thumb" for determining an appropriate number of time points but the number chosen should not be too large or too small relative to model complexity. Nonetheless, temporal autocorrelation was tested for the bivariate and multivariate regressions present in the model by regressing the residuals against lagged residuals and was found to be minimal.

Model fit was determined first by ensuring that the magnitude and direction of the significant pathways agreed with the conceptual understanding of the system of interactions depicted in Figure 4.3. Next, coefficients of determination (R^2) of the endogenous (dependent) variables of interest were examined for reasonableness (> 0.40). The chi-square probability statistic ($P > 0.05$), the chi-square minimum discrepancy test (CMIN/DF < 2), the comparative fit index (CFI > 0.90) (Bentler 1989), and the root mean squared error of approximation (RMSEA < 0.06) (Steiger and Lind 1980, Browne and Cudeck 1993, Tomer and Pugesek 2003, Schreiber et al. 2006) were examined. The Bollen-Stine bootstrap, which corrects the ML chi-square probability statistic for non-normality, was used to ascertain model fit as well ($P > 0.05$). The CFI as a fitness indicator is particularly applicable to small sample sizes and non-normal distribution

(West et al. 1995). Bentler and Bonnett (1980) and Tomer and Pugesek (2003) suggest a CFI cutoff point of greater than 0.90. Finally, the residual matrix usually was examined to ensure that differences in correlations between the modeled and observed matrices were small.

In structural equation modeling, indirect effects are calculated as the product of a sequence of direct effects along a causal pathway (Bollen 1989). Total effect for a given variable on an endogenous variable represents the overall (net) effective of all direct and indirect causal pathways in the model. Standardized path coefficients represent the relative strength of interaction between two variables. The direct and total effects were examined as indicators of the strengths of ecohydrological interaction among variables. Parametric bootstrapping was used to obtain estimates of significance for total effects inferred from the model at $P < 0.05$. In SEM, the significance values help the researcher determine whether or not the value arises from sampling fluctuations or from a causal influence (Hayduk 1987).

Of the possible representations of groundwater addressed in Chapter 3 (G_{net}, G_{perc}, G_{rec}), the groundwater recovery (G_{rec}) was used to represent groundwater flux in the SEM because it is directly within the sphere of influence of the plants, whereas G_{net} and G_{perc} fluxes are delivered by deeper groundwater flowpaths. The other groundwater components in the model could not be included, as the colinearity between ΔS, G_{perc}, and G_{net} was too great for the model to resolve.

4.3 Results

4.3.1 Model Fit

The path analyses for the various data sets except 2007 (2006-2007 combined, 2006, recharge, abundant large trees) described the observed data well (Table 4.1). Of the models parameterizations pursued, multivariate kurtosis was relatively low except for the annual subsets (2006, 2007). Also, the 2007 data set had more outliers than could be justifiably removed and require more free correlations than the other data sets to obtain a good fit ($X^2 = 9.8$, CFI = 0.99, RMSEA = 0.15).

The fitted models also matched most initial expectations for the direction (sign) of effects and explained a reasonable amount of variation in many endogenous variables (Figure 4.4). For example, in the combined 2006-2007 data set, the coefficient of variation (R^2) for change in storage, groundwater recovery, and soil moisture ranged from 0.70 to 0.94. Exceptions were ground cover (R^2=0.01) and LAI (R^2=0.10), with ET somewhere between (R^2=0.42) (Figure 4.4). The models independently applied to subgroups of the data (i.e., 2006, recharge, abundant trees) showed similar results (Figure 4.4).

4.3.2 Plant-Hydrology Interactions

The interactions of primary interest in this study were the net effects of plant water use, indexed by ET, and soil moisture, which I take to be the water available to plants. In the model fit of the combined years, the total effect path coefficients were weakly negative in both directions, implying a weak positive feedback although the path coefficients themselves were not statistically significant in the bootstrap tests (Table 4.2, Figure 4.5). In 2006, however, soil moisture had a stronger (-0.16, P = 0.10) negative effect on ET, and ET had a stronger and statistically significant (-0.08, P = 0.02) effect on soil moisture (Figure 4.5B), again implying a positive feedback loop between ET and soil moisture, this time more strongly. In the dry-year (2007) model fit, ET had a weak, but not significant, negative effect of on soil moisture (-0.03, P = 0.84), and soil moisture had a very weak, and far from statistically significant, positive effect on ET (+0.02, P=0.93) (Figure 4.5C), again implying a negative feedback loop in the dry year. Considering the bootstrapped error estimates, however, we might equally well conclude that no feedback loop existed even though ET must, to some extent, depend on overall soil moisture.

Examining relationships only among recharge swales, soil moisture strongly affected ET (-0.28, P = 0.03) but there was only a weak reverse interaction (-0.06, P = 0.10), implying a weak positive feedback but strong asymmetry (Figure 4.5D). Essentially, the opposite pattern was seen when only tree-dominated swales were fit; ET had clear effects on soil moisture (-0.17, P = 0.01), but soil moisture had almost no impact on ET rates (-0.06, P = 0.69) (Figure 4.5E). Across the entire swale sequence in wet years and in recharge zones in both years, soil moisture had a larger impact on ET

than ET had on soil moisture (Figure 4.5). Where trees were large and abundant, however, the reverse was true.

In my models, the causal linkage between soil moisture and ET was due to indirect effects of soil moisture as it altered LAI and ground-cover variables. Direct effects of LAI and ground cover on ET were positive in all model fits, suggesting that shading properties of ground cover do not significantly limit ET overall at this site (Figure 4.4). Rather, increasing vegetation surface area leads to greater evapotranspirative loss, and any negative effects of shading on ET by ground cover are overcome by the positive effect. Total effects estimates, which include indirect effects, support this observation (Table 4.2). Although canopy cover (LAI) reduced ground cover in recharge swales (Figure 4.4D), which suggests an adverse shading effect, the total effect of ground cover on ET was still positive (Table 4.2).

The effect of soil moisture on ground cover was both positive and negative depending on the conditions (wet year, recharge swales, abundant large trees). When greater-than-normal rainfall occurred in 2006, the deleterious effect of soil moisture on ground cover, although not significant (Figure 4.4), was likely due to water logging of soils. In recharge areas, plant species likely are adapted to drier conditions and therefore are negatively affected by high soil moisture. In the swales with abundant large trees and in 2007, however, the positive effect indicates that ground cover may have been slightly water-limited despite seasonally flooded conditions, due to water-table depression by tree ET in the former and less precipitation in the latter.

4.3.3 Overall Water Balance

Overall, this ridge-swale system does not appear to be water limited, but under certain circumstances (dry years, places with abundant trees) water limitation may be occurring despite the phreatotrophic character of the site. Usually, too much water limits evapotranspiration, especially for trees, as evidenced by a significant negative direct effect of soil moisture (Θ) on leaf area index (LAI) in all model fits (Figure 4.4) and a consistently negative total effects coefficient linking soil moisture and ET. An exception to this was observed in 2007, the dry year, when the total coefficient between soil moisture and ET was positive. In swales with abundant large trees, soil moisture may

have had a beneficial effect on ground cover as well, although the path coefficient was not statistically significant (Figure 4.4D), whereas in the wet year (2006) and in both years at the recharge swales, higher soil moisture led to a reduction in ground cover (Figure 4.4B, Figure 4.4C).

In terms of water levels, the strongest driver of change in storage (ΔS) in this system appears to be precipitation (Table 4.2). The negative path coefficients for ET and initial water depth and positive path coefficients for groundwater recovery (G_{rec}) were less than precipitation, indicating secondary importance in relation to precipitation. Initial water depth was negatively related (negative path coefficient) to change in storage because higher water-table elevation allows water to drain by the force of gravity more readily due to the greater elevational head. Additionally, initial water depth was the greatest driver of soil moisture (Table 4.2).

4.3.4 Ecohydrologic Process Implications for Plant Community Structure

The non-metric multidimensional scaling (NMS) ordination of species presence-absence plotted in species space reflected the importance of the water balance of each wetland unit (swale) on its species distribution (Figure 4.6). Axis 1 explained 33.3 % of the variation in the species data, and Axis 2 explained 57.3 %. Environmental variables having correlations to the axes with coefficients of variation (R^2) greater than 0.20 are shown in Figure 4.6.

Swales plotted in species space according to the degree of inundation and the type of groundwater they receive, either shallow groundwater in the rooted zone, driven by ET demand (G_{rec}), or deep groundwater, represented by net percolation (G_{perc}), where a positive G_{perc} indicates less net percolation loss and relatively more deeper groundwater discharge. Swales 38, 73, 78, and 82 (Group I) were associated with high rates of ET loss and groundwater recovery, which were reflected in the observed species. Swales 30 and 32 (Group II) had greater deep groundwater influx and less flooding and plotted out similarly. In swales 8, 14, and 17 (Group III), inundation was sustained for more days of the growing season than in other swales. Swales in the middle group (Group IV; swales 26, 28, 37, and 55) were somewhere in between these extremes. Swale 29 was an outlier, as it is a disturbed site with railroad tracks running through it (Figure 4.2).

The position of swales in species space (Figure 4.6) was also related to large-tree abundance, which was not represented explicitly in the NMS of ground-cover vegetation. Swales 26, 29, 30, and 32 had no large trees greater than 5 cm DBH within 20 m of the center transect. Swales 14, 17, 38, 73, 78, and 82 had many large trees as dominant vegetation and DBH for those trees totalled more than 100 cm. Swales 8, 28, 37, 55, and 81 had some large trees. Swales plotted in species space according to the number and DBH of large trees in the overstory, with some exceptions. Swale 14 and 17, which had large trees, did not plot with Group I. Swale 81 was ranked just below the other swales in Group 1 in terms of number of large trees but was clustered hierarchically with other swales having some large trees. Swale 26 had a similar number of trees as Group I, but it plotted in Group II due to its greater depth generating a similar flooding regime to Group II swales.

Figure 4.6 also shows recharge swales as open symbols and discharge swales as closed symbols. The recharge or discharge character, assigned by the net groundwater flux in the drier-than-normal year (2007), showed no consistent pattern with regard to the distribution of swales in species space. However, the degree of flooding, soil moisture, ET, and groundwater routing (G_{rec} or G_{perc}), which represent more specific components of the water budget, did explain some of the variation observed in the NMS axis scores (Figure 4.6).

4.4 Discussion

The wetland system in this study was not generally water-limited, but evapotranspiration was reduced by wet soils in wet years (2006) (Figure 4.4B), particularly where species present are better adapted to drier soils (recharge zones, Figure 4.4D). A slight degree of water limitation, however, is apparent in dry years (Figure 4.4C) and where large trees are abundant (Figure 4.4E). These effects influence the interactions between soil moisture and ET.

Although it is clear that ET is a significant driver of water levels (Table 4.2), the more interesting interaction is that between soil moisture, which I use as an index of water available to plants, and ET, which represents plant water use. Water levels, both

initial water depth and change in storage, help determine soil moisture, and evapotranspiration by plants removes it. Undoubtedly, the process is more complicated than my simple model would suggest. For example, water moves from soil to plant to atmosphere along a gradient from high to low energies representing differing water potentials, hydrostatic pressures, and water vapor pressures. The differential between the vapor pressure of air in leaves and the atmosphere is the primary driver of plant water loss (Lambers et al. 1998). Complicating matters, resistances to flow (e.g., stomatal closing) also regulate water flux rates along the soil-plant-atmosphere continuum; stomatal opening and closing can occur due to changes in temperature, solar insolation, and carbon dioxide levels, in addition to water availability. As a result, the manner by which transpiration affects soil moisture is not straightforward. Nonetheless, the two are strongly related, and examining their net effects provides insight into the mechanisms driving wetland hydrology. Because the organic soils in this study were fairly homogeneous between swales and remained saturated through most of the growing season, it is unlikely that soil water potential was affected considerably by soil type and texture or differential soil properties as soils dried. Furthermore, since the volumetric water content of these sandy loam soils never fell below 30% during this study, the soil moisture was maintained well above field capacity [see Figure 5.35 in Brady and Weil (2002)].

It is important to consider climate and site-specific conditions when examining the total effects of these interactions. Across all sites with various physiographic (recharge and discharge) and vegetational (having abundant large trees or not) character and across a range of climatic conditions (wet and dry years), the effects of plant water use (ET) and available water (soil moisture, Θ) on each other were weakly negative but not statistically significant (Figure 4.5). The weak effects may occur because the climatic conditions, deep groundwater flux, and tree dominance all affect the interactions in contrasting ways, thus masking individual interactions.

On a small scale, the plant-hydrology interactions are governed by the interface of plant water use and water availability. Expanding to a larger scale, the source of groundwater (G_{rec} or G_{perc}) and duration of flooding, governed by site hydrogeology,

result in interesting variability in plant community structure and ultimately determine the overall ecohydrology of the wetland.

4.4.1 Feedbacks

The terms "facilitation," "self-limiting," and "adaptation" are useful for describing observed feedbacks. Facilitation is an important, but often overlooked, component of ecological theory (Bruno et al. 2003, Begon et al. 2006), and it is an important concept for thinking about biotic-abiotic interactions as well as biotic ones. On a small scale, when conditions are particularly wet (i.e., rainfall is greater than normal), a positive feedback loop reflecting facilitation (Figure 4.5B) suggests that plant water use serves to increase ET rates by keeping moisture levels down at the roots. That is, the observed positive feedback, although not significant in the total effect of soil moisture on ET, facilitates plant transpiration. Such periodic flooding, combined with periodic drawdown, is necessary for maintaining diversity and excluding invasive species in wetland communities in Great Lakes coastal wetlands that are directly connected hydrologically to the lake (Keddy and Reznicek 1986, Wilcox 1995, Maynard and Wilcox 1997, Wilcox and Nichols 2008). Similar effects of flooding and drawdown are probably occurring in this ridge-swale ecosystem as well, given that swales plot in species space according to hydrologic gradients (Figure 4.6), as will be addressed in more detail below.

In dry years, however, drier climatic conditions led toward water limitation and a negative feedback loop in this wetland system, as soil moisture had a weak positive, although not significant, effect on ET, but ET had a weak negative, again not significant, effect on soil moisture (Figure 4.5C). When this negative feedback loop occurs, ET becomes self-limited.

Implications for vegetation change can be drawn from the observation in this study that strong one-directional effects of water availability (soil moisture) on plant water use (ET) and with weak reverse effects occur under drier conditions (i.e., recharge swales) (Figure 4.5C). In recharge zones, more plants may be adapted to soils that were not as saturated and, therefore, are adversely affected overall by an increase in soil moisture. The water content of the soil is greater than the plants can transpire away, and a

reduction in ET results if plants are stressed. The strong negative effect of soil moisture is not necessarily harmful to the plants over the growing season as long as the physiography of the swale allows for draining of the excess water. Because soil moisture drives plant water use in this context, plant community change is determined by available water (or lack thereof), and plants adapt. Alternatively, plant communities may trend toward equilibrium with the water balance.

Abundant large trees are able to transpire away the excess water, thereby reversing the interaction observed in the recharge swales (Figure 4.5E). In the case of a strong effect of ET on soil moisture such as this, a reverse, minimally weak interaction must also be present, as plants are inherently dependent on water. Therefore, the observed interaction in this study is likely to be facilitation (i.e., Figure 4.1F) but could also be self-limitation (i.e., Figure 4.1F) since the effect of soil moisture on ET was not significantly different from zero (Figure 4.5E). Nonetheless, the interaction is nearly linearly dependent; trees appear to determine, in part, the water available to them.

Because recharge swales encompass some swales with abundant large trees and some without (14, 17, 78, 82 in Figure 4.6), the discrepancy between recharge and abundant-large-tree swales suggests that trees are able to control their water availability, whereas understory vegetation (particularly herbaceous) may be subject to the hydrologic conditions it experiences.

4.4.2 Effects of Large-Tree Abundance and Hydrogeologic Setting on Plant Community

With few exceptions, the manner in which the swales plot out in species space is directly related to the number and size of trees in that particular unit, groundwater routing (shallow or deep flowpaths), and duration of flooding. The net groundwater, as represented in Figure 4.6 by the discharge (solid symbols) and recharge (open symbols) character in 2007, does not help explain variation in species composition, as open symbols occur equally in Groups I, II, and IV. Rather, the effects of the type of groundwater—shallow groundwater drawn to the root zone by ET (G_{rec}) or deep groundwater inflow (G_{perc})—and the degree of flooding affect species composition and ordination grouping more than the summed effects of the overall water budget.

The Group I association results from the combined effects of many large trees in the overstory and the hydrologic condition that they create; large trees transpire water at high rates, as evidenced by the ET vector in Figure 4.6, and drive soil-water availability, as indicated by strong negative effect of ET on soil moisture in Figure 4.5D. Groundwater influx to these swales originates from nearby surface storage and primarily represents groundwater recovery drawn to the swale by ET (G_{rec}), which the G_{rec} vector in Figure 4.6 clearly demonstrates. As a result, the presence of many large trees that drive the site hydrology has a major effect on the community composition of the understory (Figure 4.6, Group I), as well as soil-moisture conditions (Figure 4.5) and shading. Large trees may not be the only cause of high ET rates, however. In the path analysis, ground cover vegetation had a stronger causal effect on ET than canopy cover did, although the difference between the two was less pronounced in swales with abundant large trees (Table 4.2). In a preliminary path analysis in which I separated the ground cover into woody and herbaceous vegetation, woody understory vegetation appeared to be a major driver of ET, even more so than canopy vegetation. This is something that I will pursue in future studies.

Although they had large trees, swales 14 and 17 did not plot in Group I, perhaps because they did not have a large component of woody vegetation in their understory. The flooding regime of those particular swales is the likely reason for the discrepancy. Swale 17 is deeper than surrounding swales (Figure 3.8), and it is located where the water-table slope is relatively flat, such that percolation out proceeds at a slower rate. As a result, inundated conditions persist later into the growing season than in other swales. Trees, both in the understory and the canopy, cannot transpire as much water as in Group I due to saturated soils, resulting in understory vegetation that is similar to swales 8 and 14 (Figure 4.6, Group III), which also experienced flooded conditions, possibly due to deeper swale morphology (Figure 3.8).

In swales where deep groundwater flowpaths reach the surface but soils were less saturated (i.e., 30, 32), another unique understory community resulted (Group II). Swales 30 and 32 are situated in a hydrogeologic setting that allows discharge of deep groundwater flow (Figure 3.8, c). Their unique site hydrogeology determines the plant community present, as evidenced by the tight grouping of Group II, and their positioning

in relation to the G_{perc} vector in Figure 4.6. G_{perc} represents the average 2006-2007 net groundwater percolation and is a negative flux for all swales. Less negative values (i.e., following the G_{perc} vector to the right in Figure 4.6) are indicative of swales with greater deep groundwater influx.

The swales in Group IV are somewhere in between the abundant-tree sites with high ET and shallow groundwater (Group I), the deep groundwater sites (Group II), and the flooded sites (Group III). Most swales in Group IV have some large trees. The net effects of a moderate number of large trees, marginal flooding, and more (e.g., Swale 28, 37) or less (e.g., Swale 55) deep groundwater inflow resulted in the observed mixed community composition. The differentiation of swales along a vector representing groundwater loss (G_{perc}) supports findings by Skalbeck et al. (2009) that groundwater losses are as important as other sources in describing wetland hydrology and resulting vegetation communities.

4.4.3 Limitations and Weaknesses of the Model

Reconciling the bidirectional nature of ecohydrological interactions in wetlands requires interpreting the observed covariances between major drivers of wetland processes (Baker and Wiley 2009). Structural equation modeling (Bollen 1989) is a useful method for determining direct, indirect, and total effects in causal chains where multivariate analyses are required to describe interactions adequately but collinearity is strong among variables rendering traditional parametric multivariate techniques inaccurate (Pugesek 2003). This statistical modeling technique has been utilized in wetland studies (e.g., Grace and Pugesek 1997, Gough and Grace 1999, Grace and Guntenspergen 1999, Grace and Julita 1999, Baker and Wiley 2009), as well as more widely in many other ecological settings (e.g., Mitchell 1992, Grace et al. 2007). Admittedly, there are limitations to the modeling method.

In structural equation models, many alternate solutions with equally good data fits often are possible. The models presented here are not necessarily the only possible models that can describe the plant-hydrology interactions of interest. For my data set, however, these model parameterizations best described the correlation matrix of the observations, and the model fit was good. I can conclude from this only that the

hypothesized ecohydrological structure of the swales in this wetland complex is consistent with my measurements in the field. Aggregation of the variables on a monthly time scale may have obscured ontogenetic processes, as has been suggested by Fuller et al. (2003). For example, in most swales, both flooded and non-flooded states were experienced in July. However, the date when water levels fell below ground varied from swale to swale, and the monthly time steps likely were unable to capture these two states effectively. Aggregation of variables on a different time step may produce slightly different results, a comparison for future work.

The transformation of a conceptual model into a specific structural equation model carries with it the challenge of normalizing temporal scales of the interactions. For example, climate, physiography, and trees operate on a very long-term time scale. Ground cover, canopy cover, and soil moisture operate on shorter time scales, and the effects of their drivers are integrated in time to produce observed patterns. The interactions of the water balance proceed at a much faster rate. Nonetheless, because the SEM utilizes covariances in the data, neither the units nor spatial or time scales must be of the same units. Thus, the strengths of the interactions of variables operating on different spatiotemporal scales can be ascertained as long as the direct effects move in a logical pattern. To this end, the causal hypothesis in this model employed a series of transitions over time. The water-balance components operating at the shortest (daily) time scale acted upon the variables at the next time scale, that of soil moisture and vegetation (weekly). State of soil-moisture balance represented the condition of the middle of the month, and LAI and ground cover were indexed at the end of the month so that they could feed back onto the water-balance variables, which were monthly sums.

4.4.4 Ecohydrologic Dynamics at Multiple Scales

In ecosystem studies, it is important to consider multiple spatial scales, as has been previously noted by many (e.g., Allen and Starr 1982, Delcourt et al. 1983, O'Neill et al. 1986, Addicott et al 1987, Mitsch and Gosselink 2000b, Comin et al. 2004, Vondracek et al. 2005). This is especially true of ecohydrological studies (Janauer 2000, Rodriguez-Iturbe 2000). The ridge-swale wetland complex in this study provided a

unique opportunity to consider three scales of interest: an individual swale, the wetland complex, and the Great Lakes coastal wetland zone.

Whereas the results in the previous chapter included an analysis of the entire wetland complex, the path analysis in this chapter was limited to the individual swale scale. Due to multicollinearity between change in storage and deep groundwater flux, the latter could not be included in the path analysis. Instead, I examined shallow groundwater flow effects on the system of interactions and ascertained hydrogeomorphologic effects using the recharge data subset (Figure 4.4D) and ordination analyses of the vegetation data (Figure 4.6).

At the scale of the entire wetland complex, water levels fluctuated fairly uniformly over the growing season despite variability in regional groundwater upwelling and evapotranspiration rates. At this scale, regional water fluxes influence water-table dynamics. In the wet year (2006), the entire system was supplemented by regional groundwater, and the water table remained nearer to the surface than in in the dry year (2007), when the net groundwater flux was near zero (Table 3.2). These complex-scale dynamics influenced the interactions between water availability and plant water use, as evidenced by differences in path analytic results between years (Table 4.2). Furthermore, the sandy substrate that comprises the ridge-swale chronosequence allows for rapid redistribution of water between swales, suggesting that this system can be treated as a single wetland. For example, swales 14 and 17, which were categorized as recharge swales, likely fed water downslope to Swale 8, a discharge swale (Figure 4.6). The steepening in the water-table slope between swales 8 and 14 also is an indication that Swale 8 received water from upslope. Such redistribution of water also likely occurs in other parts of the ridge-swale chronosequence.

At a regional scale, the majority of Great Lakes coastal wetlands are phreatotophic (groundwater-fed) systems because coastal areas represent groundwater discharge zones (Granneman and Weaver 1999, Granneman 2000). As a result, similar processes observed in this study also must occur in other coastal wetlands. Plants will interact with local hydrology, and the specifics of the local water balance will determine the magnitude of that interaction. Climate, of course, also plays a major role, with wetter

years shifting the impact of soil moisture on evapotranspiration from being a net positive to a net negative effect (Table 4.2).

4.4.5 Implications for Climate Change

Based on other studies, it seems to be the case that succession in wetland systems in the Great Lakes and elsewhere is dependent on the hydrologic details in a particular wetland (Wilcox and Simonin 1987, Jackson et al. 1988, Doss 1983, Mitsch and Gosselink 2000b, Wilcox 2004, Burkett et al. 2005). Where groundwater discharge and other inflows exceed the rate of ET, climate and climate change are likely to have little effect on community composition (Burkett et al. 2005). As discussed above, the hydrogeologic setting and the abundance of trees, in part, determine the interaction between soil moisture and ET. Because this interaction is the underpinning of a water balance that directly affects plants, examining climate-change effects on the water balance may elucidate and assist in prediction of the larger-scale effects of climate change on coastal systems.

In highly phreatotrophic swales, as suggested by Burkett et al. (2005), climate change may have little net effect. Swales with high rates of groundwater discharge due to their hydrgeomorphic setting likely will continue to receive groundwater influx. There is some indication that deep groundwater flow is not consistent between years; net groundwater flux to the wetland complex was 3 mm in 2007 but was 200 mm in 2006 (Table 3.2). The excess in 2006 could have been due to precipitation inputs upslope from the wetland complex or from deep regional groundwater upwelling. If from deep groundwater, however, it suggests that the groundwater flowpaths are not consistent between years and may lead to vegetation change as climate changes.

What I described as “recharge swales” and swales with abundant large trees undoubtedly will be affected by the drier summer and fall conditions for the Great Lakes region that are predicted by some current climate models (Wuebbles and Hayhoe 2004). The effects on plant-hydrology interactions, however, are complicated. This site will likely proceed toward drier conditions as suppression of ET by soil moisture is reduced in both cases. Overall, plant community change is likely to proceed on a trajectory toward

more xeric conditions except where deep groundwater feeds a particular wetland. Thus, climate-change effects in coastal systems such as this likely will be mediated by groundwater. Since many coastal areas in the Great Lakes are characterized as discharge zones (Granneman and Weaver 1999, Granneman 2000), they may represent wet-zone refugia in the face of climatic changes toward drier conditions.

If water levels continue to drop in Lake Huron, as predicted by many climate models (e.g., Croley 1990, Smith 1991, Magnuson et al. 1997, Lofgren et al. 2002), a lowering of the water table will occur, which undoubtedly will reduce soil moisture and may cause vegetation change. Recharge and discharge zones may shift, followed by a resulting change in plant community. Future studies in groundwater modeling may help predict these hydrologic adjustments in the coastal zone, and the mechanisms outlined in this study provide insight for predicting the shifting mosaics of plant community composition due to climate change in Great Lakes coastal wetlands.

Table 4.1. Fit statistics of the structural equation models in Figure 4.4 for the combined 2006 and 2007 data set and for 2006, 2007, recharge swales, and swales with abundant large trees fit independently.

Year	Fit function	Value
2006 & 2007	Chi-square (X^2)	6.7
	Degrees of freedom (df)	6
	X^2/df	1.11
	Probability	0.35
	Bentler's comparative fit index (CFI)	1.00
	Normalized-fit index (NFI)	0.99
	Root mean square error of approximation (RMSEA)	0.04
	Multivariate kurtosis (c.r.)	-1.6 (-0.6)
	Bollen-Stine bootstrap	0.41
2006	Chi-square (X^2)	4.7
	Degrees of freedom (df)	6.0
	X^2/df	0.78
	Probability	0.58
	Bentler's comparative fit index (CFI)	1.00
	Normalized-fit index (NFI)	0.99
	Root mean square error of approximation (RMSEA)	0.00
	Multivariate kurtosis (c.r.)	-4.1 (-1.1)
	Bollen-Stine bootstrap	0.61
2007	Chi-square (X^2)	9.8
	Degrees of freedom (df)	5.0
	X^2/df	1.96
	Probability	0.08
	Bentler's comparative fit index (CFI)	0.99
	Normalized-fit index (NFI)	0.98
	Root mean square error of approximation (RMSEA)	0.15
	Multivariate kurtosis (c.r.)	-5.0 (-1.3)
	Bollen-Stine bootstrap	0.18
Recharge	Chi-square (X^2)	8.8
	Degrees of freedom (df)	6.0
	X^2/df	1.47
	Probability	0.18
	Bentler's comparative fit index (CFI)	0.99
	Normalized-fit index (NFI)	0.98
	Root mean square error of approximation (RMSEA)	0.10
	Multivariate kurtosis (c.r.)	-1.1 (-0.31)
	Bollen-Stine bootstrap	0.25
Abundant Trees	Chi-square (X^2)	4.5
	Degrees of freedom (df)	6.0
	X^2/df	0.75
	Probability	0.61
	Bentler's comparative fit index (CFI)	1.00
	Normalized-fit index (NFI)	0.98
	Root mean square error of approximation (RMSEA)	0.00
	Multivariate kurtosis (c.r.)	-0.5 (-0.1)
	Bollen-Stine bootstrap	0.63

Table 4.2. Standardized total effects of the path analysis representing the causal relationships among water-budget and vegetation variables for the combined 2006-2007 data set and 2006, 2007, recharge swales, and swales with abundant large trees. Bolded values were significant at $P < 0.05$ by bootstrapping (e.g. the effect of precipitation on change in storage for the 2006-2007 data set is 0.71 and is significant). (ET = evapotranspiration, Θ = volumetric soil moisture, ΔS = change in storage, G_{rec} = groundwater recovery, LAI = canopy leaf area index, GC = ground cover, P = precipitation, h_0 = initial water depth).

Year	Variable	ET	Θ	ΔS	G_{rec}	LAI	GC	P	h_0
2006 & 2007	ET	0.00	-0.08	-0.01	0.00	**0.26**	**0.62**	-0.01	-0.07
	Θ	-0.06	0.00	0.12	0.05	-0.01	-0.03	0.08	**0.90**
	ΔS	**-0.48**	0.04	0.00	**0.43**	**-0.12**	**-0.30**	**0.70**	**-0.26**
	G_{rec}	**0.93**	-0.07	-0.01	0.00	**0.24**	**0.57**	-0.01	-0.07
	LAI	0.02	**-0.31**	-0.04	-0.02	0.00	0.01	-0.03	**-0.28**
	GC	0.00	0.03	0.00	0.00	-0.10	0.00	0.00	0.03
2006	ET	0.01	-0.16	-0.03	-0.01	0.14	**0.58**	-0.02	-0.16
	Θ	**-0.08**	0.01	**0.16**	0.03	-0.01	**-0.04**	**0.11**	**1.02**
	ΔS	**-0.49**	0.08	0.01	0.20	-0.07	**-0.28**	**0.67**	**-0.20**
	G_{rec}	**0.91**	-0.14	-0.02	0.00	0.13	**0.52**	-0.02	-0.14
	LAI	**0.03**	**-0.37**	**-0.06**	-0.01	0.00	**0.02**	**-0.04**	**-0.38**
	GC	0.01	-0.15	-0.02	-0.01	-0.10	0.01	-0.02	-0.15
2007	ET	0.00	0.02	0.00	0.00	**0.35**	**0.63**	0.00	0.01
	Θ	-0.03	0.00	0.06	0.03	-0.01	-0.02	0.00	**0.83**
	ΔS	**-0.59**	-0.01	0.00	0.56	**-0.21**	**-0.38**	-0.01	**-0.51**
	G_{rec}	**0.97**	0.01	0.00	0.00	**0.34**	**0.61**	0.00	0.01
	LAI	0.01	**-0.38**	-0.02	-0.01	0.00	0.01	0.00	**-0.32**
	GC	-0.01	0.27	0.02	0.01	-0.10	-0.01	0.00	0.23
Recharge	ET	0.02	**-0.28**	-0.04	-0.01	0.12	**0.81**	-0.03	**-0.26**
	Θ	-0.06	0.02	0.13	0.02	-0.01	-0.05	0.09	**0.95**
	ΔS	**-0.44**	**0.12**	0.02	0.16	-0.05	**-0.35**	**0.70**	**-0.19**
	G_{rec}	**0.89**	**-0.24**	-0.03	-0.01	0.11	**0.71**	-0.02	**-0.23**
	LAI	0.03	**-0.45**	-0.06	-0.01	0.00	0.02	-0.04	**-0.42**
	GC	0.01	-0.09	-0.01	0.00	**-0.42**	0.00	-0.01	-0.08
Abundant Trees	ET	0.01	-0.06	-0.02	-0.01	**0.40**	**0.52**	-0.01	-0.06
	Θ	**-0.17**	0.01	**0.31**	0.17	**-0.07**	**-0.09**	**0.20**	**0.99**
	ΔS	**-0.55**	0.03	0.01	0.55	**-0.22**	**-0.29**	**0.67**	-0.18
	G_{rec}	**0.93**	-0.05	-0.02	-0.01	**0.37**	**0.48**	-0.01	-0.05
	LAI	**0.05**	-0.31	-0.09	-0.05	**0.02**	**0.03**	-0.06	-0.31
	GC	-0.02	0.11	0.03	0.02	0.05	-0.01	0.02	0.11

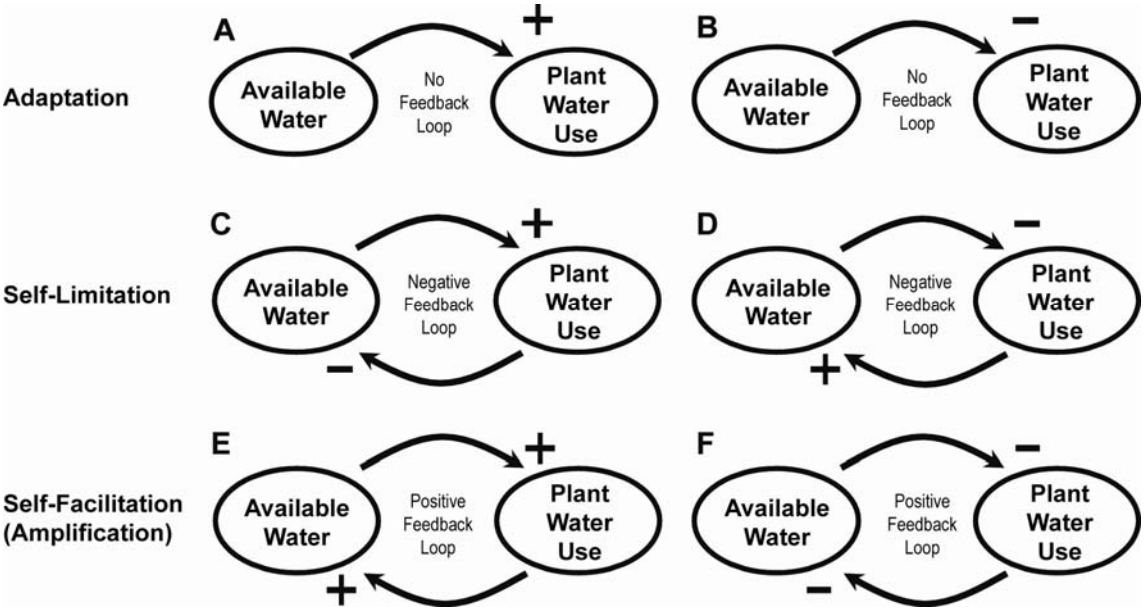

Figure 4.1. Alternate hypotheses to describe the potential net-effect interactions between plants (evapotranspiration, ET) and available water (soil moisture, Θ). A and B show linear dependency between variables, leading to adaptation. In A, increasing Θ leads to an increase in ET, suggesting a water-limited environment. In B, Θ has a deleterious effect on ET in an inundated environment. C and D represent self-limitation and a negative feedback loop, where ET leads to a reduction in Θ, and Θ increases transpiration by plants (C), or plants increase Θ by bringing water to them, and Θ then has an adverse effect on ET (D). Positive feedback loops result when both parties have either a positive or a negative effect on one another. Plants bring water to them by transpiration effects, and greater Θ leads to an increase in ET in a water-limited environment (E). Conversely, ET can reduce Θ, which limits the rate at which plants can transpire if soils become too wet (F).

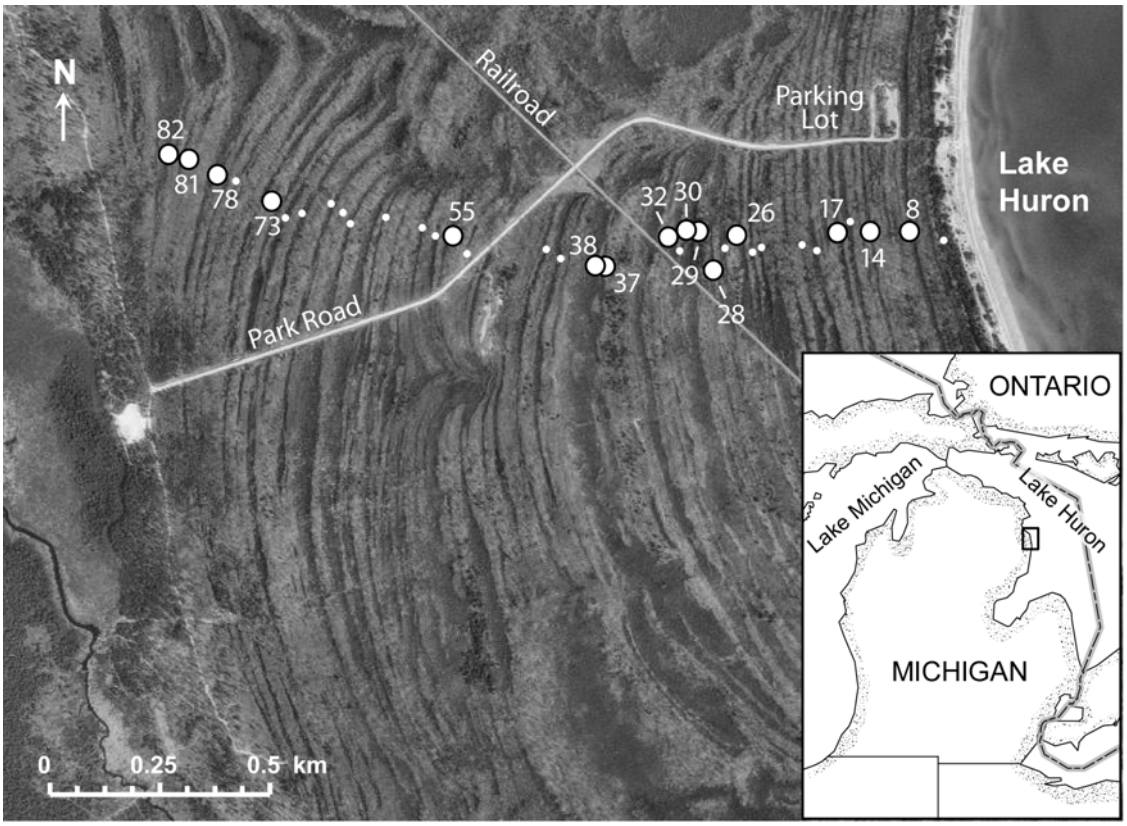

Figure 4.2. Location (inset) and air photo of the ridge-swale sequence at Negwegon State Park showing hydrologic-sampling sites (large circles, labeled) and additional vegetation-sampling sites (small circles). The lighter linear features represent the ridges, and darker features are the swales.

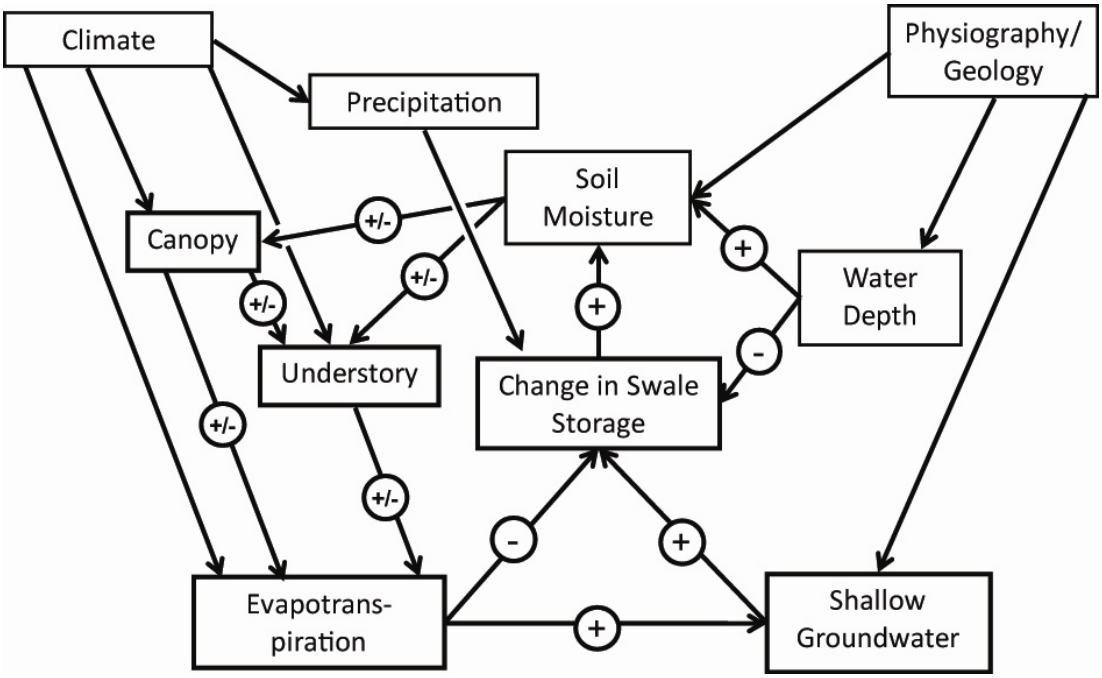

Figure 4.3. Conceptual model describing the interactions between hydrology and biology in the ridge-swale wetland system in this study. Plusses and minuses on arrows indicate hypothesized sign of path coefficients. Where a plus and a minus lie on the same arrow, both are theoretically possible. For example, canopy cover is expected to increase the transpiration component of evapotranspiration (ET) but can have a negative effect on the evaporation component through effects of shading. Likewise, canopy can adversely affect understory cover by light limitation, or it might benefit understory vegetation that is shade-tolerant.

Figure 4.4. Structural equation modeling path analysis of causal relationships among water-budget and vegetation variables. (LAI = leaf-area index, GC = ground cover, ET = evapotranspiration, G_{rec} = groundwater recovery, P = precipitation, ΔS = change in storage, h_0 = initial water depth, Θ = soil moisture). A positive change in storage (ΔS) indicates a rise in the water table. One-directional arrows indicate direct effects. For simplicity, correlation arrows are not shown. Path coefficient significance is designated by thick lines, bolded path coefficients, and by asterisks pertaining to level of significance (*$P < 0.05$, ** $P < 0.01$, *** $P < 0.001$). The coefficient of determination (R^2) within boxes for endogenous variables indicates the proportion of variation explained.

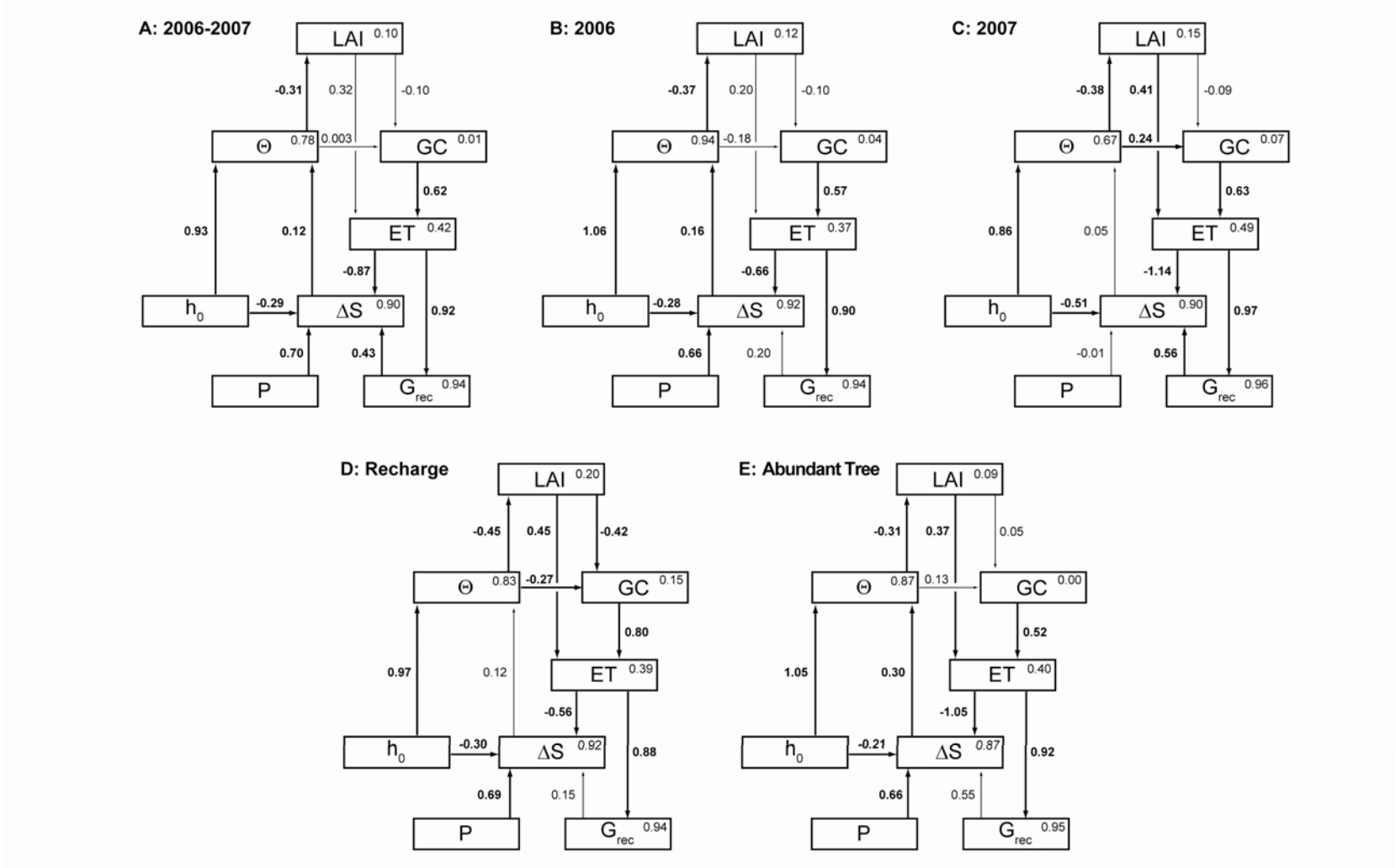
A: 2006-2007
LAI 0.10
Θ 0.78
GC 0.01
ET 0.42
h0
ΔS 0.90
P
Grec 0.94
-0.31
0.32
-0.10
0.003
0.62
0.93
0.12
-0.87
-0.29
0.92
0.70
0.43
B: 2006
LAI 0.12
Θ 0.94
GC 0.04
ET 0.37
h0
ΔS 0.92
P
Grec 0.94
-0.37
0.20
-0.10
-0.18
0.57
1.06
0.16
-0.66
-0.28
0.90
0.66
0.20
C: 2007
LAI 0.15
Θ 0.67
GC 0.07
ET 0.49
h0
ΔS 0.90
P
Grec 0.96
-0.38
0.41
-0.09
0.24
0.63
0.86
0.05
-1.14
-0.51
0.97
-0.01
0.56
D: Recharge
LAI 0.20
Θ 0.83
GC 0.15
ET 0.39
h0
ΔS 0.92
P
Grec 0.94
-0.45
0.45
-0.42
-0.27
0.80
0.97
0.12
-0.56
-0.30
0.88
0.69
0.15
E: Abundant Tree
LAI 0.09
Θ 0.87
GC 0.00
ET 0.40
h0
ΔS 0.87
P
Grec 0.95
-0.31
0.37
0.05
0.13
0.52
1.05
0.30
-1.05
-0.21
0.92
0.66
0.55

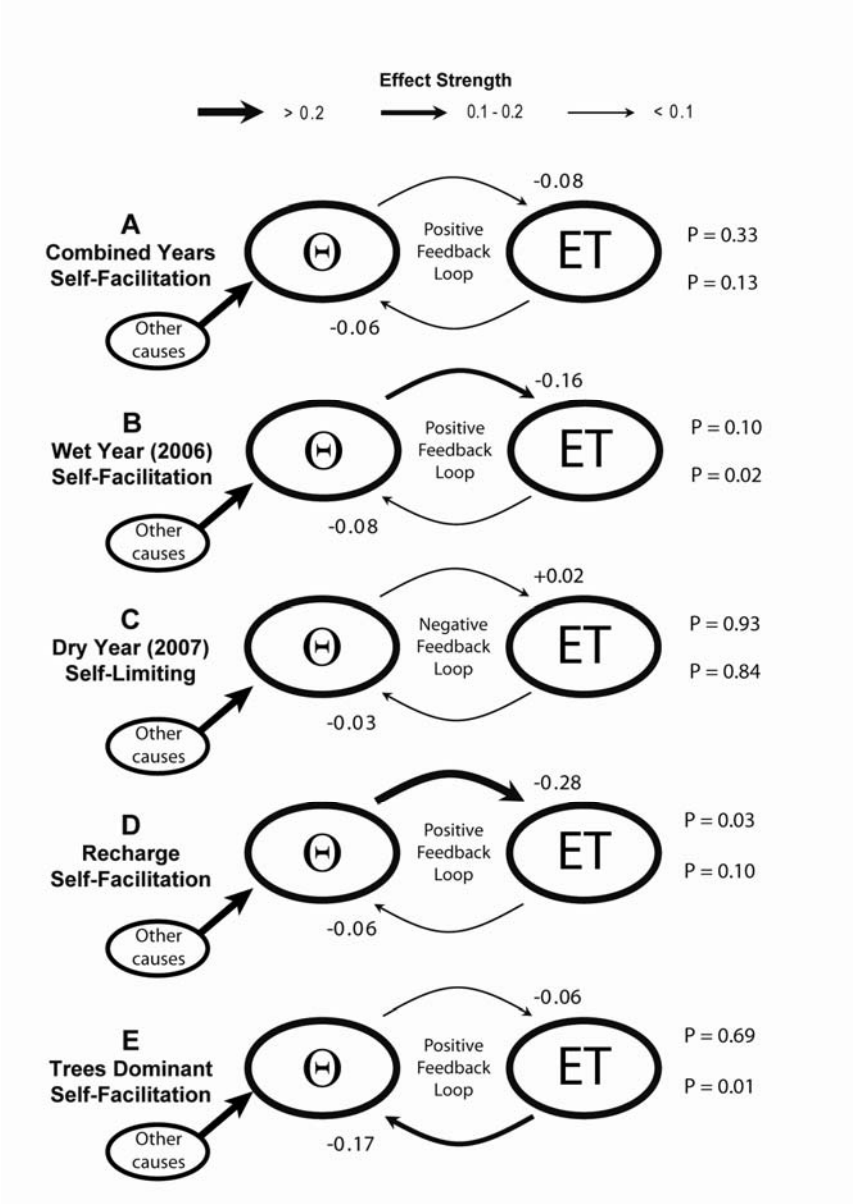

Figure 4.5. Observed net-effect interactions between plants (ET) and available water (Θ, soil moisture) for the 2006-2007 combined data set and independently for 2006, recharge swales, and swales in which large trees are abundant. Values at the ends of arrows represent the total effects (Table 4.2) from the path analysis (Figure 4.4); significance of bootstrapped samples is given at right.

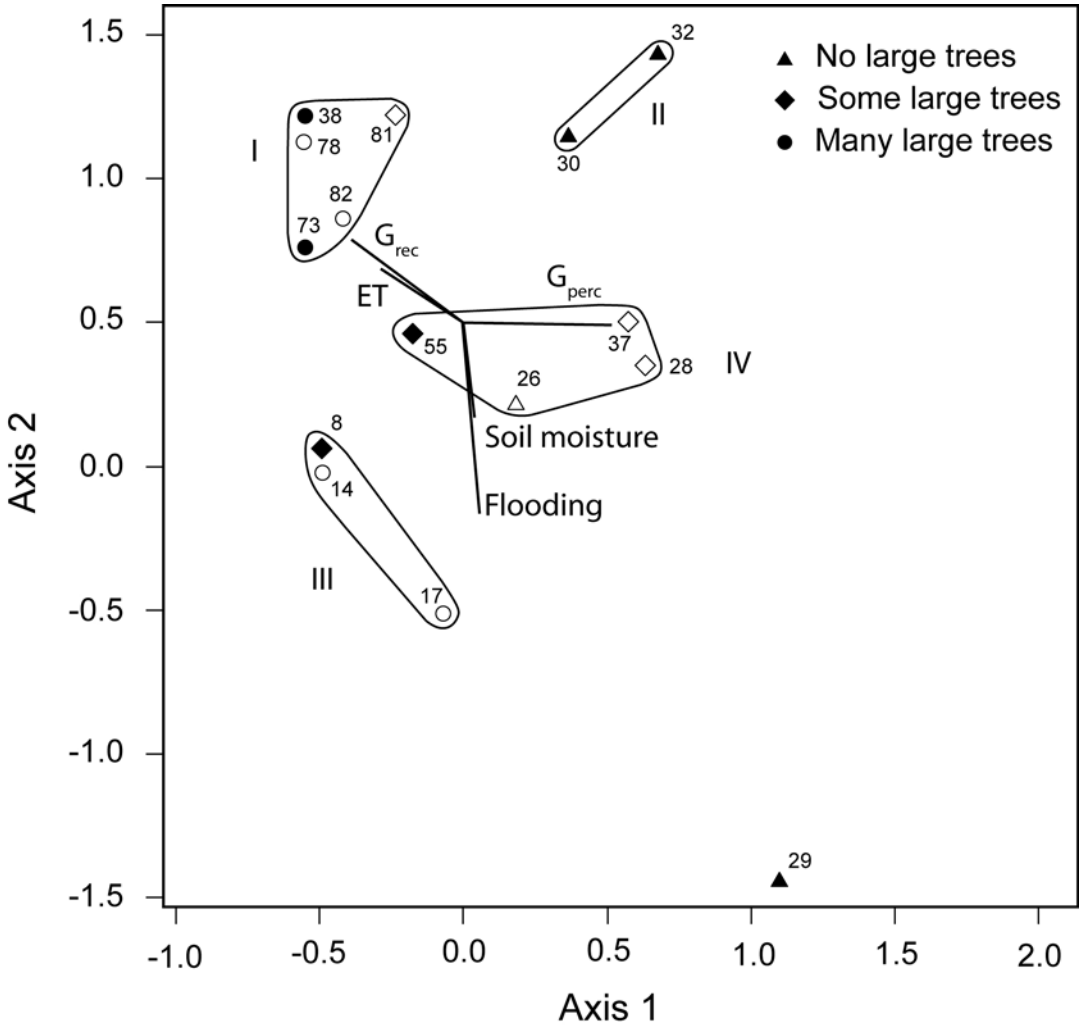

Figure 4.6. NMS ordination of understory cover in the 15 swales plotted in species space and rotated so as to maximize the relationship between G_{perc} and Axis 1. Symbols represent the three vegetation strata. Solid symbols are discharge swales (positive 2007 net groundwater flux). Open symbols are recharge swales (negative net groundwater flux). Vectors represent correlations with environmental variables for R^2 values greater than 0.20. ET is evapotranspiration. G_{rec} is average 2006-2007 groundwater recovery, the groundwater due to evaporative consumption by plants. G_{perc} is the average 2006-2007 net groundwater percolation and is a negative flux for all swales. Less negative values (i.e., following the G_{perc} vector to the right) indicate units with greater deep groundwater influx. Flooding is the summed number of days the unit was inundated in 2006 and 2007. Soil moisture refers to the volumetric soil moisture content measured in mid-August, 2007. Large trees were defined as DBH > 5 cm. Swales with "no large trees" were lacking trees with a DBH > 5 cm. Swales grouped as "some large trees" had a summed DBH between 5 and 100 cm for all trees measured within 20 m on either side of the center transect, and the "many large trees" group had a summed DBH > 100 cm.

REFERENCES CITED

Addicott, J. F., J. M. Aho, M. F. Antolin, D. K. Padilla, J. S. Richardson, and D. A. Soluk. 1987. Ecological neighborhoods: scaling environmental patterns. Oikos 49:340–346.

Allen, R. G., L. S. Pereira, D. Raes, and M. Smith. 1998. Crop evapotranspiration: guidelines for computing crop water requirements. Irrigation and Drainage Paper 56, FAO - Food and Agriculture Organization of the United Nations, Rome, Italy.

Allen, T. F. H. and T. B. Starr. 1982. Hierarchy: perspectives for ecological complexity. University of Chicago Press, Chicago, IL, USA.

Arbuckle, J. L. 2008. SPSS Statistics Base 17.0 User's Guide. SPSS Inc., Chicago, IL, USA.

Baker, M. E. and M. J. Wiley. 2009. Multiscale control of flooding and riparian-forest composition in Lower Michigan, USA. Ecology 90:145–159.

Begon, M., C. R. Townsend, and J. L. Harper. 2006. Ecology. Fourth edition. Blackwell Publishing Ltd., Malden, MA, USA.

Bentler, P. 1989. EQS Structural Equations Program Manual. BMDP Statistical Software, Los Angeles, CA, USA.

Bentler, P. M. and D. G. Bonnet. 1980. Significance tests and goodness-of-fit in the analysis of covariance structure. Psychological Bulletin 88: 588-606.

Bollen, K. A. 1989. Structural equations with latent variables. John Wiley and Sons, New York, NY, USA.

Borg, H., G. L. Stoneman, and C. G. Ward. 1988. The effect of logging and regeneration on groundwater, streamflow and stream salinity in the southern forest of Western Australia. Journal of Hydrology 99:253–271.

Brady, N. C. and R. R. Weil. 2002. The Nature and Property of Soils. Thirteenth edition. Prentice-Hall, Upper Saddle River, NJ, USA.

Browne, M. W. and R. Cudeck. 1993. Alternative ways of assessing model fit. p. 136–162. *In* K. A. Bollen and J. S. Long (eds.) Testing Structural Equation Models. Sage, Newbury Park, CA, USA.

Breda, N. J. J. 2003. Ground-based measurements of leaf area index: a review of methods, instruments and current controversies. Journal of Experimental Botany 54:2403–2417.

Bruno, J. F., J. J. Stachowicz, and M. D. Bertness. 2003. Inclusion of facilitation into ecological theory. Trends in Ecology and Evolution 18:119–125.

Burkett, V. R., D. A. Wilcox, R. Stottlemyer, W. Barrow, D. B. Fagre, J. Baron, J. Price, J. L. Nielson, C. Allen, D. L. Peterson, G. Ruggerone, and T. Doyle. 2005. Nonlinear dynamics in ecosystem response to climatic change: case studies and management implications. Ecological Complexity 2:357–394.

Chang, M. 2002. Forest Hydrology: An Introduction to Water and Forests. CRC Press, Boca Raton, FL, USA.

Comin, F. A., M. Menendez, and J. A. Herrera. 2004. Spatial and temporal scales for monitoring coastal aquatic ecosystems. Aquatic Conservation: Marine and Aquatic Ecosystems 14:S5–S17.

Croley, T. E. 1990. Laurentian Great-Lakes double-CO2 climate change hydrological impacts. Climate Change 17:27–47.

Delcourt, H. R., Delcourt, P. A. and Webb, T. 1983. Dynamic plant ecology: the spectrum of vegetation change in space and time. Quaternary Science Reviews 1:153–175.

Doss, P. K. 1993. The nature of a dynamic water table in a system of non-tidal, freshwater coastal wetlands. Journal of Hydrology 141:107–126.

Dubé, S., A. P. Plamondon, and R. L. Rothwell. 1995. Watering up after clear-cutting on forested wetlands of the St. Lawrence Lowland, Water Resources Research 31:1741–1750.

Dwire, K. A., J. B. Dauffman, and J. E. Baham. 2006. Plant species distribution in relation to water-table depth and soil redox potential in montane riparian meadows. Wetlands 26:131–146.

Fraser, C. J. D., N. T. Roulet, and M. Lafleur. 2001. Groundwater flow patterns in a large peatland. Journal of Hydrology 246: 142–154.

Fuller, B. E., A. von Eye, P. K. Wood, and B. D. Keeland. 2003. Modeling manifest variables in longitudinal designs - a two-stage approach. p. 312-351. *In* B. H. Pugesek, A. Tomer, and A. von Eye (eds.) Structural Equation Modeling: Applications in Ecological and Evolutionary Biology. Cambridge University Press, Cambridge, UK.

Gerla, P. J. 1992. The relationship of water-table changes to the capillary fringe, evapotranspiration, and precipitation in intermittent wetlands. Wetlands 12: 91–98.

Gough, L. and J. B. Grace. 1999. Predicting effects of environmental change on plant species density: experimental evaluations in a coastal wetland. Ecology 80:882–890.

Grace, J. B, T. M. Anderson, M. Smith, E. Seabloom, S. J. Andelman, D. Melinda, G. Meche, E. Weiher, L. K Allain, H. Jutila, M. Sankaran, J. Knops, M. Ritchie, and M. R. Willig. 2007. Does species diversity limit productivity in natural grassland communities? Ecology Letters 10:680–689.

Grace, J. B. and G. R. Guntensperger. 1999. The effects of landscape position of plant species density: evidence of past environmental effects in a coastal wetland. Ecoscience 6:381–391.

Grace, J. B. and H. Jutila. 1999. The relationship between species diversity and community biomass in grazed and ungrazed coastal meadows. Oikos 85:398–408.

Grace, J. B. and B. H. Pugesek. 1997. A structural equation model of plant species richness and its application to a coastal wetland. The American Naturalist 149:436–460.

Granneman, N. G. 2000. The importance of groundwater in the Great Lakes region. U.S. Geological Survey Water-Resources Investigations Report 008-4008, Lansing, MI, USA.

Grannemann, N. G., and Weaver, T. L. 1999. An annotated bibliography of selected references on the estimated rates of direct ground-water discharge to the Great Lakes: U.S. Geological Survey Water-Resources Investigations Report 98-4039, Lansing, MI, USA.

Gribovszki, Z., P. Kalicz, J. Szilagyi, and M. Kucsara. 2008. Riparian zone evapotranspiration estimation from diurnal groundwater level fluctuations. Journal of Hydrology 349:6–17.

Hale, M. G. and D. M. Orchutt. 1987. The Physiology of Plants Under Stress, John Wiley, New York, NY, USA.

Harris, S. W. and W. H. Marshall. 1963. Ecology of water-level manipulations on a northern marsh. Ecology 44:331-343.

Hayduk, L. A. 1987. Structural Equation Modeling with LISREL, The John Hopkins University Press, Baltimore, MD, USA.

Henszey, R. J., K. Pfeiffer, and J. R. Keough. 2004. Linking surface- and ground-water levels to riparian grassland species along the Platte River in central Nebraska, USA. Wetlands 24:665–687.

Hershberger, S. L. 2003. The growth of structural equation modeling: 1994-2001. Structural Equation Modeling 10:35-46.

Hill, A. J. and V. S Neary. 2007. Estimating evapotranspiration and seepage for a sinkhole wetland from diurnal surface-water cycles. Journal of the American Water Resources Association 43:1373–1382.

Jackson, S. T., R. P. Futyma, D. A. Wilcox. 1988. A paleoecological test of a classical hydrosere in the Lake Michigan dunes. Ecology 69:928–936.

Janauer, G. A. 2000. Ecohydrology: fusing concepts and scales. Ecological Engineering 16:9–16.

Kantrud, H. A., J. B. Millar, and A. G. van der Valk. 1989. Vegetation of wetlands of the Prairie Pothole Region. p. 132–187. *In* A. van der Valk (ed.) Northern Prairie Wetlands. Iowa State University Press, Ames, IA, USA.

Keddy, P. A. and A. A. Reznicek. 1986. Great Lakes vegetation dynamics: the role of fluctuating water levels and buried seeds. Journal of Great Lakes Research 12:25–36.

Kline, R. B. 1998. Principles and Practice of Structural Equation Modeling. Guilford Press, New York, NY, USA.

Laczniak, R. J., G. A. DeMeo, S. R. Reiner, J. L. Smith, and W. E. Nylund. 1999. Estimates of groundwater discharge as determined from measurements of evapotranspiration, Ash Meadows area, Nye County, Nevada. Water-Resources Investigation Report 99-4079, U.S. Geological Survey, Reston, VA.

Lafleur, M. and W. R. Rouse. 1988. The influence of surface cover and climate on energy partitioning and evaporation in a subarctic wetland. Boundary Layer Meteorology 44:327–347.

Laio, F., S. Tamea, L. Ridolfi, P. D'Odorico, and I. Rodriguez-Iturbe. 2009. Ecohydrology of groundwater-dependent ecosystems: 1. Stochastic water table dynamics. Water Resources Research 45:W05419.

Lambers, H., T. L. Ponse, F. Stuart, and S. Chapin. 1998. Plant Physiology Ecology. Springer-Verlag, New York, NY, USA.

Le Maitre, D. C., D. F. Scott, and C. Colvin. 1999. A review of information on interactions between vegetation and groundwater. Water SA 25:137–152.

Leyer, I. 2005. Predicting plant species' responses to river regulation: the role of water level fluctuations. Journal of Applied Ecology 42:239–250.

LI-COR. 1992. LAI-2000 Plant Canopy Analyzer Instruction Manual. LI-COR, Inc., Lincoln, NE, USA.

Lofgren, B. M., F. H. Quinn, A. H. Clites, R. A. Assel, A. J. Eberhardt, and C. L. Luukkonen. 2002. Evaluation of potential impacts on Great Lakes water resources based on climate scenarios of two GCMs. Journal of Great Lakes Research 28:537–554.

Loheide, S. P. 2008. A method for estimating subdaily evapotranspiration of shallow groundwater using diurnal water table fluctuations. Ecohydrology 1:59–66.

Loheide, S. P., J. J. Butler, and S. M. Gorelick, 2005. Estimation of groundwater consumption by phreatophytes using diurnal water table fluctuations: a saturated-unsaturated flow assessment. Water Resources Research 41:1–14.

Loheide, S. P., R. S. Deitchman, D. J. Cooper, E. C. Wolf, C. T. Hammersmark, and J. D. Lundquist. 2009. A framework for understanding the hydroecology of impacted wet meadows in the Sierra Nevada and Cascade Ranges, California, USA. Hydrogeology Journal 17: 229–246.

MacCallum, R. C., C. Kim, W. B. Malarkey, and J. K. Kiecolt-Glaser. 1997. Studying multivariate change using multilevel models and latent curve models. Multivariate Behavioral Research 32:215-253.

Marcotte, P., V. Roy, A. P. Plamondon, and I. Auger. 2008. Ten-year water table recovery after clearcutting and draining boreal forested wetlands of eastern Canada. Hydrological Processes 22:4163–4172.

Magnuson, J. J., K. E. Webster, R. A. Assel, C. J. Bowser, P. J. Dillon, J. G. Eaton, H. E. Evans, E. J. Fee, R. I. Hall, L. R. Mortsch, D. W. Schindler, and F. H. Quinn. 1997. Potential effects of climate changes on aquatic systems: Laurentian Great Lakes and Precambrian Shield Region. Hydrological Processes 11:825–871.

Maruyama, G. M. 1998. Basics of Structural Equation Modeling. Sage, Thousand Oaks, CA, USA.

Maynard, L. and D. A. Wilcox. 1997. Coastal Wetlands. State of the Lakes Ecosystem Conference Proceedings. Environment Canada, Burlington, ON, Canada and U.S. Environmental Protection Agency, Chicago, IL, USA. Report EPA 905-R-97-015b.

McCune, B. and J. B. Grace. 2002. Analysis of Ecological Communities. MjM Software Design, Gleneden Beach, OR, USA.

McCune, B. and M. J. Mefford. 1999. Multivariate Analysis of Ecological Data Version 4.0. MjM Software, Gleneden Beach, OR, USA.

Meyboom, P. 1966. Unsteady groundwater flow near a willow ring in hummocky moraine. Journal of Hydrology 4:38–62.

Mitchell, R. J. 1992. Testing evolutionary and ecological hypotheses using path analysis and structural equation modeling. Functional Ecology: 6:123–129.

Mitsch, W. J. and J. G. Gosselink. 2000a. The value of wetlands: importance of scale and landscape setting. Ecological Economics 35:25–33.

Mitsch, W. J. and J. G. Gosselink. 2000b. Wetlands. Third edition. John Wiley & Sons, Inc., New York, NY, USA.

National Oceanographic and Atmospheric Administration (NOAA). 2008. Annual Climatological Summary (Alpena County Regional Airport). http://www4.ncdc.noaa.gov/cgi-win/wwcgi.dll?wwDI~StnSrch~StnID~20010361.

Noest, V. 1994. A hydrology-vegetation interaction model for predicting the occurrence of plant species in dune slacks. Journal of Environmental Management 40:119–128.

O'Neill, R.V., D. L. DeAngelis, J. B. Waide, and T. F. H. Allen. 1986. A Hierarchical Concept of Ecosystems. Princeton University Press, Princeton, NJ, USA.

Peck, A. J. and D. R. Williamson. 1987. Effects of forest clearings on groundwater. Journal of Hydrology 94:47– 65.

Poiani, K. A., W. C. Johnson, G. A. Swanson, and T. C. Winter. 1996. Climate change and northern prairie wetlands: simulations of long-term dynamics. Limnology and Oceanography 41:871–881.

Posner, R. N., J. M. Bell, S. J. Baedke, T. A. Thompson, and D. A. Wilcox. 2005. Aqueous geochemistry as an indicator of subsurface geology and hydrology of a beach-ridge/wetland complex in Negwegon State Park, MI. Geological Society of America Abstracts with Programs 37:300.

Pugesek, B. H. 2003. Concepts of structural equation modeling in biological research. p. 42–59. *In* B. H. Pugesek, A. Tomer, and A. von Eye (eds.) Structural Equation Modeling: Applications in Ecological and Evolutionary Biology. Cambridge University Press, Cambridge, UK.

Ridolfi, L., P. D'Odorico, and F. Laio. 2006. Effect of vegetation–water table feedbacks on the stability and resilience of plant ecosystems. Water Resources Research 42:W01201.

Riekerk, H. 1989. Influence of silvicultural practices on the hydrology of pine flatwoods in Florida. Water Resources Research 25:713–719.

Rodriguez-Iturbe, I. 2000. Ecohydrology: a hydrologic perspective of climate-soil-vegetation dynamics. Water Resources Research 36:3–9.

Rodriguez-Iturbe, I., P. D'Odorico, F. Laio, L. Ridolfi, and S. Tamea. 2007. Challenges in humid land ecohydrology: interactions of water table and unsaturated zone with climate, soil, and vegetation. Water Resources Research 43:W09301.

Roy, V., J.-C. Ruel, and A. P. Plamondon. 2000. Establishment, growth and survival of natural regeneration after clearcutting and drainage on forested wetlands. Forest Ecology and Management 129:253– 267.

Sanderson, J. S. and D. J. Cooper. 2008. Ground water discharge by evapotranspiration in wetlands of an arid intermountain basin. Journal of Hydrology 351:344–359.

Schreiber, J. B., F. K. Stage, J. King, A. Nora, and E. A. Barlow. 2006. Reporting structural equation modeling and confirmatory factor analysis results: a review. Journal of Educational Research 99:323–337.

Skalbeck, J. D., D. M. Reed, R. J. Hunt, and J. D. Lambert. 2009. Relating groundwater to seasonal wetlands in southeastern Wisconsin, USA. Hydrogeology Journal 17:215–228.

Smith, J. B. 1991. The potential impacts of climate change on the Great-Lakes. Bulletin of the American Meteorological Society 72:21–28.

Sorbom, D. 1989. Model modification. Psychometrika 54:371–383.

Steiger, J. H. and J. M. Lind. 1980. Statistically based tests for the number of common factors. Paper presented at the annual meeting of the Psychometric Society, Iowa City, IA, USA.

Sun, G., H. Riekerk, and L. V. Kornhak. 2000. Ground-water-table rise after forest harvesting on cypress-pine flatwoods in Florida. Wetlands 20:101–112.

Tamea, S., F. Laio, L. Ridolfi, P. D'Odorico, and I. Rodriguez-Iturbe. 2009. Ecohydrology of groundwater-dependent ecosystems: 2. Stochastic soil moisture dynamics. Water Resources Research 45:W05420.

Tomer, A. and B. H. Pugesek. 2003. Guidelines for the implementation and publication of structural equation models. p. 125–140. *In* B. H. Pugesek, A. Tomer, and A. von Eye (ed.s). Structural Equation Modeling: Applications in Ecological and Evolutionary Biology. Cambridge University Press, Cambridge, UK.

Tóth, J. 1963. A theoretical analysis of groundwater flow in small drainage basins. Journal of Geophysical Research 68:4795–4812.

Trousdell, K. B. and M. D. Hoover. 1955. A change in ground-water level after clearcutting of loblolly pine in the coastal plain. Journal of Forestry 53:493–498.

Troxell, H. C. 1936. The diurnal fluctuation in the groundwater and flow of the Santa Ana River and its meaning. EOS Transactions, American Geophysical Union 17:496–505.

van der Kamp, G. and M. Hayashi. 2009. Groundwater-wetland ecosystem interaction in the semiarid glaciated plains of North America. Hydrogeology Journal 17:203–214.

van Geest, G. J., H. Coops, R. M. M. Roijackers, A. D. Buijse, and M. Scheffer. 2005. Succession of aquatic vegetation driven by reduced water-level fluctuations in floodplain lakes. Journal of Applied Ecology 42:251–260.

Vondracek, B., K. L. Blann, C. B. Cox, J. Frost Nerbonne, K. G. Mumford, B. A. Nerbonne, L. A. Sovell, and J. K. H. Zimmerman. 2005. Environmental Management 36:775–791.

West, S. G., J. F. Finch, and P. J. Curran. 1995. Structural equation models with nonnormal variables: problems and remedies. p. 56–75. *In* R. Hoyle (ed.) Structural Equation Modeling: Issues, Concepts, and Applications. Sage, Newbury Park, CA, USA.

White, W. N. 1932. A method of estimating groundwater supplies based on discharge by plants and evaporation from soil. Water-Supply Paper 659-A, U.S. Geological Survey. Washington, DC, USA.

Williams, T. M. and D. J. Lipscomb. 1981. Water table rise after cutting on coastal plain soils. Southern Journal of Applied Forestry 5:46–48.

Wilcox, D. A. 1995. The role of wetlands as nearshore habitat in Lake Huron. p. 223–245. *In* M. Munawar, T. Edsall, and J. Leach (eds.) The Lake Huron Ecosystem: Ecology, Fisheries and Management. Ecovision World Monograph Series, S.P.B. Academic Publishing, The Netherlands.

Wilcox, D. A. 2004. Implications of hydrologic variability on the succession of plants in Great Lakes wetlands. Aquatic Ecosystem Management 7:223–231.

Wilcox, D. A., S. J. Baedke, and T. A. Thompson. 2005. Groundwater contribution to hydrology-driven development of wetland plant communities. Geological Society of America Abstracts with Programs 37:244.

Wilcox, D. A. and S. J. Nichols. 2008. The effects of water-level fluctuations on vegetation in a Lake Huron wetland. Wetlands 28:487–501.

Wilcox, D. A. and H. A. Simonin. 1987. A chronosequence of aquatic macrophyte communities in dune ponds. Aquatic Botany 28:227.

Wilde, S. A., E. C. Steinbrenner, R. S. Pierce, R. C. Dosen, and D. T. Pronin. 1953. Influence of forest cover on the state of the ground water table. Soil Science Society Proceedings 17:65– 67.

Wright, S. 1921. Correlation and causation. Journal of Agricultural Research 20:557–585.

Wuebbles, D. J. and K. Hayhoe. 2004. Climate change projections for the United States Midwest. Mitigation and Adaptation Strategies for Global Change 9:335–363.

CHAPTER 5

Conclusion

5.1 Purpose

The intent of my research was to investigate interactions between plants and hydrology in a ridge-swale coastal wetland system in the Laurentian Great Lakes. Specifically, I was interested in the system of feedbacks that link water-balance dynamics at two scales—the water table and the soil root zone—and vegetation. Although general one-way effects of vegetation on water levels and the reverse have been observed, we do not have a comprehensive explanation for the broader bidirectional influences and feedbacks that drive wetland development and maintenance in the landscape. This research helps to further our understanding of these interactions in wetland ecosystems. Compounding this complexity, the underlying geology, physiography, and climate (precipitation in particular) of a specific wetland unit affect the system of interactions as well. A better understanding of these ecohydrological interactions has implications for the effects of climate change on Great Lakes coastal wetlands.

5.2 Summary of Chapter Findings

In Chapter 2, I developed modifications to a method for estimating evapotranspiration (ET) and shallow groundwater flux from water-table fluctuations typically used in semiarid riparian wetlands and applied it to a structurally and vegetatively complex ridge-swale wetland system in the rain-prone Great Lakes region. Modifications to the method included 1) weighting the specific yield to account for above- and below-ground water levels, 2) using regression analysis to relate ET estimated from water-table fluctuation to Penman-Monteith potential ET for days when the method failed, and 3) allowing flexibility in assigning the nighttime period of recovery occurring

in the absence of ET. From this, I was able to estimate ET and groundwater fluxes over two annual growing seasons for 15 wetland units in the complex. Mean daily evapotranspiration (ET) rates ranged from 5.5 mm d^{-1} to 8.1 mm d^{-1}. The regular pattern of upland sandy ridges with narrow intervening swales and a water table that infrequently fell below rooting depth likely allowed for substantial evapotranspirative loss.

In Chapter 3, I examined transient water-table dynamics resulting from interactions between groundwater hydrology and evapotranspiration using water-balance analysis. I explored how variation in unit hydrology arises through interactions between plants, as indexed by ET, and site hydrology, represented by the water balance. I found that differences in the fluxes controlling the water balance give interesting spatial and temporal variation to this wetland complex. Spatial variation in the underlying stratigraphy ultimately leads to differences in groundwater water flux. The absolute flux rates are strongly influenced by annual climatic variability, but some swales always receive greater groundwater loading than others. Evapotranspiration by plants both brings water to the swale, and removes it. Where water availability in the rooted zone was greater, ET generally proceeded at higher rates, although some evidence of ET suppression in very wet swales was apparent. Where groundwater availability was relatively low, plant ET had a greater control over water availability. The type of plant community seemed to have a secondary effect on ET, explaining some variability among swales having similar water availability, but the relationship was not well-defined until the next chapter.

Chapter 4 more directly investigated the specific ecohydrological dynamics between plant water use, indexed by ET, and water available to plants, indexed by volumetric soil moisture content. Using path analytic methods in a structural equation model to implement the conceptual model of interactions between plants and hydrology in the ridge-swale system studied, I found that bi-directional negative interactions prevail across wet climatic conditions, physiographic and hyrogeologic character, and abundance of large trees. In dry years, when water is more limited, soil moisture may lead to higher rates of ET. The strengths of effects between soil moisture and ET vary depending on site-specific factors such as loss by percolation to groundwater and the abundance and size of trees. Community composition is related to whether a swale receives shallow or

deep groundwater and the degree of inundation. Both plant-hydrology interactions and community composition can be related to the hydrogeologic setting of a particular swale.

5.3 Synthesis

As in most ecosystems, climatic variability (precipitation in particular) strongly affected water-table dynamics but, in this case, only under wet conditions. As a result, annual precipitation influenced causal interactions between soil water availability and plant water use. In a wet year, a strong positive feedback was observed, whereas a weaker interaction was observed in a dry year, along with some indication of water limitation.

Underlying geology also had a substantial effect on plant-hydrology interactions in two important ways. Sandy substrates permitted considerable water loss from the system over the growing season, which lowered the water table across the wetland complex and reduced soil moisture. Secondly, where recharge conditions were present, and localized influx of deep groundwater was absent, the effect was even more pronounced, and water availability had a stronger causal effect on plant water use.

Although climate and underlying geology had the most perceptible impact on the feedbacks, my results suggest that effects of vegetation are also important, especially when considering ecosystem response to climate change. Soil moisture had a strong negative effect on ET despite potential adaptations by plants to wet conditions. At the same time, plants (particularly tree species) regulated soil moisture in a way that facilitated ET, especially under wet climatic conditions. In this way, plants helped create drier conditions than they would have experienced otherwise.

5.4 Issues of Scale

In ecosystem studies, it is important to consider multiple spatial scales, as previously noted by many (e.g., Allen and Starr 1982, Delcourt et al. 1983, O'Neill et al. 1986, Addicott et al 1987, Mitsch and Gosselink 2000, Comin et al. 2004, Vondracek et al. 2005). This is especially true of ecohydrological studies (Janauer 2000, Rodriguez-Iturbe 2000). The question, however, is not which scale is of greatest importance; rather, the key is to address all possible scales to which the data are applicable. The ridge-swale

wetland complex in this study provided a unique opportunity to consider multiple scales. The three scales of interest were an individual swale, the wetland complex, and the Great Lakes coastal wetland zone. As is often the case, the differentiation between scales is not straightforward. For example, I sampled only a portion of each swale along a transect perpendicular to the ridges but used that portion as a representation of a swale. The outer boundary of the wetland complex is well-defined, but whether the upland ridges and their vegetation should have been considered part of the wetland complex in this study is still unclear; the upland trees likely influenced wetland water levels but clearly are not wetland species and would not be delineated as part of the wetland in a conventional sense.

Scaling up to a regional level also brings challenges. While this system may not be similar descriptively to all other coastal wetlands, such systems are similar by process; plants interact with hydrology, and the resulting dynamics depend on climate, hydrogeology, and evapotranspiration. Moreover, coastal areas represent groundwater discharge zones on the landscape (Granneman and Weaver 1999, Granneman 2000), and coastal wetlands, therefore, are primarily groundwater-fed systems such as the one in this study. Although the exact details may vary, the mechanisms governing plant-hydrology interactions apply ubiquitously.

5.5 Implications for Climate Change

As climatic conditions in the Great Lakes tend toward predicted drier conditions in summer and fall, and wet years become fewer (Wuebbles and Hayhoe 2004), plant communities of coastal wetland systems likely will proceed on a trajectory toward more xeric conditions, especially in recharge zones. Groundwater discharge, governed by site-specific hydrogeologic factors however, may mediate climate-change effects. Still, site-specific characteristics and antecedent conditions undoubtedly will influence wetland response. Nonetheless, the important hydrologic players will not be limited to precipitation and surface water; groundwater and evapotranspiration may play a large role in determining wetland response to climate change as well.

If water levels continue to drop in Lake Huron, as predicted by some climate models (e.g., Croley 1990, Smith 1991, Magnuson et al. 1997, Lofgren et al. 2002),

groundwater flow paths that currently discharge to the lake may intersect the landscape in the future, generating more wetland area. Furthermore, following a major drop in base level, the water table will adjust accordingly. Recharge and discharge zones may shift, followed by a resulting change in plant community. Groundwater modeling studies can provide an important tool for predicting these hydrologic adjustments in the coastal zone, and the mechanisms outlined in this study provide insight for predicting the shifting mosaics of plant community composition due to climate change in Great Lakes coastal wetlands.

REFERENCES CITED

Addicott, J. F., J. M. Aho, M. F. Antolin, D. K. Padilla, J. S. Richardson, and D. A. Soluk. 1987. Ecological neighborhoods: scaling environmental patterns. Oikos 49:340–346.

Allen, T. F. H. and T. B. Starr. 1982. Hierarchy: Perspectives for Ecological Complexity. University of Chicago Press, Chicago, IL, USA.

Comin, F. A., M. Menendez, and J. A. Herrera. 2004. Spatial and temporal scales for monitoring coastal aquatic ecosystems. Aquatic Conservation: Marine and Aquatic Ecosystems 14:S5–S17.

Croley, T. E. 1990. Laurentian Great-Lakes double-CO2 climate change hydrological impacts. Climate Change 17:27–47.

Magnuson, J. J., K. E. Webster, R. A. Assel, C. J. Bowser, P. J. Dillon, J. G. Eaton, H. E. Evans, E. J. Fee, R. I. Hall, L. R. Mortsch, D. W. Schindler, and F. H. Quinn. 1997. Potential effects of climate changes on aquatic systems: Laurentian Great Lakes and Precambrian Shield Region. Hydrological Processes 11:825–871.

Delcourt, H. R., P. A. Delcourt, and T. Webb. 1983. Dynamic plant ecology: the spectrum of vegetation change in space and time. Quaternary Science Reviews 1:153–175.

Granneman, N. G. 2000. The importance of groundwater in the Great Lakes region. U.S. Geological Survey Water-Resources Investigations Report 008-4008, Lansing, MI, USA.

Grannemann, N. G. and Weaver, T. L. 1999. An annotated bibliography of selected references on the estimated rates of direct ground-water discharge to the Great Lakes. U.S. Geological Survey Water-Resources Investigations Report 98–4039, Lansing, MI, USA.

Janauer, G. A. 2000. Ecohydrology: fusing concepts and scales. Ecological Engineering 16:9–16.

Lofgren, B. M., F. H. Quinn, A. H. Clites, R. A. Assel, A. J. Eberhardt, and C. L. Luukkonen. 2002. Evaluation of potential impacts on Great Lakes water resources based on climate scenarios of two GCMs. Journal of Great Lakes Research 28:537–554.

Mitsch, W. J. and J. G. Gosselink. 2000. The value of wetlands: importance of scale and landscape setting. Ecological Economics 35:25–33.

O'Neill, R.V., D. L. DeAngelis, J. B. Waide, J. B. and T. F. H. Allen. 1986. A hierarchical concept of ecosystems. Princeton University Press, Princeton, NJ, USA.

Rodriguez-Iturbe, I. 2000. Ecohydrology: a hydrologic perspective of climate-soil-vegetation dynamics. Water Resources Research 36:3–9.

Smith, J. B. 1991. The potential impacts of climate change on the Great-Lakes. Bulletin of the American Meteorological Society 72:21–28.

Vondracek, B., K. L. Blann, C. B. Cox, J. Frost Nerbonne, K. G. Mumford, B. A. Nerbonne, L. A. Sovell, and J. K. H. Zimmerman. 2005. Land use, spatial scale, and stream systems: lessons from an agricultural region. Environmental Management 36:775–791.

Wuebbles, D. J. and K. Hayhoe. 2004. Climate change projections for the United States Midwest. Mitigation and Adaptation Strategies for Global Change 9:335–363.

APPENDIX

Structural Equation Model Output

2006-2007 Data Set

The model is nonrecursive.
Sample size = 87

Variable Correlations

Variable 1		Variable 2	Correlation
h_0	↔	P	-0.17
ET error	↔	h_0	0.40
G_{rec} error	↔	P	-0.10
ΔS error	↔	LAI error	0.41
LAI error	↔	G_{rec} error	0.25
ET error	↔	Θ error	-0.23
ET error	↔	P	-0.02
ΔS error	↔	GC error	0.01
G_{rec} error	↔	GC error	0.20
G_{rec} error	↔	h_0	-0.24

Assessment of normality

Variable	min	max	skew	c.r.	kurtosis	c.r.
P	45.72	100.84	1.24	4.73	0.26	0.50
h_0	-64.37	16.77	0.02	0.09	-0.75	-1.43
GC	0.07	1.50	0.53	2.03	-0.24	-0.47
Grec	91.20	229.73	0.58	2.22	-0.13	-0.25
LAI	2.35	5.39	0.72	2.76	-0.42	-0.80
DS	-342.30	191.09	-0.13	-0.51	-1.10	-2.09
Q	0.24	1.00	-0.40	-1.51	-0.59	-1.11
ET	126.64	304.61	0.56	2.15	-0.08	-0.15
Multivariate					-1.62	-0.60

Model Correlations

	P	h_0	GC	G_{rec}	LAI	ΔS	Θ	ET
P	1.00							
h_0	-0.17	1.00						
GC	0.00	0.03	1.00					
Grec	-0.03	0.16	0.59	1.00				
LAI	0.02	-0.27	-0.09	0.27	1.00			
DS	0.74	-0.55	-0.28	-0.46	0.14	1.00		
Q	-0.07	0.87	0.00	0.00	-0.31	-0.35	1.00	
ET	-0.01	0.23	0.60	0.97	0.21	-0.49	0.06	1.00

Sample Correlations

	P	h_0	GC	G_{rec}	LAI	ΔS	Θ	ET
P	1.00							
h_0	-0.17	1.00						
GC	-0.03	0.02	1.00					
Grec	-0.04	0.16	0.58	1.00				
LAI	0.08	-0.26	-0.09	0.29	1.00			
DS	0.75	-0.54	-0.30	-0.46	0.17	1.00		
Q	-0.02	0.87	0.01	0.00	-0.34	-0.33	1.00	
ET	-0.03	0.23	0.59	0.97	0.24	-0.50	0.06	1.00

Bootstrap Standard Errors - Standardized Total Effects

	P	h_0	GC	G_{rec}	LAI	ΔS	Θ	ET
GC	0.01	0.10	0.00	0.01	0.11	0.02	0.11	0.01
G_{rec}	0.01	0.06	0.06	0.01	0.10	0.01	0.07	0.02
LAI	0.02	0.09	0.01	0.01	0.00	0.03	0.10	0.01
ΔS	0.05	0.05	0.05	0.18	0.06	0.01	0.04	0.06
Θ	0.05	0.03	0.02	0.04	0.01	0.07	0.01	0.04
ET	0.01	0.07	0.07	0.01	0.10	0.01	0.08	0.01

Bootstrap Bias-Corrected Lower Bounds - Standardized Total Effects

	P	h_0	GC	G_{rec}	LAI	ΔS	Θ	ET
GC	-0.01	-0.15	-0.02	-0.01	-0.33	-0.02	-0.17	-0.03
G_{rec}	-0.03	-0.19	0.45	-0.02	0.04	-0.04	-0.21	0.88
LAI	-0.07	-0.44	0.00	-0.06	0.00	-0.10	-0.49	0.00
ΔS	0.61	-0.36	-0.41	0.09	-0.24	0.00	-0.04	-0.60
Θ	-0.03	0.83	-0.08	-0.01	-0.05	-0.04	0.00	-0.13
ET	-0.03	-0.21	0.49	-0.03	0.04	-0.05	-0.23	0.00

Bootstrap Bias-Corrected Upper Bounds - Standardized Total Effects

	P	h_0	GC	G_{rec}	LAI	ΔS	Θ	ET
GC	0.04	0.23	0.01	0.03	0.12	0.05	0.26	0.01
G_{rec}	0.00	0.07	0.68	0.00	0.42	0.01	0.07	0.97
LAI	0.01	-0.09	0.03	0.00	0.02	0.01	-0.10	0.05
ΔS	0.80	-0.17	-0.20	0.79	-0.02	0.02	0.12	-0.36
Θ	0.18	0.97	0.01	0.16	0.00	0.26	0.02	0.02
ET	0.00	0.07	0.73	0.00	0.45	0.01	0.08	0.02

Bootstrap Bias-Corrected Two-Tailed Significance - Standardized Total Effects

	P	h_0	GC	G_{rec}	LAI	ΔS	Θ	ET
GC	0.56	0.72	0.54	0.51	0.39	0.56	0.71	0.56
G_{rec}	0.21	0.32	0.00	0.15	0.02	0.21	0.34	0.00
LAI	0.09	0.00	0.07	0.06	0.07	0.09	0.00	0.09
ΔS	0.00	0.00	0.00	0.01	0.02	0.20	0.30	0.00
Θ	0.13	0.00	0.11	0.09	0.09	0.13	0.20	0.13
ET	0.21	0.32	0.00	0.16	0.02	0.21	0.33	0.20

2006 Data Set

The model is nonrecursive.
Sample size = 45

Variable Correlations

Variable 1		Variable 2	Correlation
h_0	↔	P	-0.56
ET error	↔	h_0	0.11
G_{rec} error	↔	P	0.06
ΔS error	↔	LAI error	0.51
LAI error	↔	G_{rec} error	0.28
ET error	↔	Θ error	-0.42
ET error	↔	P	-0.04
ΔS error	↔	GC error	-0.04
G_{rec} error	↔	GC error	0.29
G_{rec} error	↔	h_0	-0.40

Assessment of normality

Variable	min	max	skew	c.r.	kurtosis	c.r.
P	58.93	100.84	0.68	1.85	-1.50	-2.05
h_0	-49.39	13.77	-0.01	-0.04	-0.73	-1.00
GC	0.07	1.50	0.59	1.61	-0.18	-0.25
Grec	101.84	229.53	0.46	1.27	-0.18	-0.24
LAI	2.35	5.39	0.63	1.73	-0.59	-0.81
DS	-312.51	191.09	-0.34	-0.94	-1.28	-1.75
Q	0.50	1.00	-0.18	-0.48	-0.74	-1.02
ET	134.67	304.61	0.48	1.31	0.04	0.06
Multivariate					-4.13	-1.10

Model Correlations

	P	h_0	GC	G_{rec}	LAI	ΔS	Θ	ET
P	1.00							
h_0	-0.56	1.00						
GC	0.07	-0.14	1.00					
Grec	0.05	-0.16	0.60	1.00				
LAI	0.17	-0.35	-0.02	0.29	1.00			
DS	0.80	-0.64	-0.21	-0.36	0.27	1.00		
Q	-0.46	0.95	-0.19	-0.30	-0.35	-0.47	1.00	
ET	0.04	-0.06	0.57	0.97	0.20	-0.42	-0.22	1.00

Sample Correlations

	P	h_0	GC	G_{rec}	LAI	ΔS	Θ	ET
P	1.00							
h_0	-0.56	1.00						
GC	0.06	-0.11	1.00					
Grec	0.04	-0.15	0.60	1.00				
LAI	0.05	-0.28	-0.03	0.31	1.00			
DS	0.80	-0.64	-0.24	-0.38	0.15	1.00		
Q	-0.48	0.95	-0.18	-0.30	-0.32	-0.47	1.00	
ET	0.04	-0.06	0.58	0.97	0.23	-0.43	-0.24	1.00

Bootstrap Standard Errors - Standardized Total Effects

	P	h_0	GC	G_{rec}	LAI	ΔS	Θ	ET
GC	0.02	0.15	0.01	0.01	0.16	0.03	0.15	0.01
G_{rec}	0.01	0.09	0.10	0.01	0.14	0.02	0.09	0.04
LAI	0.02	0.13	0.01	0.02	0.01	0.03	0.13	0.02
ΔS	0.07	0.09	0.08	0.24	0.08	0.01	0.06	0.09
Θ	0.05	0.03	0.02	0.04	0.01	0.07	0.01	0.03
ET	0.01	0.10	0.11	0.01	0.16	0.02	0.10	0.01

Bootstrap Bias-Corrected Lower Bounds - Standardized Total Effects

	P	h_0	GC	G_{rec}	LAI	ΔS	Θ	ET
GC	-0.06	-0.43	0.00	-0.05	-0.44	-0.09	-0.43	-0.01
G_{rec}	-0.05	-0.32	0.32	-0.04	-0.17	-0.07	-0.32	0.82
LAI	-0.10	-0.61	0.00	-0.06	0.00	-0.15	-0.60	0.00
ΔS	0.54	-0.36	-0.45	-0.28	-0.24	0.00	-0.01	-0.68
Θ	0.03	0.97	-0.10	-0.03	-0.05	0.03	0.00	-0.15
ET	-0.05	-0.38	0.34	-0.04	-0.19	-0.08	-0.37	0.00

Bootstrap Bias-Corrected Upper Bounds - Standardized Total Effects

	P	h_0	GC	G_{rec}	LAI	ΔS	Θ	ET
GC	0.01	0.16	0.03	0.00	0.21	0.02	0.16	0.05
G_{rec}	0.00	0.03	0.70	0.00	0.39	0.00	0.03	0.98
LAI	-0.01	-0.08	0.05	0.01	0.02	-0.01	-0.08	0.07
ΔS	0.82	-0.02	-0.15	0.67	0.09	0.04	0.22	-0.34
Θ	0.21	1.11	-0.01	0.14	0.01	0.30	0.04	-0.02
ET	0.00	0.03	0.76	0.00	0.44	0.00	0.03	0.04

Bootstrap Bias-Corrected Two-Tailed Significance - Standardized Total Effects

	P	h_0	GC	G_{rec}	LAI	ΔS	Θ	ET
GC	0.21	0.36	0.18	0.26	0.50	0.22	0.37	0.21
G_{rec}	0.05	0.09	0.00	0.21	0.40	0.06	0.10	0.00
LAI	0.01	0.02	0.01	0.20	0.21	0.01	0.02	0.01
ΔS	0.00	0.03	0.00	0.42	0.39	0.06	0.10	0.00
Θ	0.01	0.00	0.01	0.28	0.27	0.02	0.06	0.02
ET	0.06	0.09	0.00	0.21	0.41	0.06	0.10	0.06

2007 Data Set

The model is nonrecursive.
Sample size = 42

Variable Correlations

Variable 1		Variable 2	Correlation
h_0	↔	P	-0.66
ET error	↔	h_0	0.68
G_{rec} error	↔	P	0.22
ΔS error	↔	LAI error	0.53
LAI error	↔	G_{rec} error	0.09
ET error	↔	Θ error	-0.19
ET error	↔	P	-0.56
ΔS error	↔	GC error	-0.12
G_{rec} error	↔	GC error	0.02
G_{rec} error	↔	h_0	-0.37
GC error	↔	P	-0.56

Assessment of normality

P_MM	min	max	skew	c.r.	kurtosis	c.r.
P	45.72	60.96	0.63	1.67	-1.50	-1.98
h_0	-64.37	16.77	0.44	1.16	-0.66	-0.88
GC	0.07	1.28	0.41	1.09	-0.53	-0.70
Grec	91.20	229.73	0.74	1.95	0.01	0.01
LAI	2.35	5.39	0.83	2.19	-0.20	-0.27
DS	-342.30	13.17	-0.47	-1.25	-1.39	-1.84
Q	0.24	1.00	0.13	0.34	-1.04	-1.37
ET	126.64	284.55	0.67	1.76	-0.17	-0.22
Multivariate					-4.95	-1.27

Model Correlations

	P	h_0	GC	G_{rec}	LAI	ΔS	Θ	ET
P	1.00							
h_0	-0.66	1.00						
GC	-0.68	0.22	1.00					
Grec	-0.68	0.41	0.61	1.00				
LAI	0.20	-0.31	-0.18	0.22	1.00			
DS	0.79	-0.83	-0.54	-0.73	0.22	1.00		
Q	-0.53	0.81	0.25	0.24	-0.38	-0.62	1.00	
ET	-0.75	0.50	0.64	0.98	0.18	-0.80	0.31	1.00

Sample Correlations

	P	h_0	GC	G_{rec}	LAI	ΔS	Θ	ET
P	1.00							
h_0	-0.62	1.00						
GC	-0.61	0.11	1.00					
Grec	-0.67	0.35	0.57	1.00				
LAI	0.15	-0.29	-0.16	0.27	1.00			
DS	0.78	-0.82	-0.48	-0.70	0.20	1.00		
Q	-0.36	0.81	0.10	0.12	-0.43	-0.60	1.00	
ET	-0.73	0.44	0.59	0.98	0.24	-0.78	0.18	1.00

Bootstrap Standard Errors - Standardized Total Effects

	P	h_0	GC	G_{rec}	LAI	ΔS	Θ	ET
GC	0.09	0.15	0.11	0.28	0.13	0.13	0.14	0.16
G_{rec}	0.05	0.12	0.10	0.14	0.10	0.07	0.13	0.10
LAI	0.12	0.14	0.12	0.32	0.08	0.14	0.16	0.19
ΔS	0.39	0.12	0.31	0.96	0.21	0.10	0.12	0.46
Θ	0.27	0.15	0.28	0.80	0.20	0.36	0.10	0.47
ET	0.05	0.13	0.10	0.15	0.11	0.07	0.14	0.10

Bootstrap Bias-Corrected Lower Bounds - Standardized Total Effects

	P	h_0	GC	G_{rec}	LAI	ΔS	Θ	ET
GC	-0.25	-0.05	-0.35	-0.07	-0.34	-0.14	-0.07	-0.55
G_{rec}	-0.05	-0.20	0.43	-0.10	0.14	-0.08	-0.24	0.86
LAI	-0.04	-0.55	-0.09	-0.74	-0.06	-0.26	-0.64	-0.16
ΔS	-0.50	-0.71	-0.88	-0.34	-0.60	-0.08	-0.30	-1.29
Θ	-0.56	0.54	-0.66	-0.44	-0.46	-0.69	-0.08	-1.05
ET	-0.06	-0.21	0.44	-0.11	0.13	-0.09	-0.27	-0.08

Bootstrap Bias-Corrected Upper Bounds - Standardized Total Effects

	P	h_0	GC	G_{rec}	LAI	ΔS	Θ	ET
GC	0.02	0.53	0.04	0.98	0.17	0.38	0.50	0.08
G_{rec}	0.01	0.27	0.78	0.13	0.55	0.10	0.25	1.07
LAI	0.20	-0.04	0.22	0.16	0.18	0.26	-0.03	0.35
ΔS	0.37	-0.32	-0.17	1.86	-0.05	0.12	0.16	-0.25
Θ	0.09	1.05	0.23	1.86	0.16	0.71	0.12	0.43
ET	0.01	0.28	0.80	0.13	0.57	0.10	0.25	0.12

Bootstrap Bias-Corrected Two-Tailed Significance - Standardized Total Effects

	P	h_0	GC	G_{rec}	LAI	ΔS	Θ	ET
GC	0.91	0.11	0.75	0.66	0.49	0.83	0.11	0.76
G_{rec}	0.88	0.92	0.00	0.85	0.00	0.78	0.93	0.00
LAI	0.87	0.03	0.73	0.63	0.67	0.79	0.03	0.74
ΔS	0.97	0.01	0.01	0.18	0.02	0.78	0.94	0.02
Θ	0.90	0.00	0.84	0.74	0.79	0.93	0.78	0.84
ET	0.88	0.92	0.00	0.85	0.00	0.78	0.93	0.78

Recharge Data Set

The model is nonrecursive.
Sample size = 48

Variable Correlations

Variable 1		Variable 2	Correlation
h_0	↔	P	-0.17
ET error	↔	h_0	0.74
G_{rec} error	↔	P	-0.12
ΔS error	↔	LAI error	0.11
LAI error	↔	G_{rec} error	0.43
ET error	↔	Θ error	-0.13
ET error	↔	P	-0.01
ΔS error	↔	GC error	-0.15
G_{rec} error	↔	GC error	0.42
G_{rec} error	↔	h_0	-0.15

Assessment of normality

Variable	min	max	skew	c.r.	kurtosis	c.r.
P	45.72	100.84	1.28	3.61	0.38	0.53
h_0	-64.37	16.77	0.13	0.38	-0.74	-1.05
GC	0.07	1.28	0.62	1.76	-0.44	-0.62
Grec	91.20	206.02	0.58	1.64	-0.45	-0.64
LAI	2.35	4.49	0.92	2.59	0.24	0.33
DS	-342.30	144.42	-0.15	-0.43	-1.06	-1.49
Q	0.24	1.00	-0.33	-0.94	-0.34	-0.48
ET	126.64	267.56	0.45	1.29	-0.62	-0.87
Multivariate					-1.13	-0.31

Model Correlations

	P	h_0	GC	G_{rec}	LAI	ΔS	Θ	ET
P	1.00							
h_0	-0.17	1.00						
GC	0.01	-0.08	1.00					
Grec	-0.02	0.25	0.61	1.00				
LAI	0.03	-0.40	-0.28	0.13	1.00			
DS	0.74	-0.57	-0.29	-0.52	0.17	1.00		
Q	-0.07	0.90	-0.13	0.10	-0.44	-0.38	1.00	
ET	0.01	0.33	0.63	0.97	0.03	-0.54	0.16	1.00

Sample Correlations

	P	h_0	GC	G_{rec}	LAI	ΔS	Θ	ET
P	1.00							
h_0	-0.17	1.00						
GC	-0.07	-0.17	1.00					
Grec	-0.06	0.21	0.57	1.00				
LAI	0.07	-0.34	-0.26	0.22	1.00			
DS	0.76	-0.54	-0.28	-0.52	0.15	1.00		
Q	-0.02	0.90	-0.14	0.04	-0.49	-0.35	1.00	
ET	-0.04	0.29	0.58	0.98	0.12	-0.55	0.13	1.00

Bootstrap Standard Errors - Standardized Total Effects

	P	h_0	GC	G_{rec}	LAI	ΔS	Θ	ET
GC	0.02	0.14	0.01	0.01	0.15	0.02	0.15	0.01
G_{rec}	0.02	0.10	0.08	0.02	0.14	0.03	0.11	0.05
LAI	0.03	0.12	0.02	0.04	0.01	0.04	0.12	0.02
ΔS	0.07	0.11	0.12	0.41	0.07	0.01	0.06	0.14
Θ	0.06	0.04	0.04	0.08	0.01	0.09	0.01	0.05
ET	0.02	0.12	0.09	0.02	0.16	0.03	0.13	0.01

Bootstrap Bias-Corrected Lower Bounds - Standardized Total Effects

	P	h_0	GC	G_{rec}	LAI	ΔS	Θ	ET
GC	-0.05	-0.33	-0.01	-0.04	-0.68	-0.08	-0.36	-0.01
G_{rec}	-0.07	-0.41	0.57	-0.05	-0.17	-0.10	-0.44	0.79
LAI	-0.11	-0.62	0.00	-0.09	0.00	-0.16	-0.66	0.00
ΔS	0.57	-0.38	-0.58	-0.60	-0.20	0.00	0.02	-0.67
Θ	-0.04	0.86	-0.12	-0.05	-0.05	-0.06	0.00	-0.16
ET	-0.09	-0.49	0.64	-0.06	-0.19	-0.12	-0.52	0.00

Bootstrap Bias-Corrected Upper Bounds - Standardized Total Effects

	P	h_0	GC	G_{rec}	LAI	ΔS	Θ	ET
GC	0.02	0.19	0.03	0.01	-0.11	0.02	0.21	0.04
G_{rec}	0.00	-0.02	0.89	0.01	0.35	0.01	-0.02	0.97
LAI	0.01	-0.16	0.07	0.02	0.02	0.01	-0.18	0.08
ΔS	0.83	-0.01	-0.17	0.71	0.08	0.05	0.26	-0.21
Θ	0.21	1.03	0.01	0.16	0.01	0.31	0.05	0.01
ET	0.00	-0.02	0.98	0.01	0.41	0.01	-0.02	0.05

Bootstrap Bias-Corrected Two-Tailed Significance - Standardized Total Effects

	P	h_0	GC	G_{rec}	LAI	ΔS	Θ	ET
GC	0.40	0.61	0.32	0.35	0.01	0.39	0.62	0.34
G_{rec}	0.08	0.03	0.00	0.32	0.48	0.08	0.03	0.00
LAI	0.09	0.00	0.06	0.34	0.24	0.10	0.00	0.07
ΔS	0.00	0.04	0.01	0.65	0.41	0.07	0.02	0.01
Θ	0.14	0.00	0.10	0.40	0.29	0.14	0.07	0.10
ET	0.08	0.03	0.00	0.31	0.49	0.09	0.03	0.07

Abundant Tree Data Set

The model is nonrecursive.
Sample size = 33

Variable Correlations

Variable 1		Variable 2	Correlation
h_0	↔	P	-0.18
ET error	↔	h_0	0.47
G_{rec} error	↔	P	-0.20
ΔS error	↔	LAI error	0.55
LAI error	↔	G_{rec} error	0.32
ET error	↔	Θ error	-0.20
ET error	↔	P	-0.14
ΔS error	↔	GC error	0.00
G_{rec} error	↔	GC error	0.28
G_{rec} error	↔	h_0	-0.26

Assessment of normality

Variable	min	max	skew	c.r.	kurtosis	c.r.
P	45.72	100.84	1.19	2.78	0.09	0.10
h_0	-58.77	16.77	0.35	0.81	-0.56	-0.66
GC	0.07	1.50	0.92	2.15	1.08	1.26
Grec	91.20	229.73	0.39	0.91	-0.58	-0.67
LAI	2.87	5.39	0.55	1.29	-1.05	-1.24
DS	-330.83	191.09	-0.11	-0.25	-0.98	-1.15
Q	0.24	1.00	-0.20	-0.48	-0.25	-0.29
ET	126.64	304.61	0.44	1.03	-0.44	-0.52
Multivariate					-0.54	-0.12

Model Correlations

	P	h_0	GC	G_{rec}	LAI	ΔS	Θ	ET
P	1.00							
h_0	-0.18	1.00						
GC	0.00	0.10	1.00					
Grec	-0.15	0.24	0.56	1.00				
LAI	-0.01	-0.27	0.04	0.39	1.00			
DS	0.74	-0.54	-0.28	-0.56	0.10	1.00		
Q	0.03	0.89	0.04	0.02	-0.30	-0.23	1.00	
ET	-0.11	0.32	0.55	0.98	0.33	-0.58	0.09	1.00

Sample Correlations

	P	h_0	GC	G_{rec}	LAI	ΔS	Θ	ET
P	1.00							
h_0	-0.18	1.00						
GC	0.06	-0.01	1.00					
Grec	-0.08	0.15	0.52	1.00				
LAI	0.09	-0.36	0.04	0.39	1.00			
DS	0.75	-0.52	-0.18	-0.48	0.21	1.00		
Q	0.08	0.89	0.01	-0.04	-0.37	-0.22	1.00	
ET	-0.06	0.24	0.50	0.98	0.33	-0.51	0.05	1.00

Bootstrap Standard Errors - Standardized Total Effects

	P	h_0	GC	G_{rec}	LAI	ΔS	Θ	ET
GC	0.04	0.18	0.02	0.06	0.19	0.06	0.18	0.04
G_{rec}	0.03	0.12	0.11	0.05	0.14	0.04	0.12	0.04
LAI	0.04	0.17	0.02	0.09	0.03	0.06	0.17	0.04
ΔS	0.10	0.15	0.11	0.59	0.15	0.03	0.09	0.18
Θ	0.08	0.08	0.05	0.22	0.06	0.12	0.03	0.09
ET	0.03	0.13	0.12	0.07	0.16	0.04	0.13	0.03

Bootstrap Bias-Corrected Lower Bounds - Standardized Total Effects

	P	h_0	GC	G_{rec}	LAI	ΔS	Θ	ET
GC	-0.04	-0.24	-0.07	-0.03	-0.33	-0.07	-0.25	-0.12
G_{rec}	-0.07	-0.28	0.24	-0.12	0.05	-0.11	-0.29	0.85
LAI	-0.17	-0.60	0.00	-0.27	0.00	-0.26	-0.62	0.00
ΔS	0.49	-0.36	-0.50	-0.29	-0.49	-0.04	-0.11	-0.86
Θ	0.06	0.89	-0.21	-0.05	-0.21	0.08	-0.04	-0.36
ET	-0.08	-0.32	0.26	-0.13	0.05	-0.12	-0.32	-0.04

Bootstrap Bias-Corrected Upper Bounds - Standardized Total Effects

	P	h_0	GC	G_{rec}	LAI	ΔS	Θ	ET
GC	0.12	0.46	0.02	0.23	0.42	0.19	0.44	0.03
G_{rec}	0.04	0.18	0.67	0.02	0.61	0.06	0.18	1.00
LAI	0.00	0.06	0.09	0.01	0.08	0.00	0.06	0.14
ΔS	0.85	0.06	-0.13	1.62	-0.04	0.07	0.19	-0.35
Θ	0.36	1.15	-0.03	0.67	-0.01	0.54	0.07	-0.05
ET	0.04	0.20	0.72	0.02	0.68	0.06	0.19	0.07

Bootstrap Bias-Corrected Two-Tailed Significance - Standardized Total Effects

	P	h_0	GC	G_{rec}	LAI	ΔS	Θ	ET
GC	0.44	0.51	0.39	0.31	0.79	0.44	0.51	0.43
G_{rec}	0.56	0.68	0.00	0.39	0.03	0.55	0.68	0.00
LAI	0.06	0.10	0.03	0.10	0.04	0.06	0.10	0.05
ΔS	0.00	0.11	0.00	0.17	0.02	0.53	0.64	0.00
Θ	0.01	0.00	0.01	0.13	0.02	0.01	0.53	0.01
ET	0.57	0.69	0.00	0.39	0.03	0.56	0.69	0.53

Bayesian Standardized Total Effects

Data Set	Variable	ET	Θ	ΔS	G_{rec}	LAI	GC	P	h_0
2006 & 2007	ET	0.00	-0.07	-0.01	0.00	0.25	0.62	-0.01	-0.07
	Θ	-0.06	0.00	0.12	0.05	-0.01	-0.04	0.08	0.90
	ΔS	-0.48	0.04	0.00	0.42	-0.12	-0.30	0.70	-0.26
	G_{rec}	0.93	-0.07	-0.01	0.00	0.23	0.57	-0.01	-0.06
	LAI	0.02	-0.31	-0.04	-0.02	0.00	0.01	-0.03	-0.28
	GC	0.00	0.04	0.01	0.00	-0.09	0.00	0.00	0.03
2006	ET	0.01	-0.14	-0.02	0.00	0.14	0.57	-0.01	-0.14
	Θ	-0.08	0.01	0.17	0.03	-0.01	-0.05	0.11	1.02
	ΔS	-0.50	0.07	0.01	0.18	-0.07	-0.28	0.66	-0.21
	G_{rec}	0.92	-0.13	-0.02	0.00	0.13	0.51	-0.01	-0.13
	LAI	0.03	-0.37	-0.06	-0.01	0.00	0.02	-0.04	-0.37
	GC	0.01	-0.13	-0.02	0.00	-0.10	0.01	-0.01	-0.13
2007	ET	-0.03	0.01	0.04	0.03	0.35	0.61	0.00	0.02
	Θ	-0.07	-0.03	0.09	0.07	-0.02	-0.05	-0.01	0.82
	ΔS	-0.61	-0.02	-0.03	0.58	-0.22	-0.39	-0.04	-0.52
	G_{rec}	0.94	0.02	0.04	0.03	0.33	0.59	0.00	0.02
	LAI	0.01	-0.37	-0.01	-0.01	0.00	0.01	0.00	-0.31
	GC	-0.04	0.27	0.06	0.04	-0.10	-0.03	-0.01	0.24
Recharge	ET	0.01	-0.26	-0.03	0.00	0.11	0.80	-0.02	-0.24
	Θ	-0.06	0.01	0.13	0.02	-0.01	-0.04	0.09	0.94
	ΔS	-0.44	0.11	0.01	0.16	-0.05	-0.35	0.70	-0.19
	G_{rec}	0.90	-0.23	-0.03	0.00	0.09	0.71	-0.02	-0.21
	LAI	0.03	-0.45	-0.06	-0.01	0.00	0.02	-0.04	-0.42
	GC	0.00	-0.08	-0.01	0.00	-0.41	0.00	-0.01	-0.07
Abundant Trees	ET	0.00	-0.02	0.00	0.00	0.36	0.51	0.00	-0.01
	Θ	-0.18	0.00	0.32	0.17	-0.07	-0.09	0.21	0.98
	ΔS	-0.56	0.01	0.00	0.52	-0.21	-0.29	0.65	-0.20
	G_{rec}	0.93	-0.02	0.00	0.00	0.34	0.47	0.00	-0.01
	LAI	0.05	-0.29	-0.09	-0.04	0.02	0.03	-0.06	-0.28
	GC	-0.03	0.15	0.05	0.03	0.04	-0.02	0.03	0.15

Bayesian Standard Deviation and Convergence Statistic

Data Set	Variable	ET	Θ	ΔS	G_{rec}	LAI	GC	P	h_0	Convergence Statistic
2006 & 2007	ET	0.01	0.08	0.01	0.01	0.11	0.07	0.01	0.07	<1.002
	Θ	0.04	0.01	0.08	0.04	0.01	0.02	0.05	0.03	
	ΔS	0.07	0.04	0.01	0.19	0.06	0.06	0.05	0.05	
	G_{rec}	0.03	0.08	0.01	0.01	0.10	0.06	0.01	0.07	
	LAI	0.01	0.10	0.03	0.01	0.00	0.01	0.02	0.09	
	GC	0.01	0.11	0.02	0.01	0.12	0.01	0.01	0.10	
2006	ET	0.01	0.11	0.02	0.01	0.16	0.11	0.01	0.11	<1.002
	Θ	0.04	0.01	0.07	0.05	0.02	0.03	0.05	0.03	
	ΔS	0.09	0.06	0.01	0.25	0.09	0.08	0.08	0.09	
	G_{rec}	0.04	0.10	0.02	0.01	0.15	0.10	0.01	0.10	
	LAI	0.02	0.14	0.04	0.02	0.01	0.01	0.02	0.15	
	GC	0.02	0.17	0.03	0.01	0.18	0.01	0.02	0.17	
2007	ET	0.06	0.16	0.07	0.07	0.12	0.09	0.01	0.14	1.004
	Θ	0.22	0.06	0.30	0.25	0.08	0.14	0.05	0.10	
	ΔS	0.14	0.11	0.06	0.37	0.09	0.11	0.12	0.09	
	G_{rec}	0.07	0.15	0.07	0.06	0.11	0.09	0.01	0.14	
	LAI	0.07	0.16	0.11	0.08	0.03	0.05	0.02	0.14	
	GC	0.10	0.16	0.12	0.12	0.13	0.07	0.02	0.16	
Recharge	ET	0.01	0.13	0.03	0.01	0.16	0.09	0.02	0.12	<1.002
	Θ	0.04	0.01	0.09	0.05	0.01	0.03	0.06	0.04	
	ΔS	0.12	0.06	0.01	0.31	0.08	0.10	0.07	0.10	
	G_{rec}	0.05	0.11	0.03	0.01	0.14	0.09	0.02	0.11	
	LAI	0.02	0.13	0.05	0.02	0.01	0.02	0.03	0.12	
	GC	0.01	0.16	0.02	0.01	0.15	0.01	0.02	0.15	
Abundant Trees	ET	0.03	0.14	0.05	0.04	0.17	0.13	0.03	0.14	<1.002
	Θ	0.08	0.03	0.12	0.17	0.05	0.05	0.08	0.06	
	ΔS	0.13	0.09	0.03	0.47	0.12	0.10	0.10	0.11	
	G_{rec}	0.04	0.13	0.05	0.03	0.16	0.12	0.03	0.13	
	LAI	0.04	0.19	0.07	0.06	0.02	0.02	0.04	0.18	
	GC	0.04	0.19	0.07	0.06	0.20	0.03	0.05	0.20	